GEORGIA INSTITUTE OF TECHNOLOGY
ENGINEERING EXPERIMENT STATION

PROJECT INITIATION

Date: November 6, 1975

Project Title: Antenna Pattern Analysis for Target Vehicles

Project No.: A-1780

Project Director: Mr. H. L. Bassett

Sponsor: Armament Development & Test Center (AFSC); ADTC/PMR; Eglin AFB, Fla 32542

Agreement Period: From 9/15/75 Until 1/15/76 (Perf. Period)

Type Agreement: Contract No. F08635-76-C-0075

Amount: $34,155

Reports Required: Monthly Status Reports; Final Technical Report

Sponsor Contact Person:

Technical Matters
ADTC/DLMQ
Eglin AFB, Florida 32542

Contractual Matters
(Thru GTRI)
ADTC/PMR
Eglin AFB, Fla 32542

Defense Priority Rating: DO-A7 under DMS Reg. 1

Assigned to: Electromagnetics Laboratory

COPIES TO:

- Project Director
- Director, EES
- Assistant Director
- Division Chief
- EES Accounting
- Patent Coordinator
- EES Supply Services
- Security—Reports—Property Office
- General Office Services
- Library, Technical Reports Section
- Office of Computing Services
- Project File
- Other SueCorbin; Bonnee Wettlaufer

RA-3 (8-75)

GEORGIA INSTITUTE OF TECHNOLOGY
OFFICE OF CONTRACT ADMINISTRATION

SPONSORED PROJECT TERMINATION

Date: August 30, 1976

Project Title: Antenna Pattern Analysis for Target Vehicles

Project No: A-1780

Project Director: H. L. Bassett

Sponsor: Armament Development & Test Center; Eglin AFB, Florida 32542

Effective Termination Date: 7/27/76 (Final Report submitted)

Clearance of Accounting Charges: 7/31/76

Grant/Contract Closeout Actions Remaining:

- X Final Invoice and Closing Documents
- _ Final Fiscal Report
- _ Final Report of Inventions
- X Govt. Property Inventory & Related Certificate
- _ Classified Material Certificate
- _ Other _____

Assigned to: Electromagnetics (~~School~~/Laboratory)

COPIES TO:

Project Director
Division Chief (EES)
School/Laboratory Director
Dean/Director—EES
Accounting Office
Procurement Office
Security Coordinator (OCA)
Reports Coordinator (OCA) ✓
Library, Technical Reports Section
Office of Computing Services
Director, Physical Plant
EES Information Office
Project File (OCA)
Project Code (GTRI)
Other _____

CA—4 (3/76)

A-1780

Contract No. F0835-76-C-0075

ANTENNA PATTERN ANALYSIS FOR TARGET VEHICLES

Monthly Technical Progress Report No. 1
15 September 1975 thru 14 October 1975
GIT/EES Project A-1780

Prepared by

Electromagnetics Laboratory
Engineering Experiment Station
Georgia Institute of Technology
Atlanta, Georgia 30332

H. L. Bassett and J. W. Cofer, Jr.

for

Headquarters Armament Development and Test Center (AFSC)
Eglin Air Force Base, Florida 32542

Mr. G. Hatcher, Technical Monitor
Guided Weapons Division
Targets Branch

OBJECTIVE

Antenna radiation pattern analyses by computer simulations will be performed for antenna systems utilized by the TDU-X tow target, BOMARC, and wing tip pod for the BQM-34A drone. Portions of the analysis will be verified by scale model antenna radiation patterns.

WORK SUMMARY

There are three parallel efforts being performed: (1) a one-fifth size model of the TDU-X is being fabricated and is about 90% complete, (2) full-scale principal plane radiation patterns of the command receiver antenna are being run as well as an efficiency test, and (3) the computer simulations are being done for the TDU-X antenna radiation patterns.

MAJOR EFFORTS

Scale model radiation patterns will begin on the TDU-X model. Additional analyses will be made of the command antenna obtained from Mr. G. Hatcher.

WORK SCHEDULE

The program is on schedule. The complete TDU-X analysis will be completed during the first 3 months of the program. This includes the scale model testing.

VISIT TO TARGETS BRANCH

Georgia Tech personnel visited Eglin AFB during October and had discussions with Messrs. Hatcher, Chancellor, and Hayes of the Targets Branch. The TDU-X tow target and BOMARC target maintainence facilities were visited. The antennas and antenna locations were the subjects of the visit.

PLANNED WORK

The computer analyses will be continued. The program for the circumferential slot will be finished, and patterns will be calculated for the DIGIDOPS scoring antenna system for the TDU-X tow target.

A-1780

Contract No. F0835-76-C-0075

ANTENNA PATTERN ANALYSIS FOR TARGET VEHICLES

Monthly Technical Progress Report No. 2
15 October 1975 thru 14 November 1975
GIT/EES Project A-1780

Prepared by

Electromagnetics Laboratory
Engineering Experiment Station
Georgia Institute of Technology
Atlanta, Georgia 30332

H. L. Bassett

for

Headquarters Armament Development and Test Center (AFSC)
Eglin Air Force Base, Florida 32542

Mr. G. Hatcher, Technical Monitor
Guided Weapons Division
Targets Branch

OBJECTIVE

Antenna radiation pattern analyses by computer simulations will be performed for antenna systems utilized by the TDU-X tow target, BOMARC, and wing tip pod for the BQM-34A drone. Portions of the analysis will be verified by scale model antenna radiation patterns.

WORK SUMMARY

The scale model has been completed; scaled scoring antennas have been mounted; and antenna radiation pattern measurements are being made. The computer simulations are continuing. Patterns have been computed for the scoring antennas for the cases of "no blockage" and "blockage." These will be discussed with the Project Monitor.

MAJOR EFFORTS

Scale model radiation patterns have begun on the TDU-X scoring antenna system. A photograph of the one-fifth size model is presented in Figure 1. Note the pairs of slot antennas located on the top and bottom of the vehicle. These slot antennas are loaded with Teflon.

Radiation pattern measurements have been completed on the Command antenna, which was mounted onto a 14-inch diameter metal cylindrical ground plane. The antenna possesses a very broad beam radiation pattern. The approximate gain of the antenna was measured to be 20 dB below that of a standard gain dipole.

WORK SCHEDULE

The program is slightly behind schedule, but the overall goals should be met during the scheduled time frame.

PERSONNEL VISITS

Technical discussions have been held with Mr. W. Hayes concerning the X-band augmentation radar antenna system. Mr. Hayes plans to send to

Georgia Tech a package containing drawings pertinent to this effort.

Mr. G. Hatcher of the Targets Branch will visit Georgia Tech on 21 November 1975 for a project review.

PLANNED WORK

The computer simulations will continue. The remaining TDU-X antenna system parameters will be programmed and the patterns will be computed. Principal plane radiation pattern measurements of these scaled antennas will be performed.

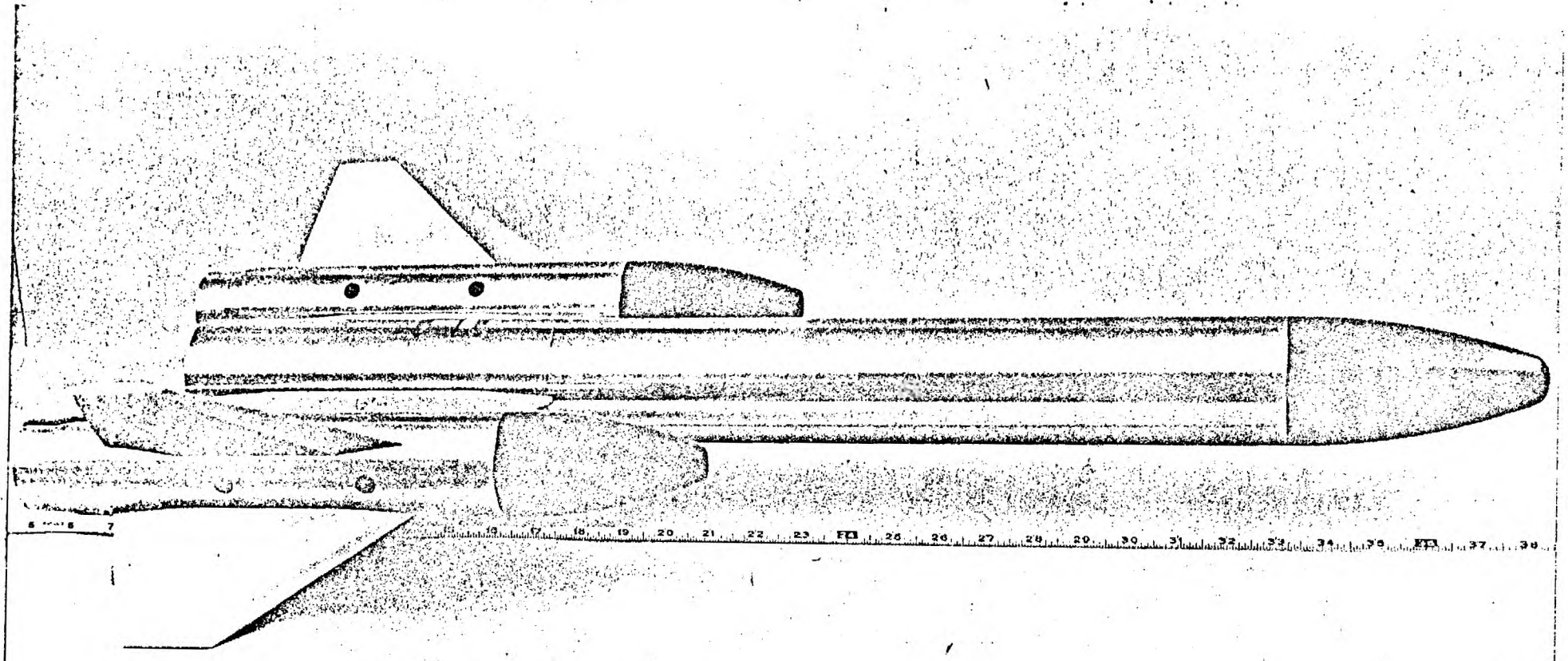

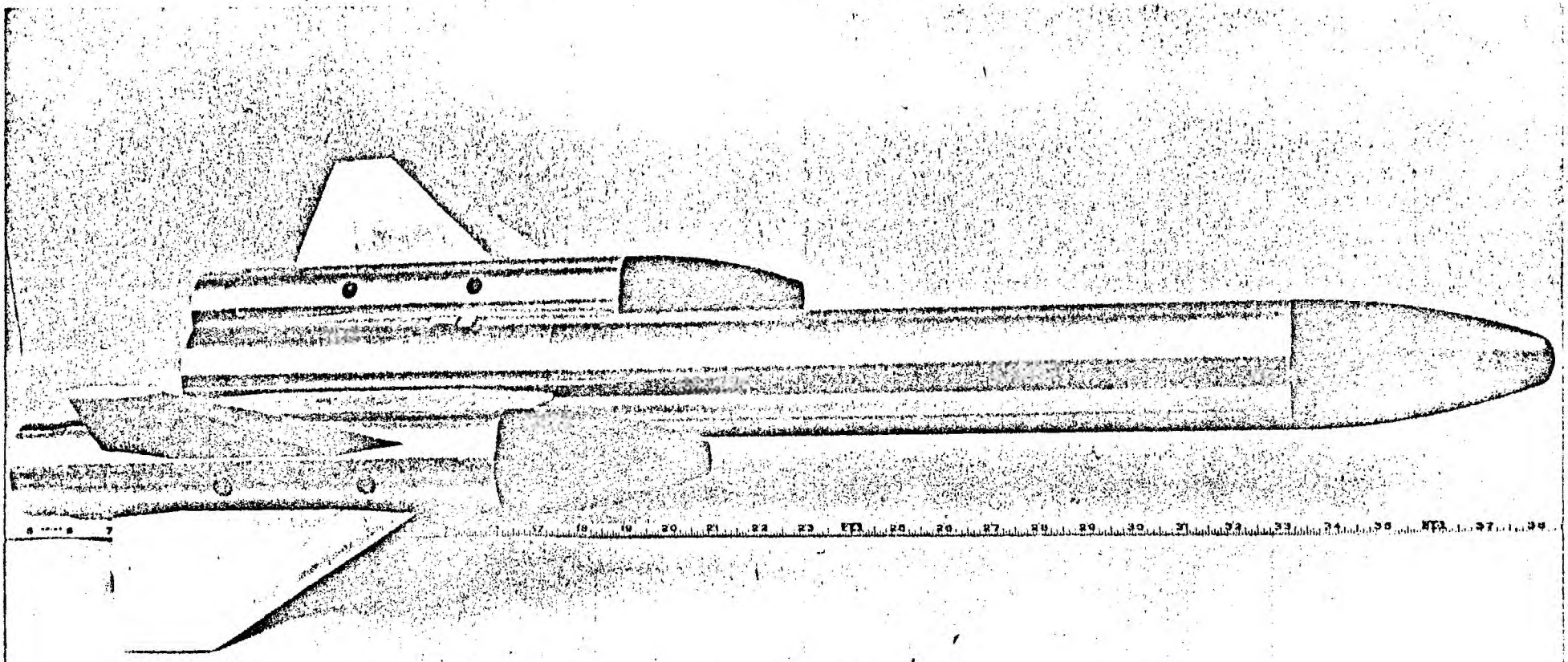

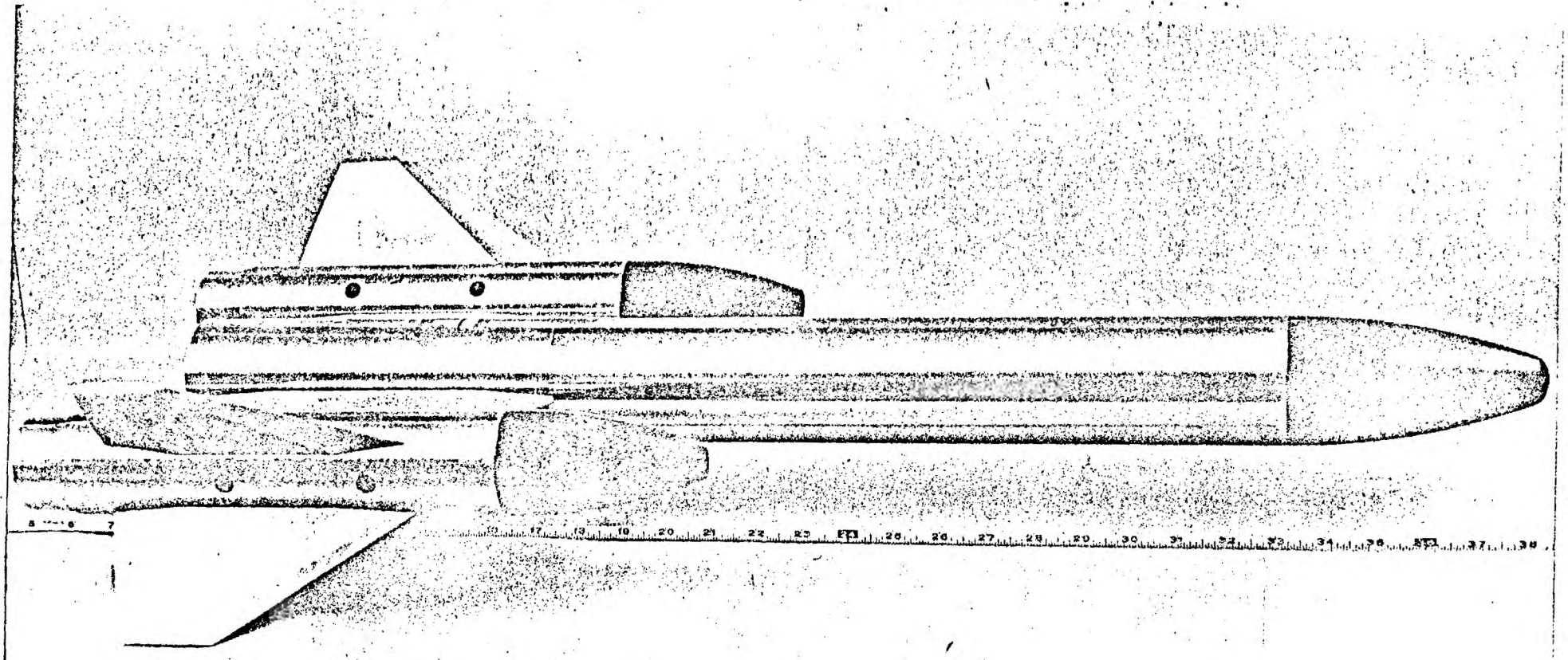

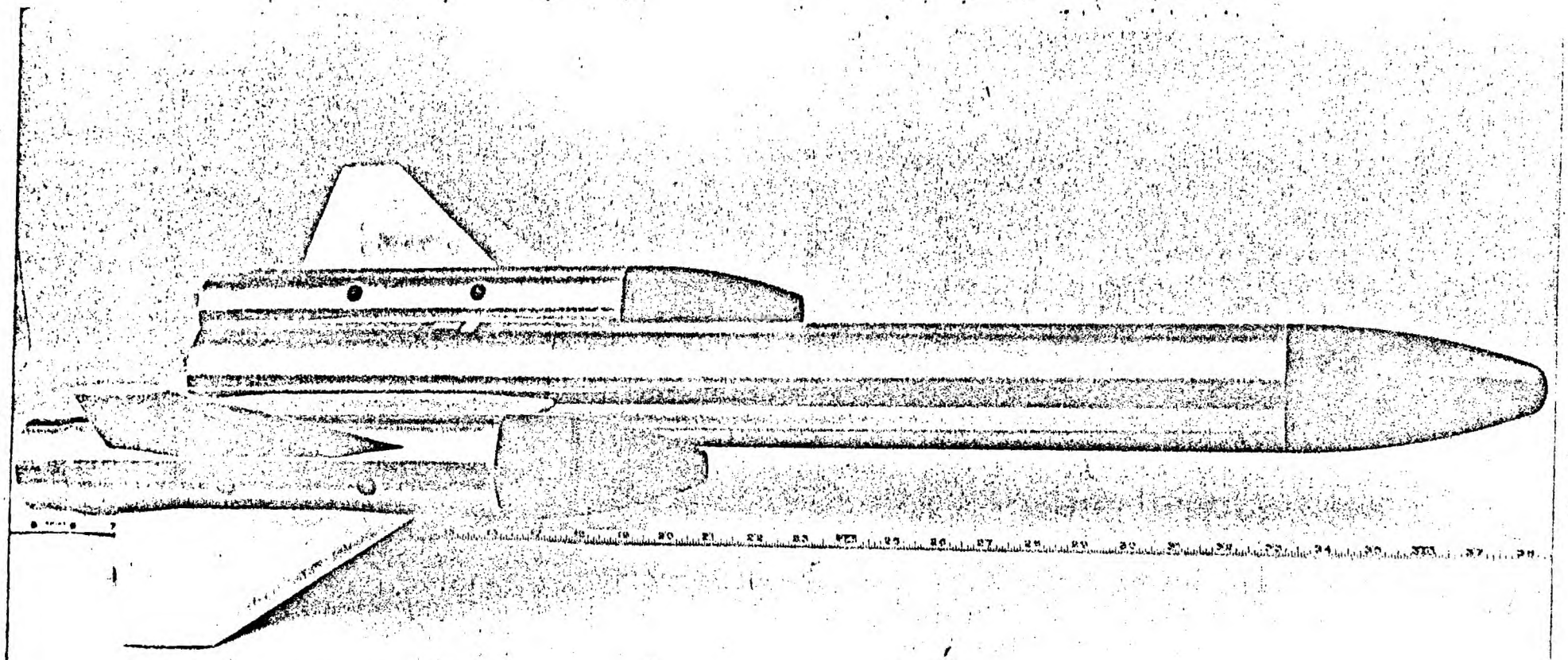

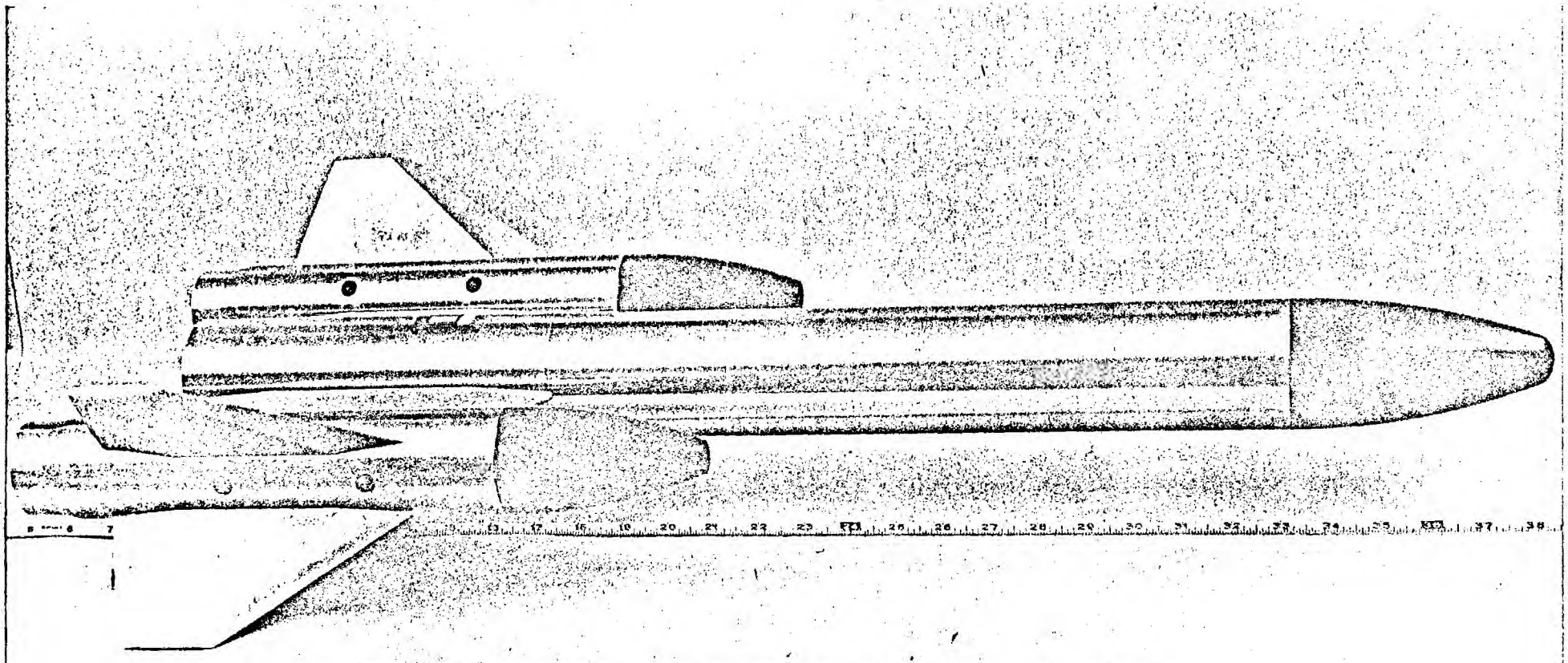

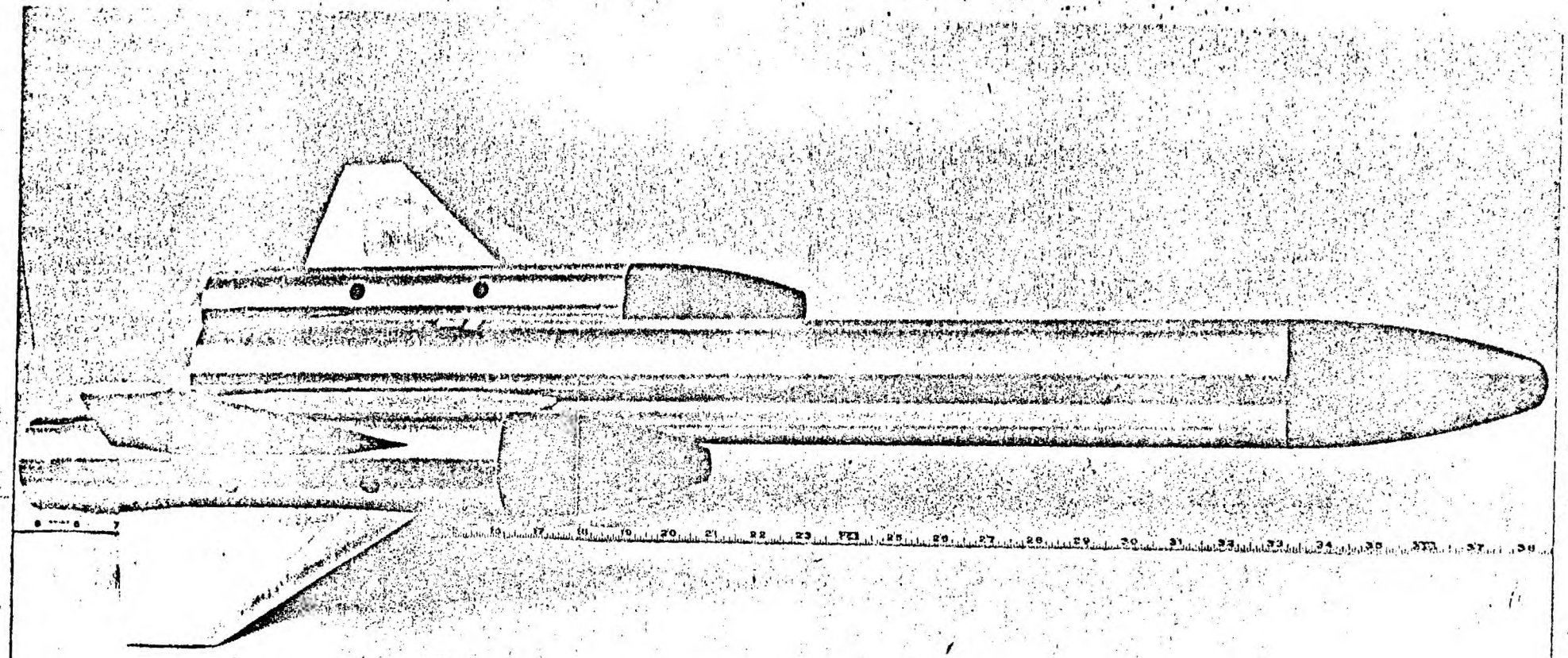

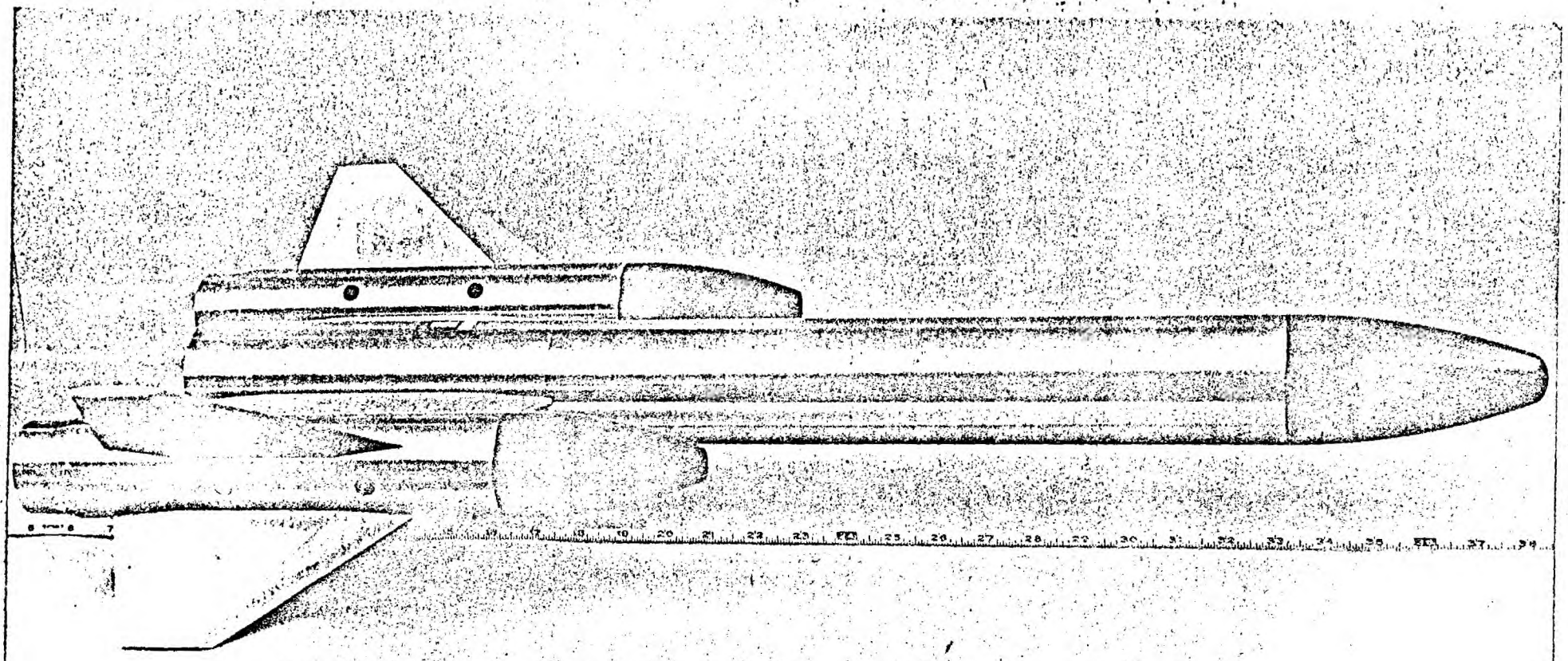

A-1780

Contract No. F0835-76-C-0075

Antenna Pattern Analysis For Target Vehicles

Monthly Technical Progress Report No. 3
15 November 1975 through 14 December 1975
GIT/EES Project A-1780

Prepared by

Electromagnetics Laboratory
Engineering Experiment Station
Georgia Institute of Technology
Atlanta, Georgia 30332

H. L. Bassett

for

Headquarters Armament Development and Test Center (AFSC)
Eglin Air Force Base, Florida 32542

Mr. G. Hatcher, Technical Monitor
Guided Weapons Division
Targets Branch

OBJECTIVE

Antenna radiation pattern analyses by computer simulations will be performed for antenna systems utilized by the TDU-X tow target, BOMARC, and wing tip pod for the BWM-34A drone. Portions of the analysis will be verified by scale model antenna radiation patterns.

WORK SUMMARY

Scale model radiation pattern measurements have been completed on the TDU-X scoring antenna, telemetry antenna and L-Band antenna systems. A photograph of the TDU-X scale model mounted on the antenna range is presented in Figure 1. Computer simulations have been completed on the TDU-X scoring antennas. These will be discussed with the project monitor on 18 December 1975.

MAJOR EFFORTS

As noted in the Work Summary, the TDU-X scale model radiation patterns have been completed with the exception of the X-Band antenna. These patterns are being made on the "old" type antenna. The tail coverage of the scoring antenna system is suprisingly good as noted in the scale model antenna radiation patterns and in the computer simulations.

Isolation measurements between the Telemetry antenna and L-Band augmentation antenna have been completed. These measurements indicate a minimum of 20 dB isolation in the 1 GHz to 2 GHz frequency range. Typically, the isolation is greater than 30 dB.

The attached 3-D contour plot indicates the calculated coverage for the TDU-X scoring antennas (Figure 2) as they are currently positioned. As indicated from both the computed data and the scale model data, the proposed positioning of the DIGIDOPS antennas will provide the required coverage. The scale model of the wing tip pod of the BQM-34A drone is being fabricated. The scoring antenna radiation pattern measurements will be completed on this model

during December.

WORK SCHEDULE

The program is slightly behind schedule, mainly due to the adverse weather conditions on the antenna pattern range. It is felt that the work will be completed as scheduled.

PLANNED WORK

The TDU-X X-Band antenna radiation patterns will be completed during the coming month. In addition, the antennas on the wing tip pod of the BQM-34A drone will be analyzed. Comparisons of scale model data versus computed data will be made to verify the computer simulations.

FUNDS

As of 1 December, 1975, approximately $13,000 out of the total $34,155 have been expended. This leaves sufficient funds to complete the contractual requirements.

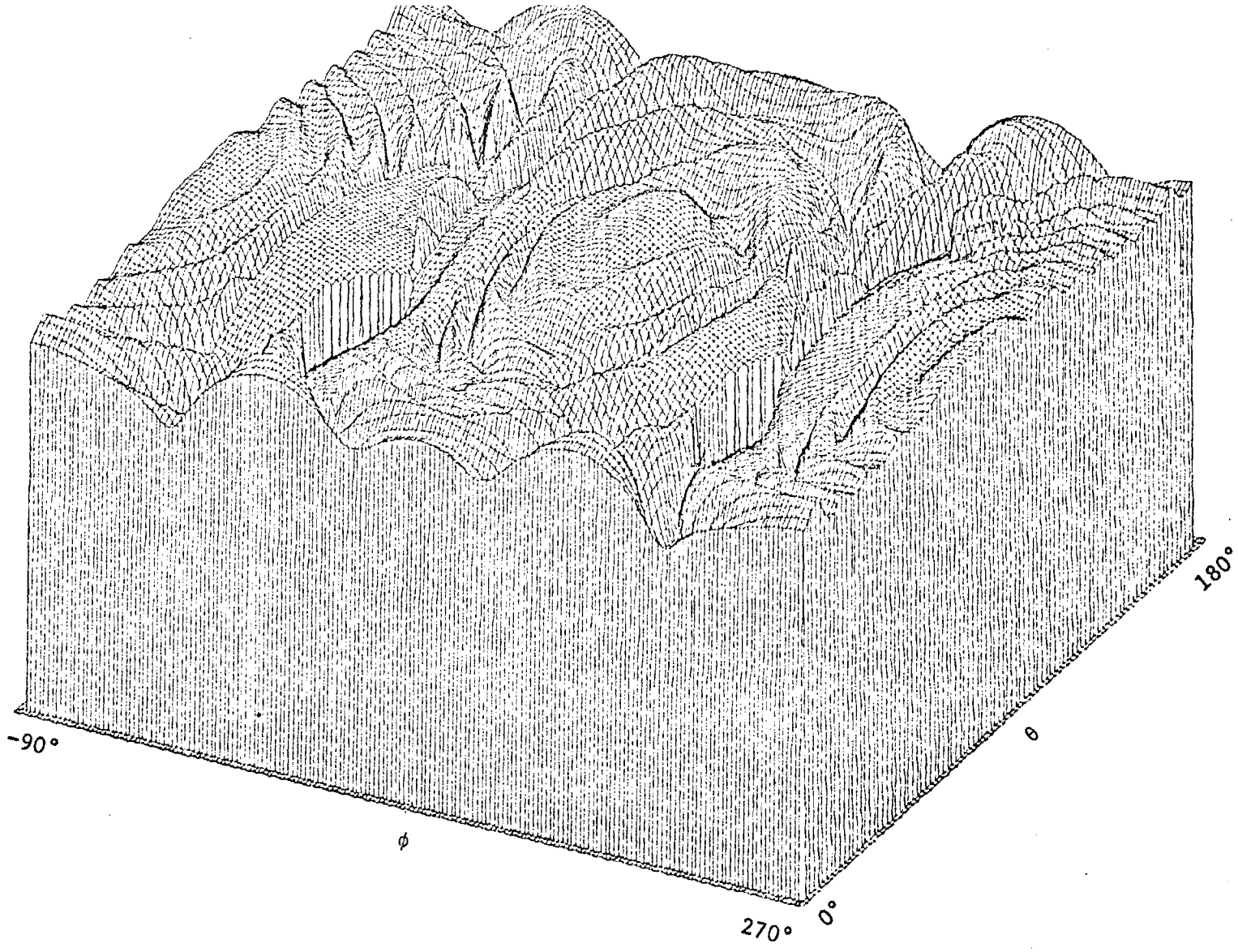

Figure 2. Calculated radiation pattern ($E_\theta^2 + E_\phi^2$) for two pairs of crossed slots (positioned on top and bottom as indicated by ADTC) on a conducting right circular cylinder having the same diameter as the TDU-X target. Wing and pod blockage was included.

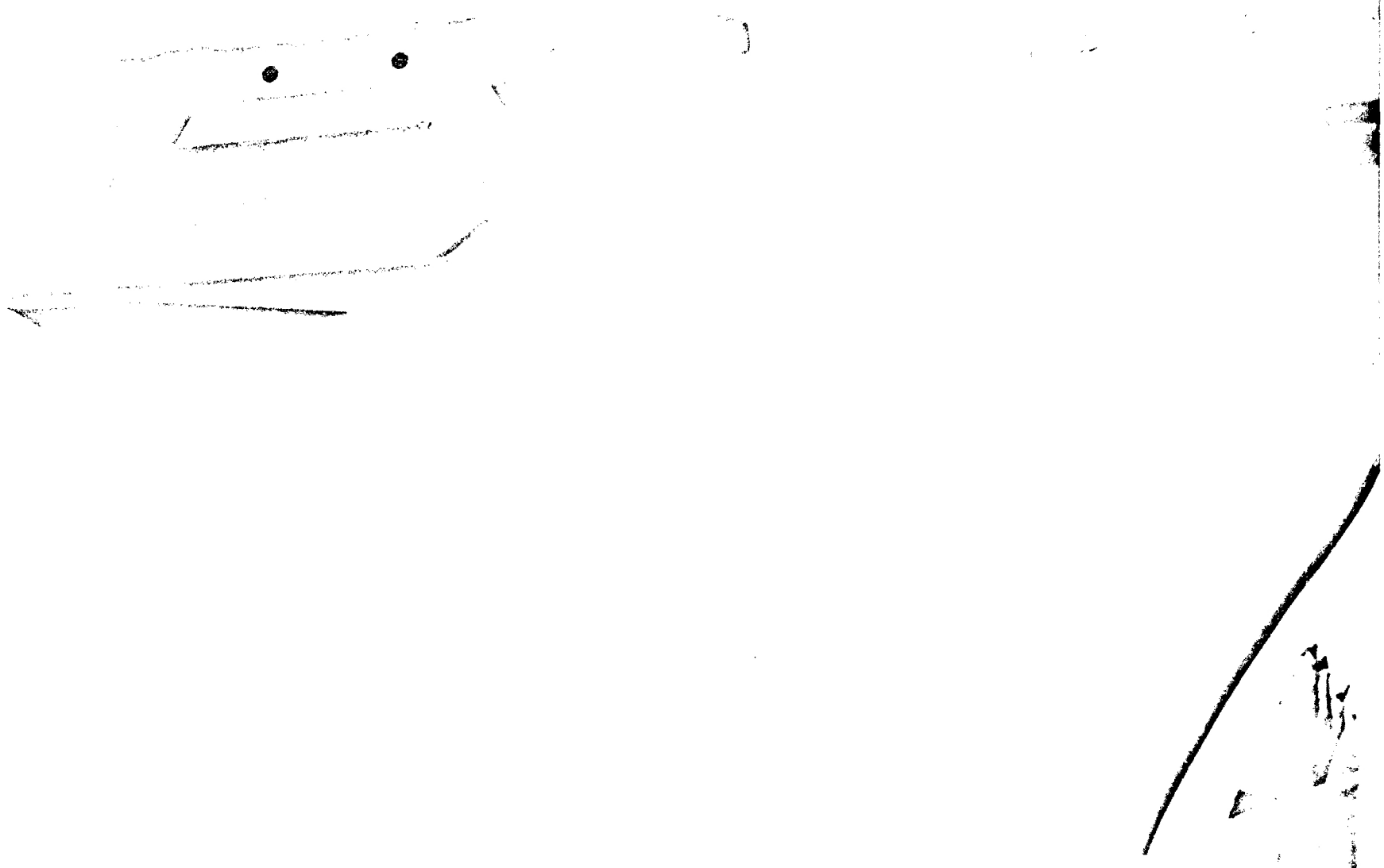

Figure 1. TDU-X Scale Model on Antenna Range

Contract No. F0835-76-C-0075

Antenna Pattern Analysis for Target Vehicles

Monthly Technical Progress Report No. 4

15 December 1975 through 14 January 1976

GIT/EES Project A-1780

Prepared by

Systems and Techniques Laboratory
Engineering Experiment Station
Georgia Institute of Technology
Atlanta, Georgia 30332

H. L. Bassett
C. E. Summers

for

Headquarters Armament Development and Test Center (AFSC)
Eglin Air Force Base, Florida 32542

Mr. G. Hatcher, Technical Monitor, DLMQ
Guided Weapons Division
Targets Branch

OBJECTIVE

Antenna radiation pattern analyses by computer simulations will be performed for antenna systems utilized by the TDU-X tow target, BOMARC, and wing tip pod for the BQM-34 A drone. Portions of the analysis will be verified by scale model antenna radiation patterns.

WORK SUMMARY

Scale model radiation pattern measurements have been completed on the TDU-X tow target. The scoring antennas, located on the target as designated by the Technical Project Monitor, provide good rear hemispherical coverage. In fact, the tail coverage for both polarizations is more than adequate. The coverage provided by the telemetry antenna, command antenna, and the L-Band augmentation antenna also provide adequate lower hemispherical coverage.

Full-scale measurements were made on the X-Band augmentation antennas, both the current antenna and the proposed conical spiral, and good rear coverage is provided by both.

Scale model radiation pattern measurements have been completed on the wing tip pod. These patterns will be discussed with the Technical Monitor at the earliest possible date.

Drawings are in the shop for the BOMARC model fabrication.

MAJOR EFFORTS

The computer analysis for the DIGIDOPS antenna on the TDU-X Tow Target was completed including an analysis of the slot positions. The DIGIDOPS antenna was modeled from the superposition of an axial slot and a circumferential slot located on an infinite cylinder of radius 7 inches. The slot positions were varied to determine the optimum location of the slots on the target. Gains and power distribution curves were plotted and compared and three dimensional plots were made of all of the patterns generated.

Figure 1 shows the total power $(E_\Phi^2 + E_\theta^2)$ for two crossed slots located at the original position. The patterns for the slots located at different positions are almost indistinguishable from this plot. Figure 2 shows the same pattern which has had the blockage from the wings added.

The two DIGIDOPS antennas were varied in their spacings by 0, $\lambda/4$, $\lambda/2$. The gains of these new patterns were calculated and found to be within 1 dB

of each other. The power distribution curves show (figure 3) that there was no significant change in the coverage effected by moving the slots. The original position of the DIGIDIPS offered as good a coverage as any other.

The contour plots of the measured data on the TDU-X antenna system are almost complete. The data from the scoring antenna plots will be compared with the computed data to determine the feasibility of utilizing computer simulations only for positioning antennas on the target vehicles.

A single scale model wing tip pod was used to determine scoring antenna pattern coverage for the BQM-34 A drone. The patterns indicate very good front and rear coverage with poor upper hemisphere coverage. These patterns will be further discissed with the Technical Monitor.

WORK SCHEDULE

The program is behind schedule on a time basis and is on-schedule on a cost basis. A no-cost extension to the contract has been requested. This additional time will allow the BOMARC patterns to be completed and will provide the necessary time for a detailed comparison of measured patterns versus the computed patterns.

PLANNED WORK

The BOMARC scale model will be fabricated, and the scoring antenna radiation patterns for this model will be measured. Antenna location positions have been obtained from the Technical Monitor.

Comparisons of computed data versus the scale model pattern data for the TDU-X will be completed during the next reporting period.

FUNDS

As of 1 January, 1976, approximately $20K out of the total $34,155 has been expended. This leaves sufficient funds to complete the contractual requirements.

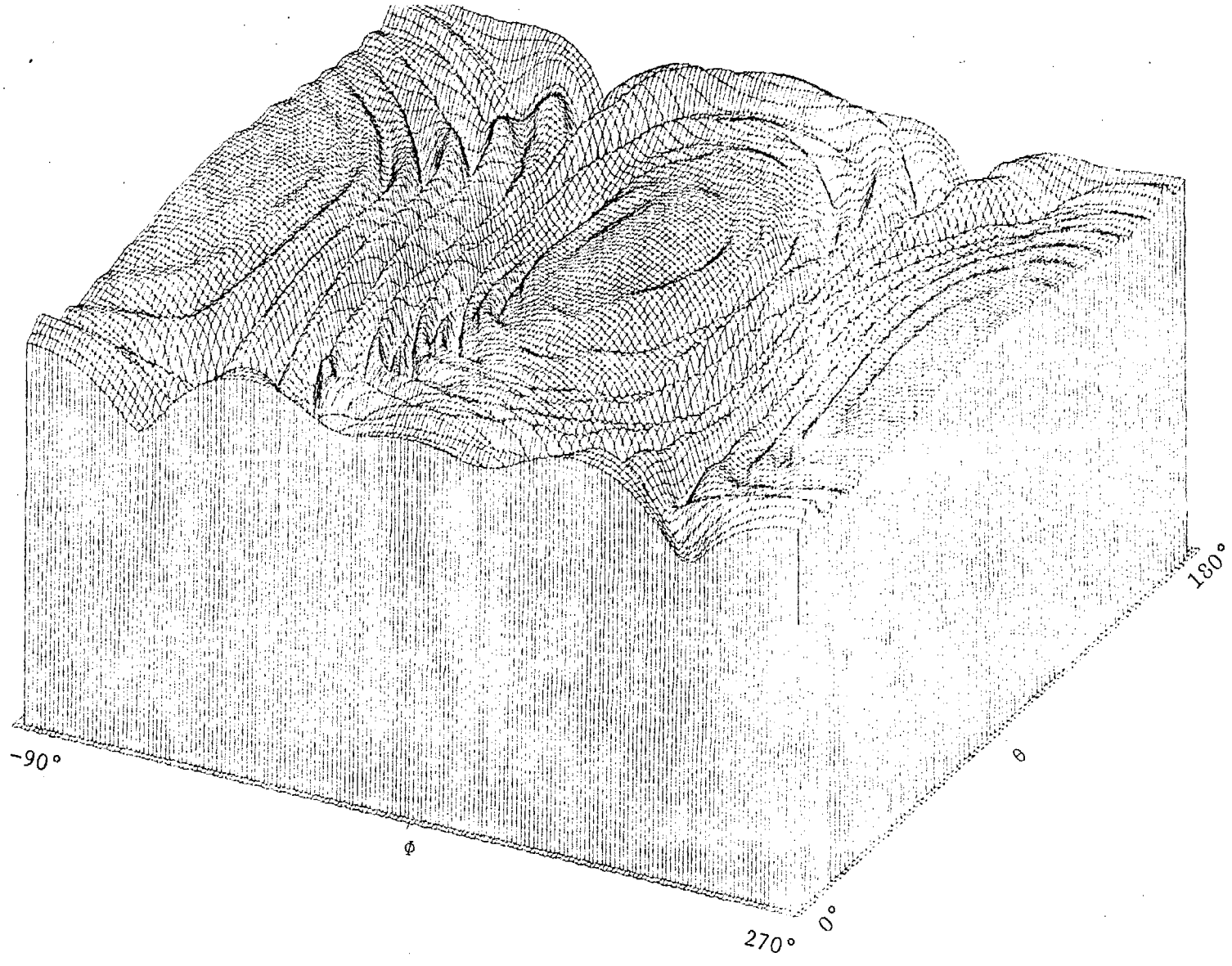

Figure 1. Calculated radiation pattern ($E_\theta^2 + E_\phi^2$) for two pairs of crossed slots (positioned on top and bottom as indicated by ADTC) on a conducting right circular cylinder having the same diameter as the TDU-X target. Wing and pod blockage was not included.

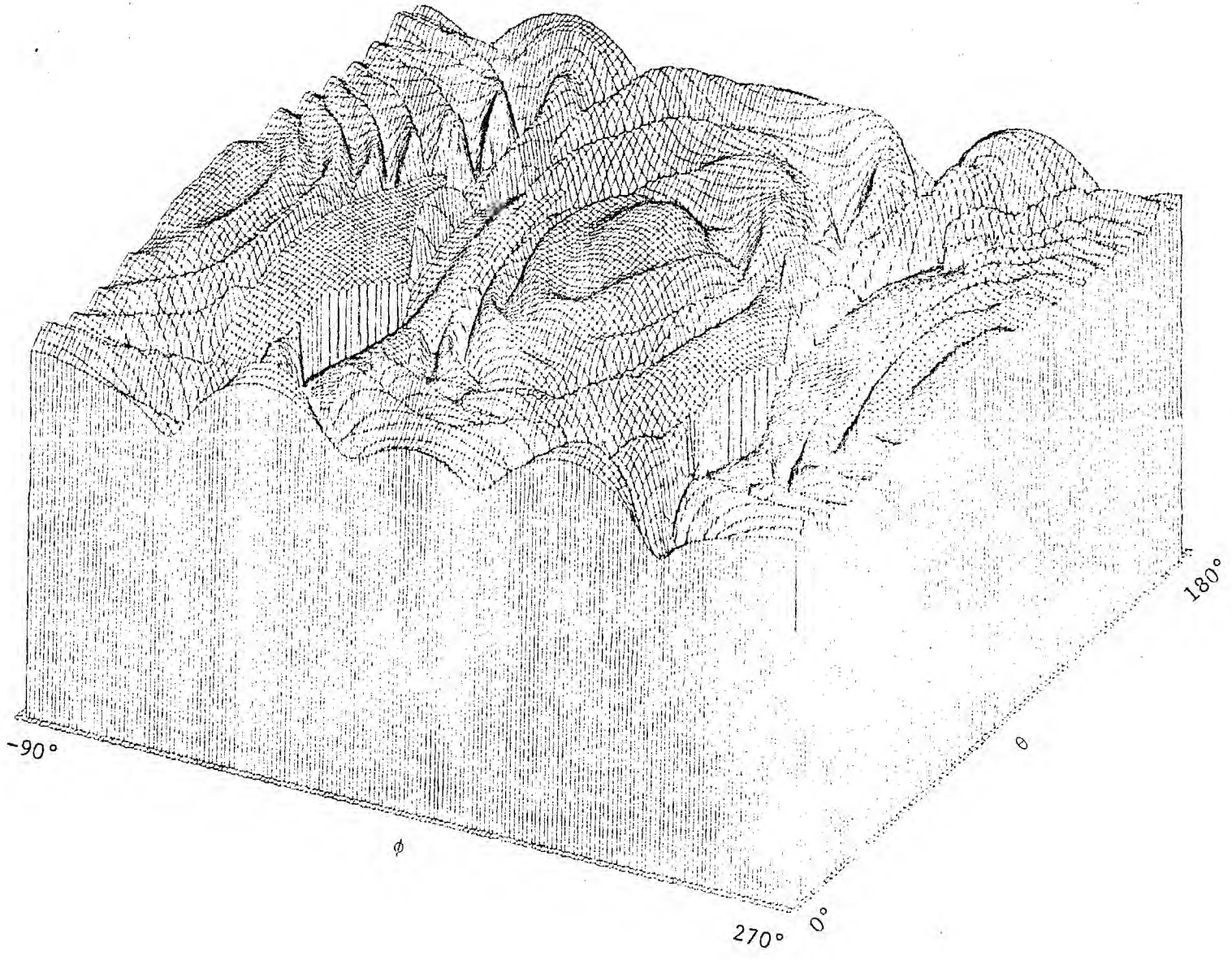

Figure 2. Calculated radiation pattern ($E_\theta^2 + E_\phi^2$) for two pairs of crossed slots (positioned on top and bottom as indicated by ADTC) on a conducting right circular cylinder having the same diameter as the TDU-X target. Wing and pod blockage was included.

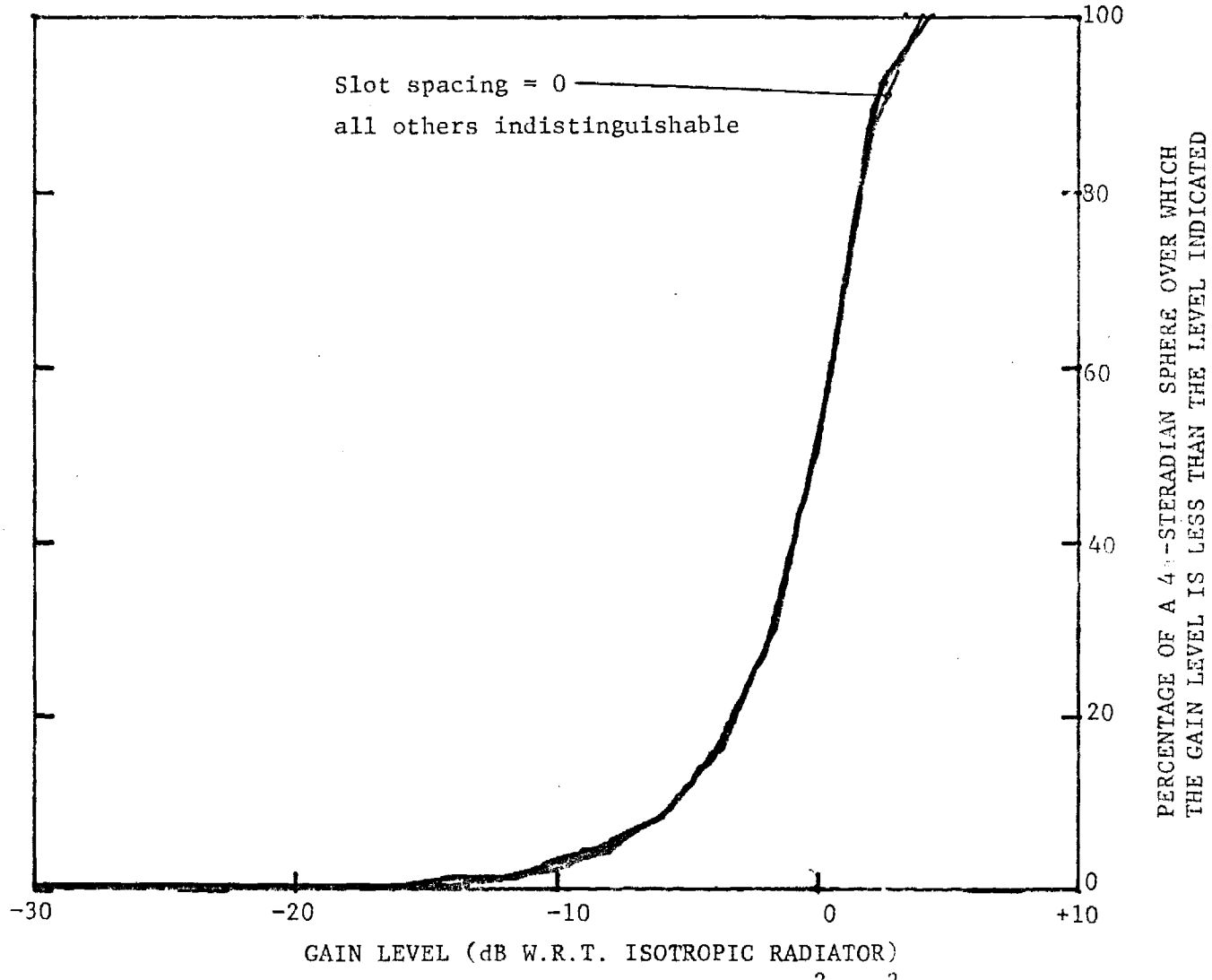

Figure 3. Power distribution function (total power, $(E_{\theta}^2 + E_{\phi}^2)$ for two pairs of crossed slots (one pair each on top and bottom) on the TDU-X target. Slot positions are indicated. No wing and pod blockage included.

A1780

Contract No. F0835-76-C-0075

Antenna Pattern Analysis for Target Vehicles

Monthly Technical Progress Report No. 5

15 January 1976 through 14 February 1976

EES/GIT Project A-1780

Prepared by

Systems and Techniques Laboratory
Engineering Experiment Station
Georgia Institute of Technology
Atlanta, Georgia 30332

H. L. Bassett
C. E. Summers

for

Headquarters Armament Development and Test Center (AFSC)
Eglin Air Force Base, Florida 32542

Mr. G. Hatcher, Technical Monitor, DLMQ
Guided Weapons Division
Targets Branch

OBJECTIVE

Antenna radiation pattern analyses by computer simulations will be performed for antenna systems utilized by the TDU-X tow target, BOMARC, and wing tip pod for the BQM-34A drone. Portions of the analysis will be verified by scale model antenna radiation patterns.

WORK SUMMARY

Scale model antenna radiation pattern measurements have been completed on the TDU-X tow target and the BQM-34A drone. Computer calculations of the radiation pattern coverage for antenna systems on the TDU-X tow target and the BOMARC have been completed, and the BQM-34A drone analysis is 90% complete. Thus, the remaining tasks to be completed are those of BOMARC scoring antenna scale model measurements and the BQM-34A computer calculations.

Comparisons have been made of the measured scale model radiation patterns and the computed patterns of the TDU-X scoring antennas. The patterns compare favorably, indicating that the computer simulation is an excellent technique for determining the best location of antennas on a target for optimum coverage, and if precise coverage data are required, scale model measurements should be sufficient. In Figures 1-12 are shown both the scale model principal plane radiation patterns and the calculated patterns for the TDU-X scoring antennas. As indicated by the plots, reasonably good agreement exists. Shown in Figures 13 and 14 are measured and calculated patterns for the TDU-X scoring antennas. The final two Figures, 15 and 16, are the calculated patterns for the BOMARC scoring antennas.

MAJOR EFFORTS

Each task, as outlined in the statement of work, has been completed with the exception of scale model BOMARC scoring antennas and computer simulations of the wing tip pod scoring antennas. These will be completed soon.

WORK SCHEDULE

A no cost extension to the contract has been requested so that the BOMARC scale model patterns can be completed.

PLANNED WORK

Scale model BOMARC scoring antenna radiation patterns will be completed along with wing tip pod computer simulations. Work has been initiated on the Final Report.

FUNDS

As of 1 February, 1976, approximately $29,500 of the total $34,155 has been expended. This leaves sufficient funds to complete the contract.

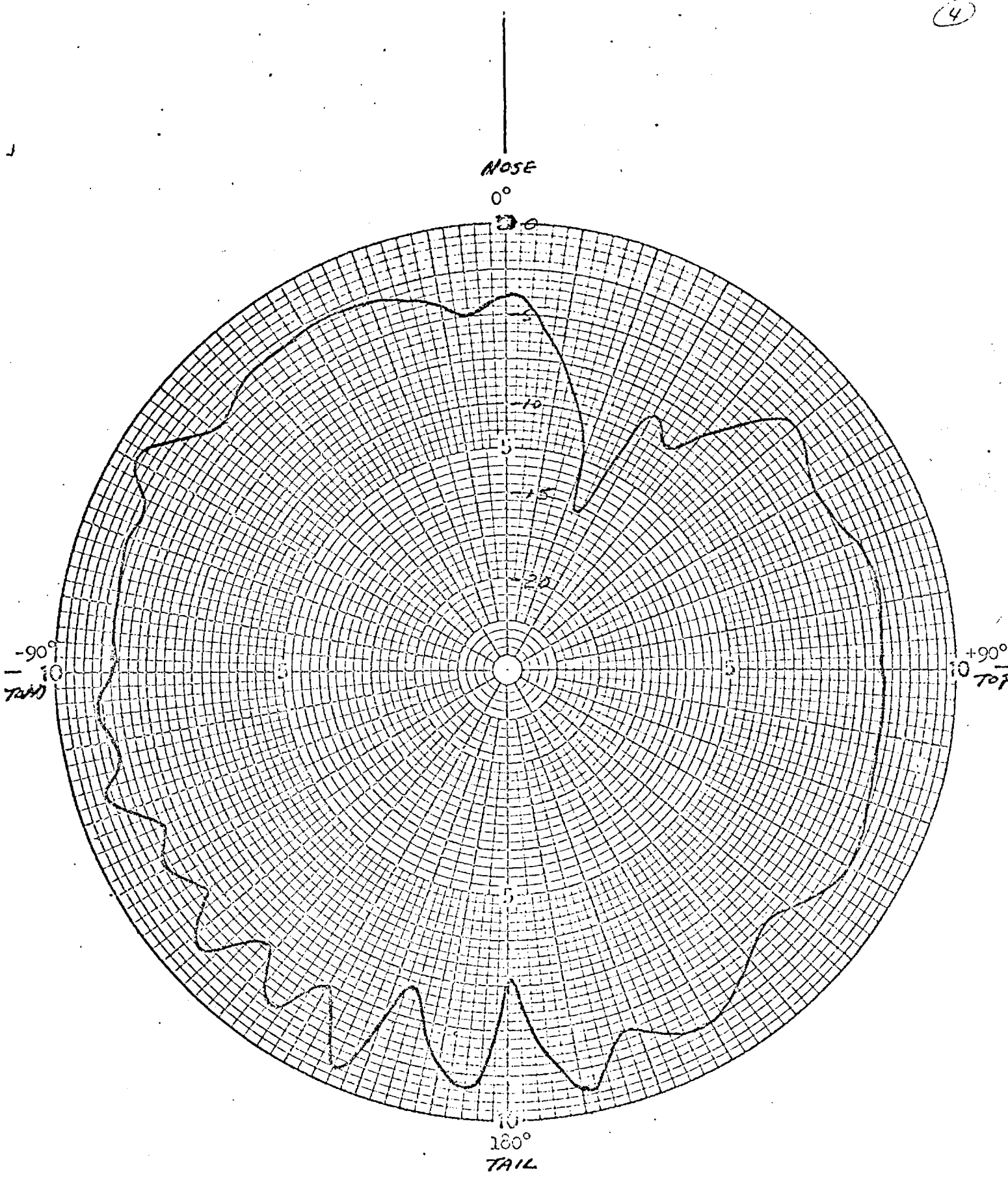

ROLL ANGLE 90°
PITCH VARIABLE

Figure 1. Principal Plane Plot, TDU-X Scoring Antennas, Horizontal Polarization, Two Antennas Located at Top and Bottom.

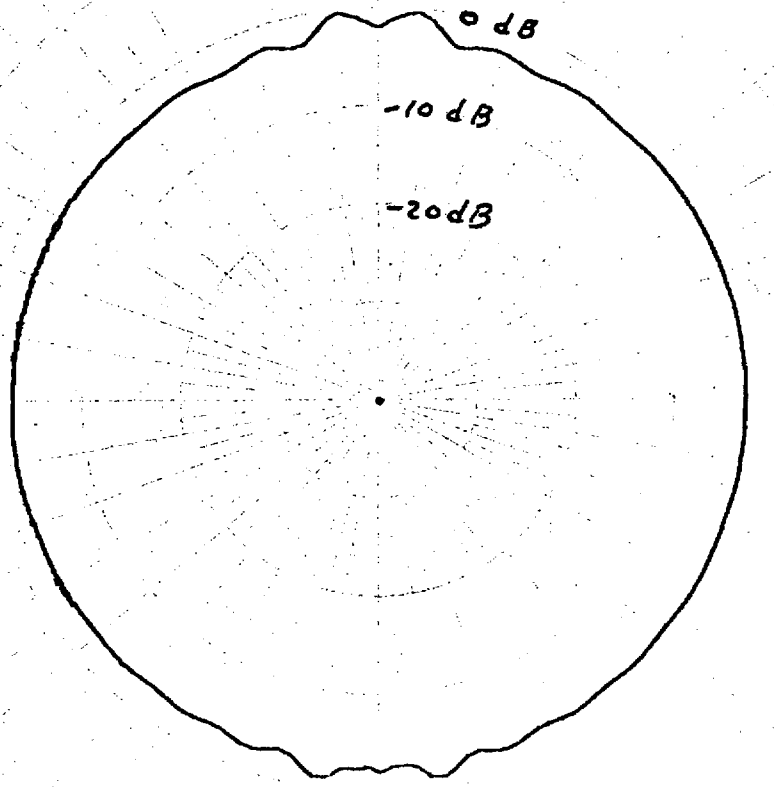

Figure 2. See Caption Figure 1. Computed data E_θ, $\phi = 90°$

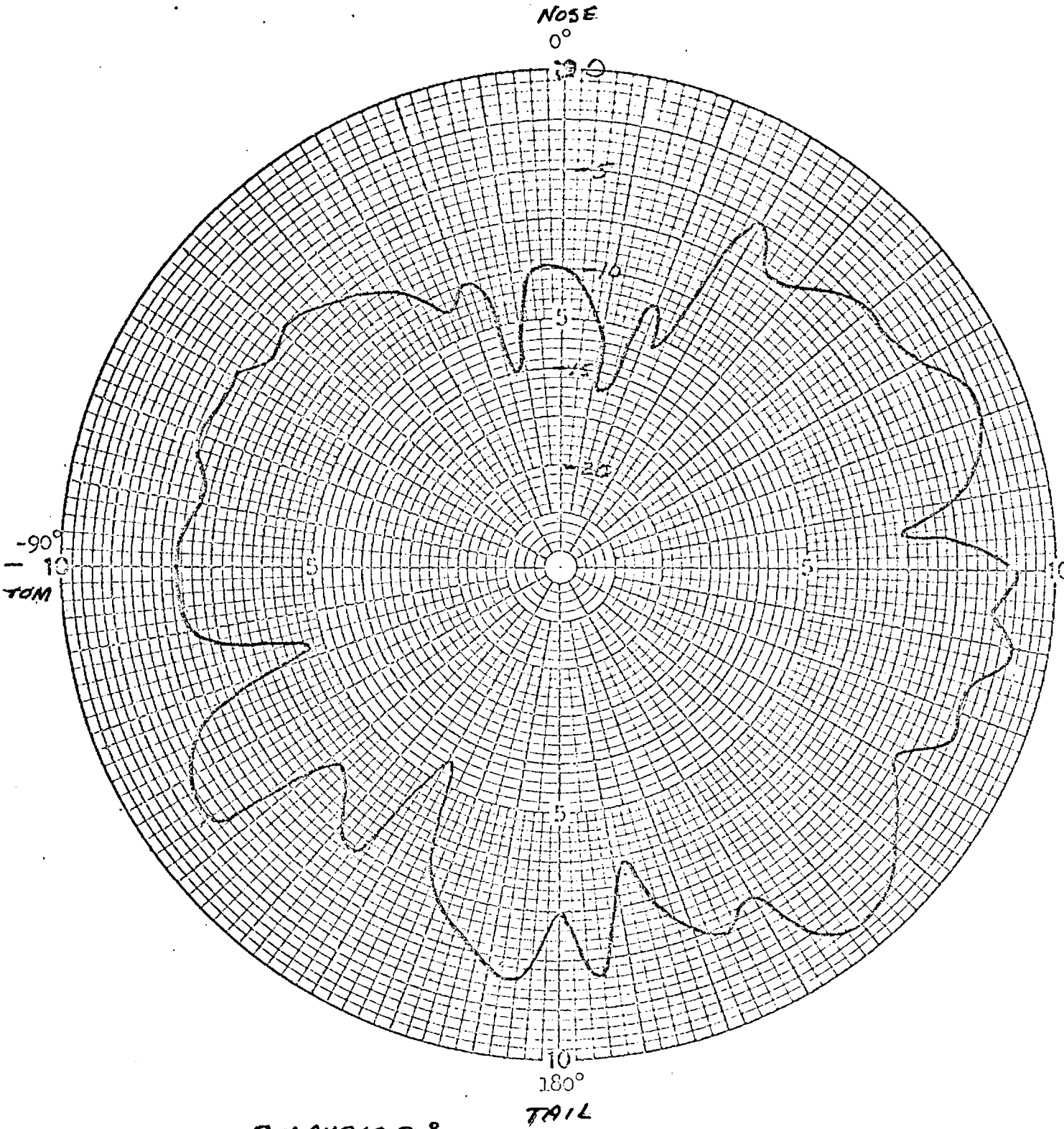

ROLL ANGLE 90°
PITCH VARIABLE

Figure 3. Principal Plane Plot, TDU-X Scoring Antennas, Vertical Polarization, Two Antennas at Top and Bottom

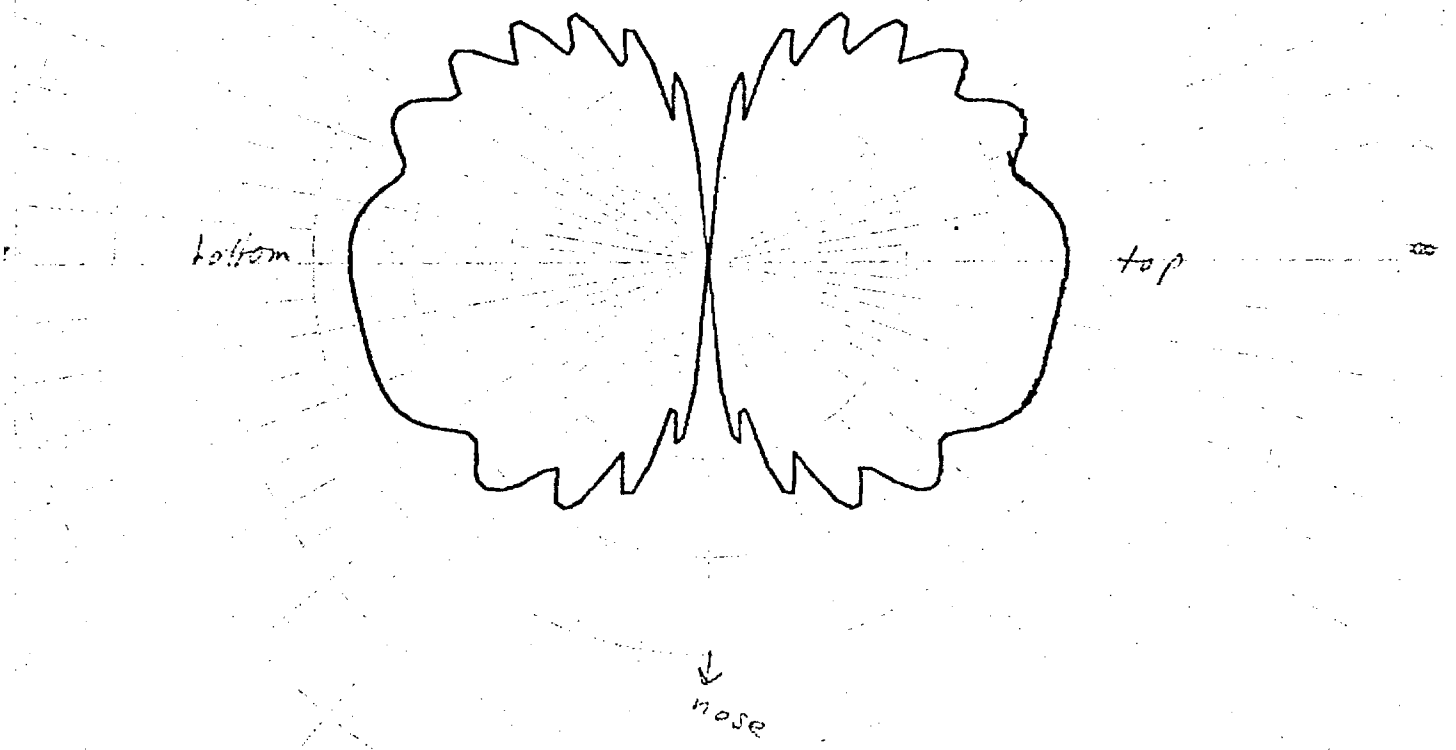

Figure 4. See Caption Figure 3. Computed data E_ϕ, $\phi = 90°$

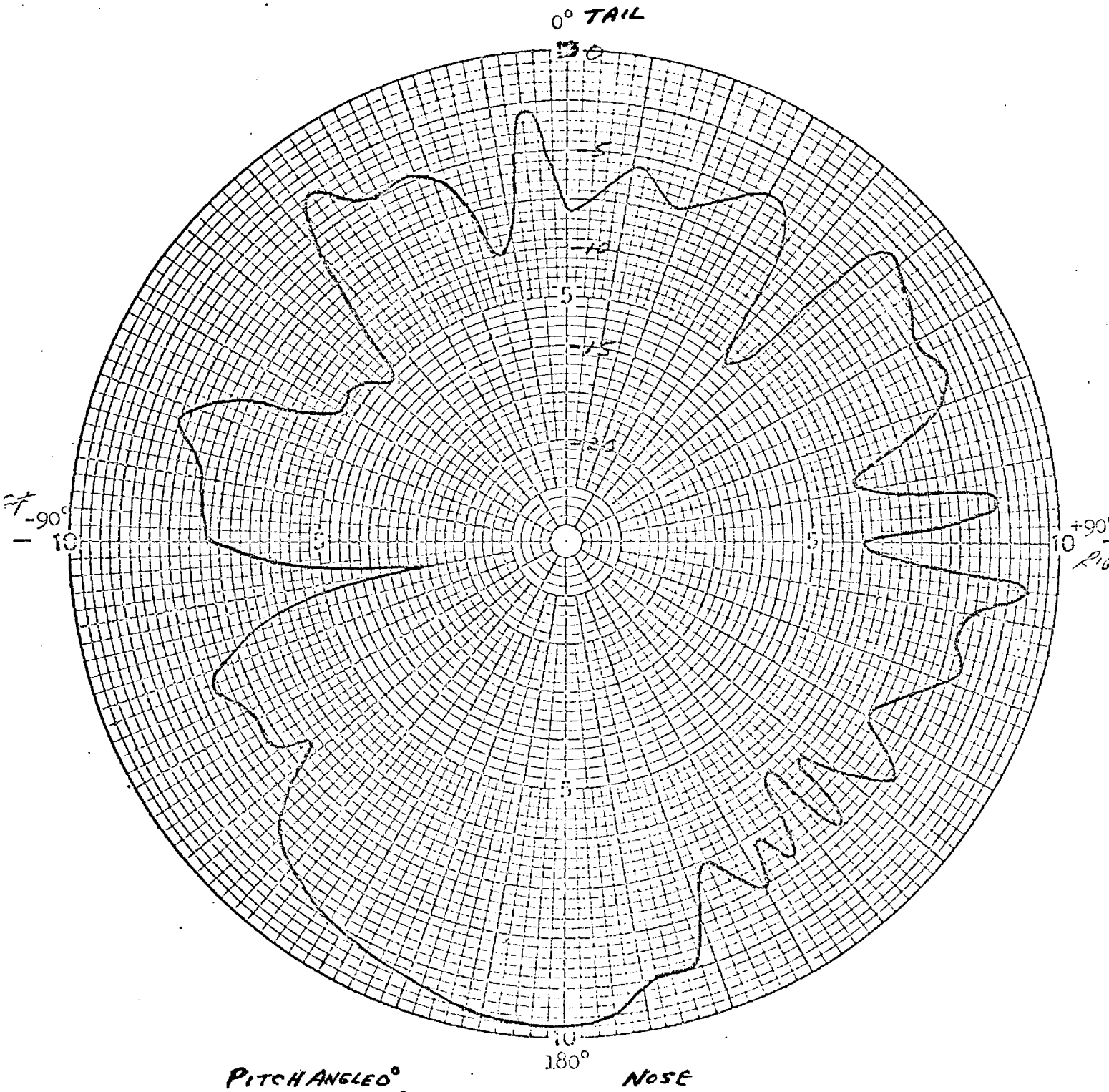

PITCH ANGLE 0°
ROLL ANGLE 0°
YAW ANGLE VARIABLE

Figure 5. Principal Plane Plot, TDU-X Scoring Antennas, Vertical Polarization, Two Antennas Located at Top and Bottom

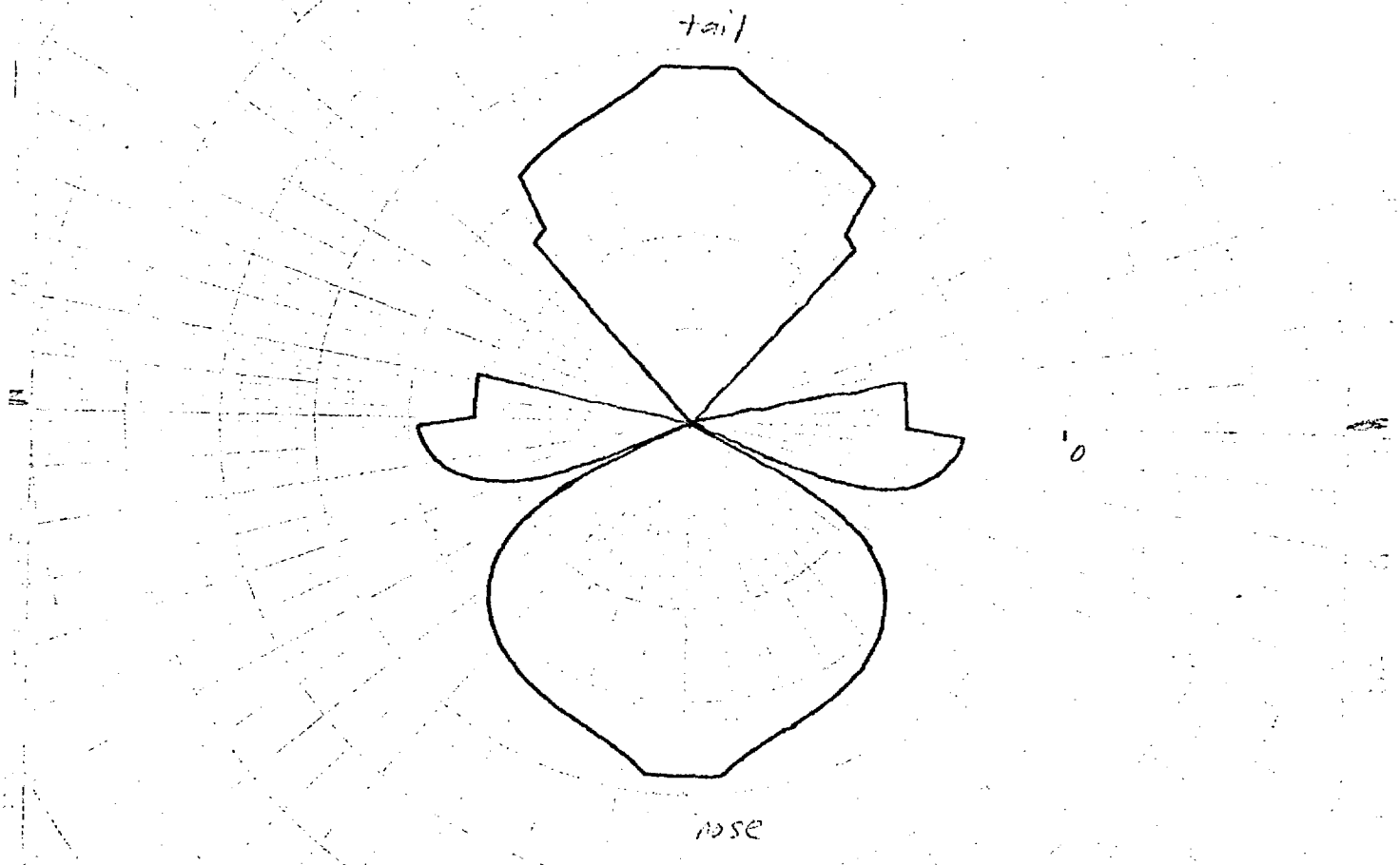

Figure 6. See caption Figure 5. Computed data E_ϕ, $\phi = 0°$

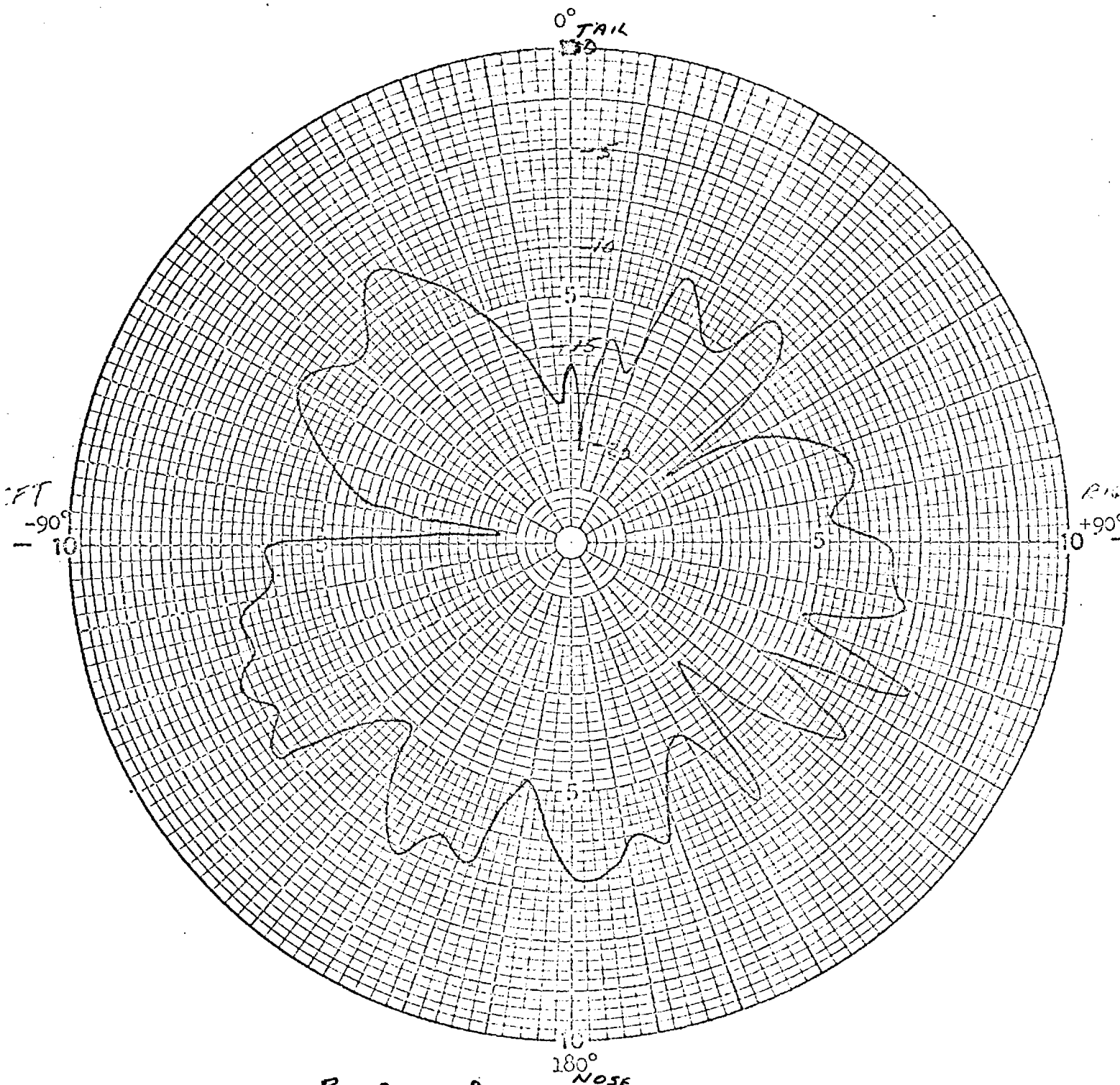

ROLL ANGLE 0°
PITCH ANGLE 0°
YAW VARIABLE

Figure 7. Principal Plane Plot, TDU-X Scoring Antennas
Horizontal Polarization, Two Antennas Located at Top and Bottom

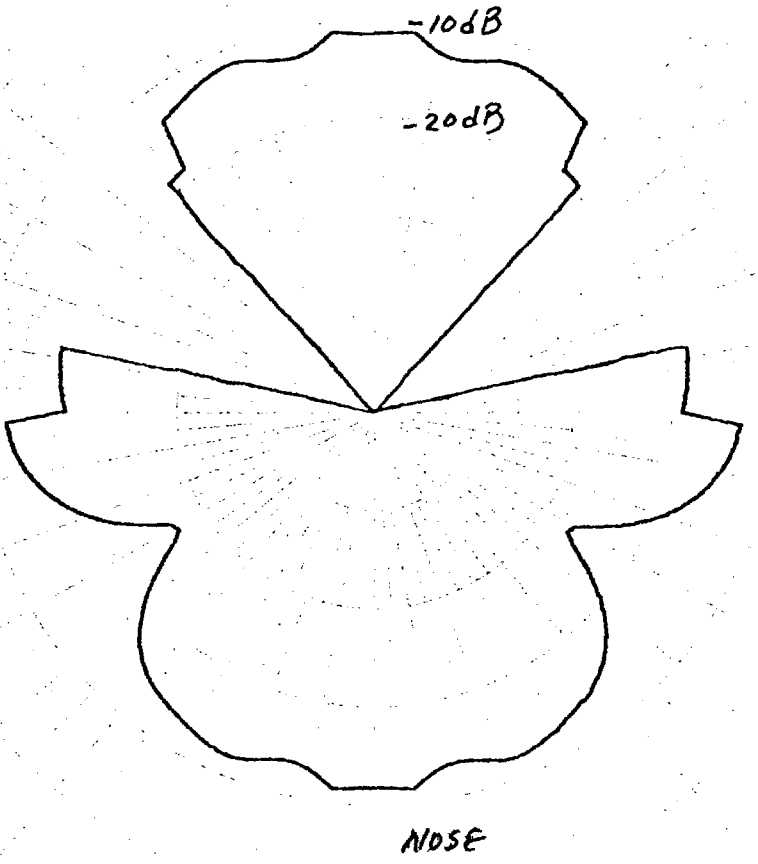

Figure 8. ~~See~~ caption Figure 7. Computed data $E\theta$, $\phi = 0°$

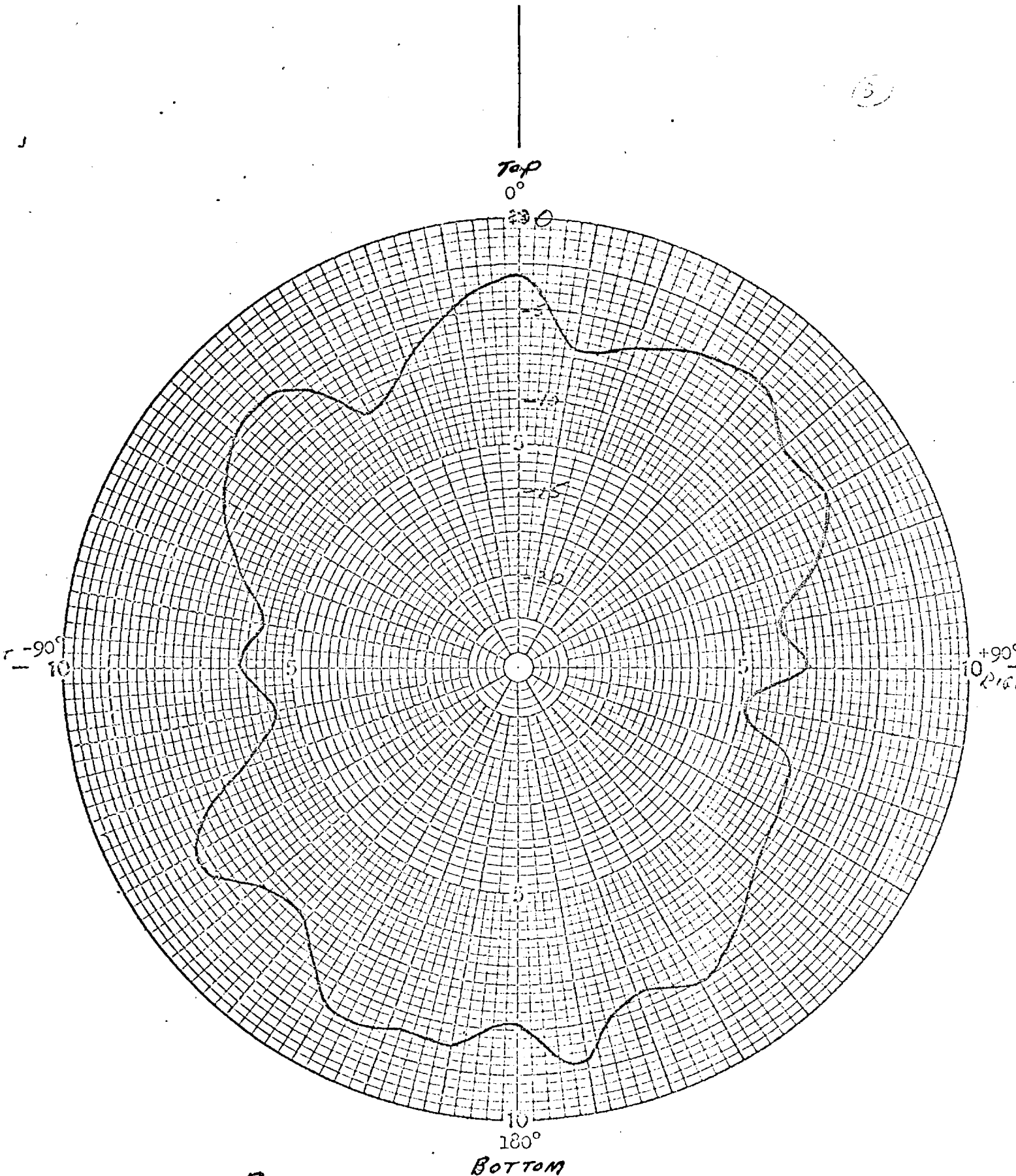

PITCH ANGLE 90°
YAW ANGLE 0°
ROLL ANGLE VARIABLE

Figure 9. Principal Plane Plot, TDU-X Scoring Antennas, Horizontal Polarization, Two Antennas Located at Top and Bottom

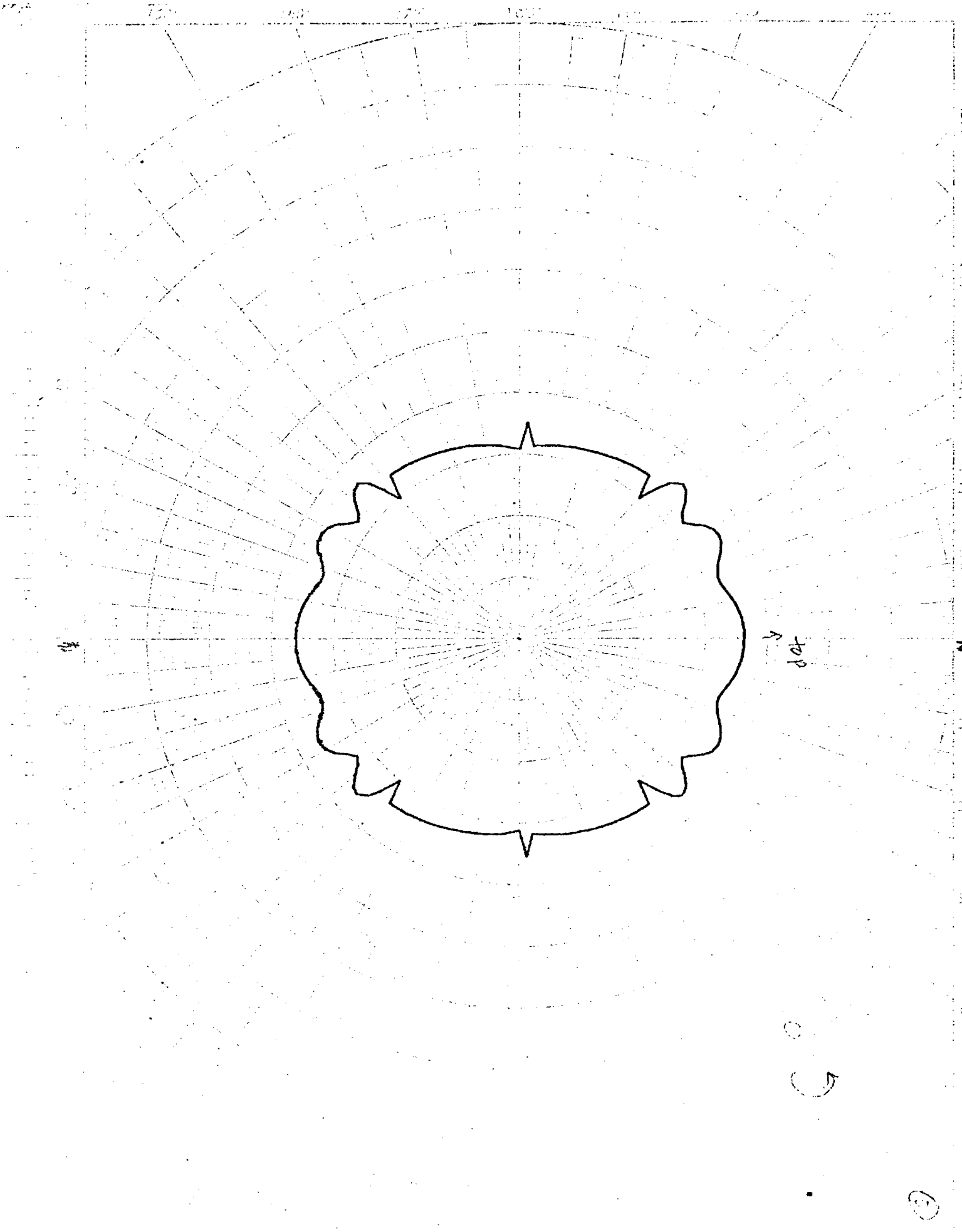

Figure 10. See caption Figure 9. Computed data E_θ, $\theta = 90°$

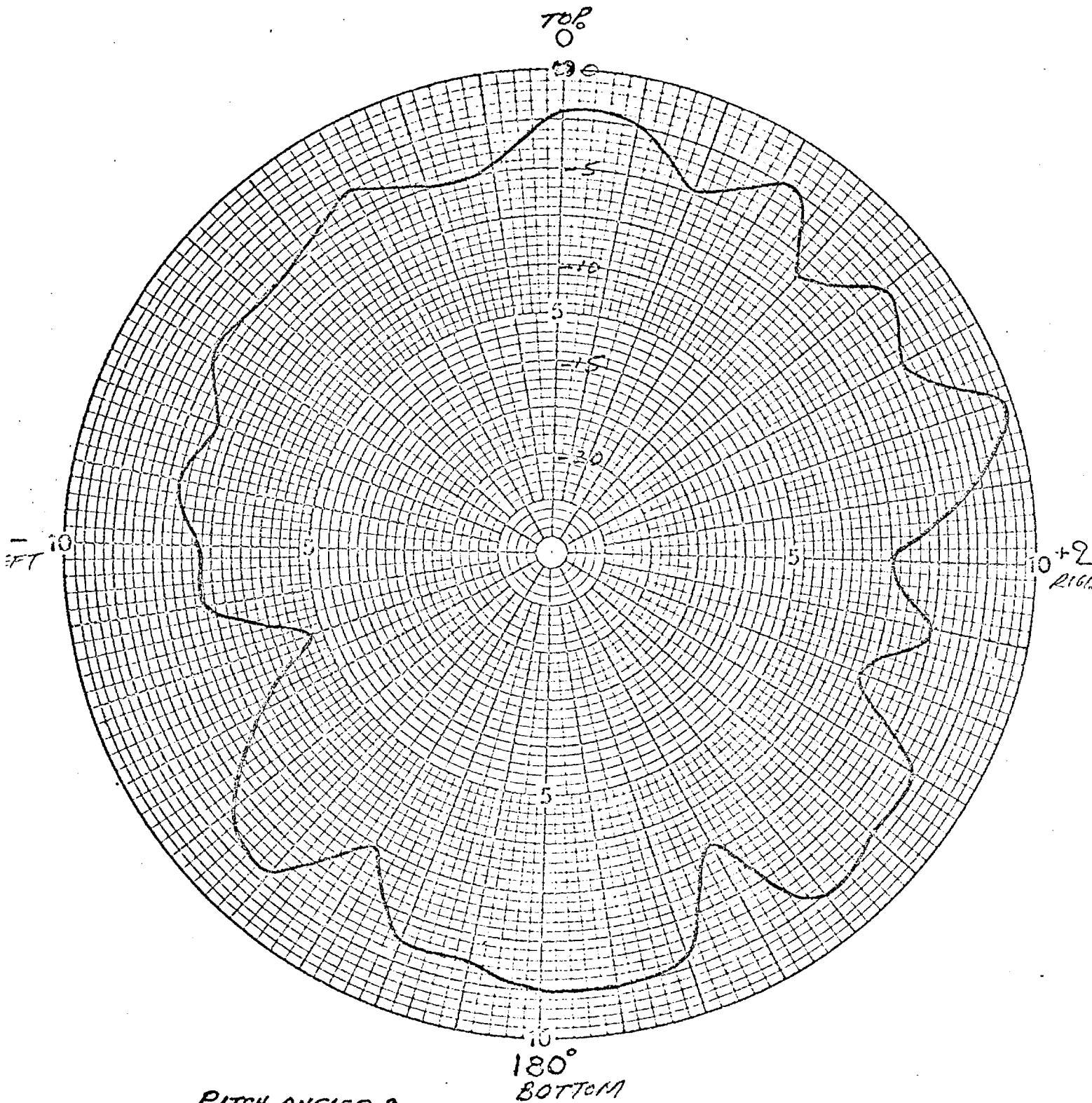

PITCH ANGLE 90°
YAW ANGLE 0°
ROLL ANGLE VARIABLE

Figure 11. Principal Plane Plots, TDU-X SCORING ANTENNAS, Vertical Polarization, Two Antennas at Top and Bottom

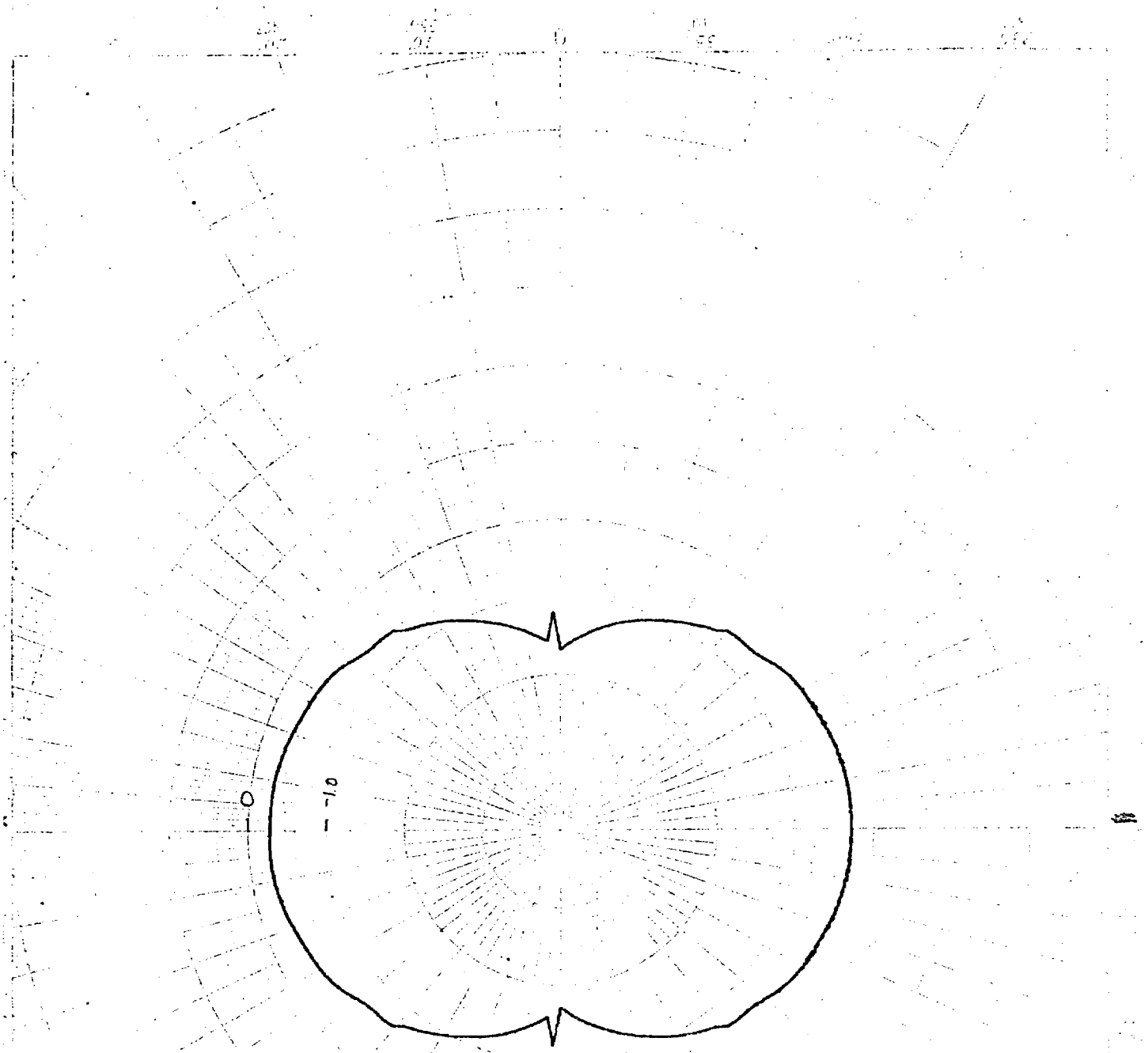

Figure 12. See caption Figure 11. Computed data E_ϕ, $\theta = 90°$

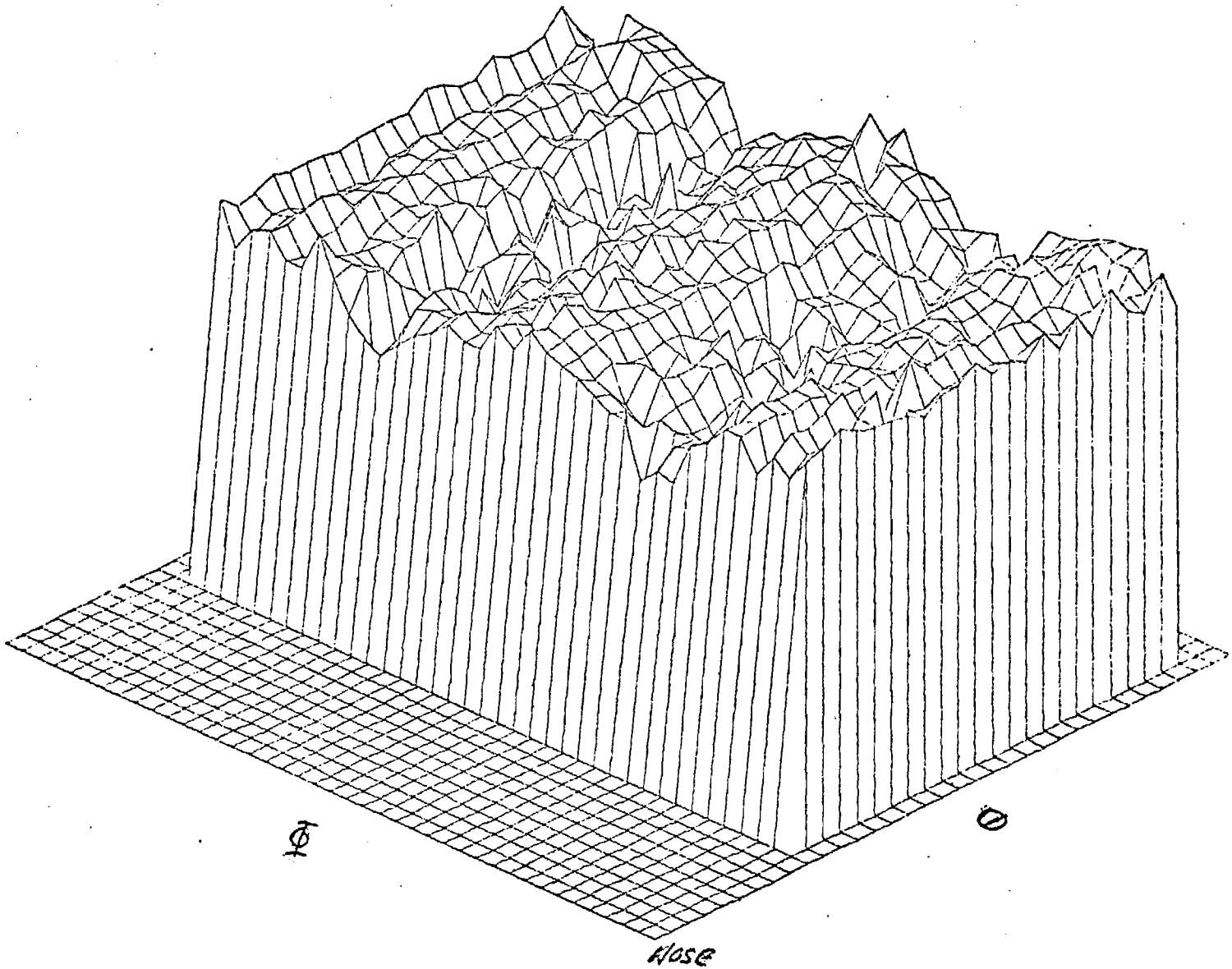

Figure 13. Measured radiation pattern, Vertical Polarization for TOU-X Scoring Antennas - scale model.

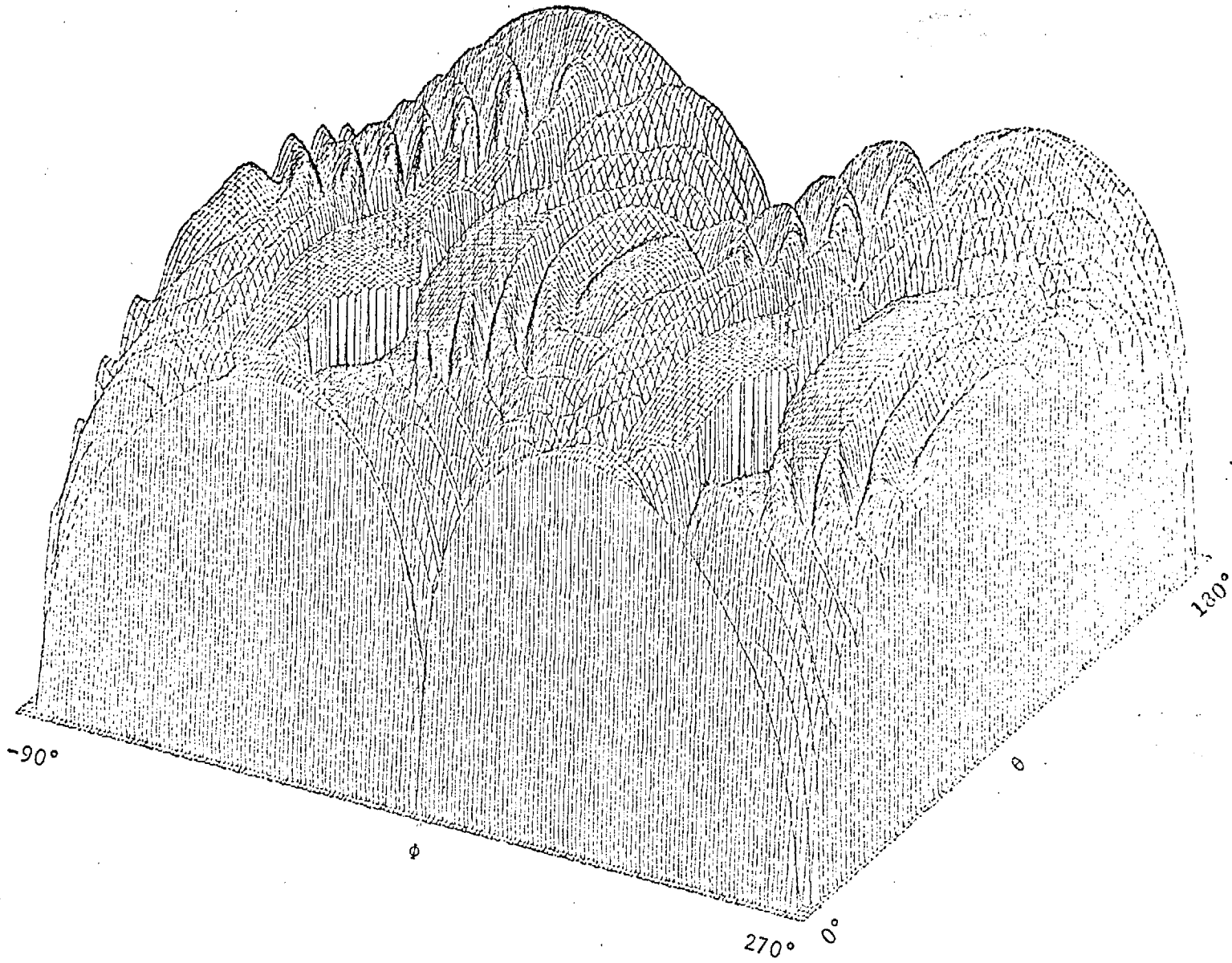

Figure 14. Calculated radiation pattern (E_Φ^2) for two pairs of crossed slots (positioned on top and bottom as indicated by ADTC) on a conducting right circular cylinder having the same diameter as the TDU-X target. Wing and pod blockage was included.

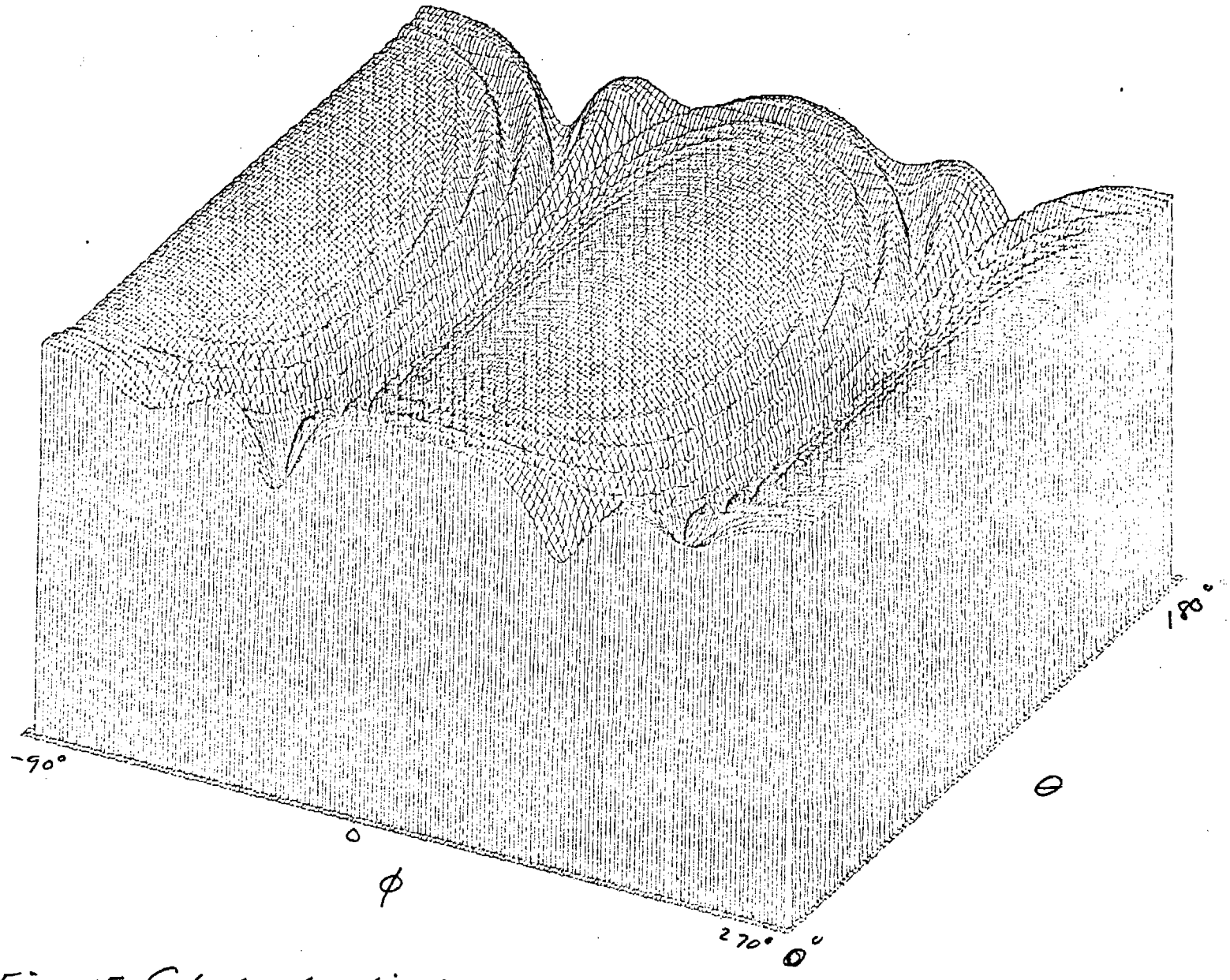

Figure 15. Calculated radiation pattern $(E_\theta)^2$ for two pairs of crossed slots positioned on BOMARC (right and left).

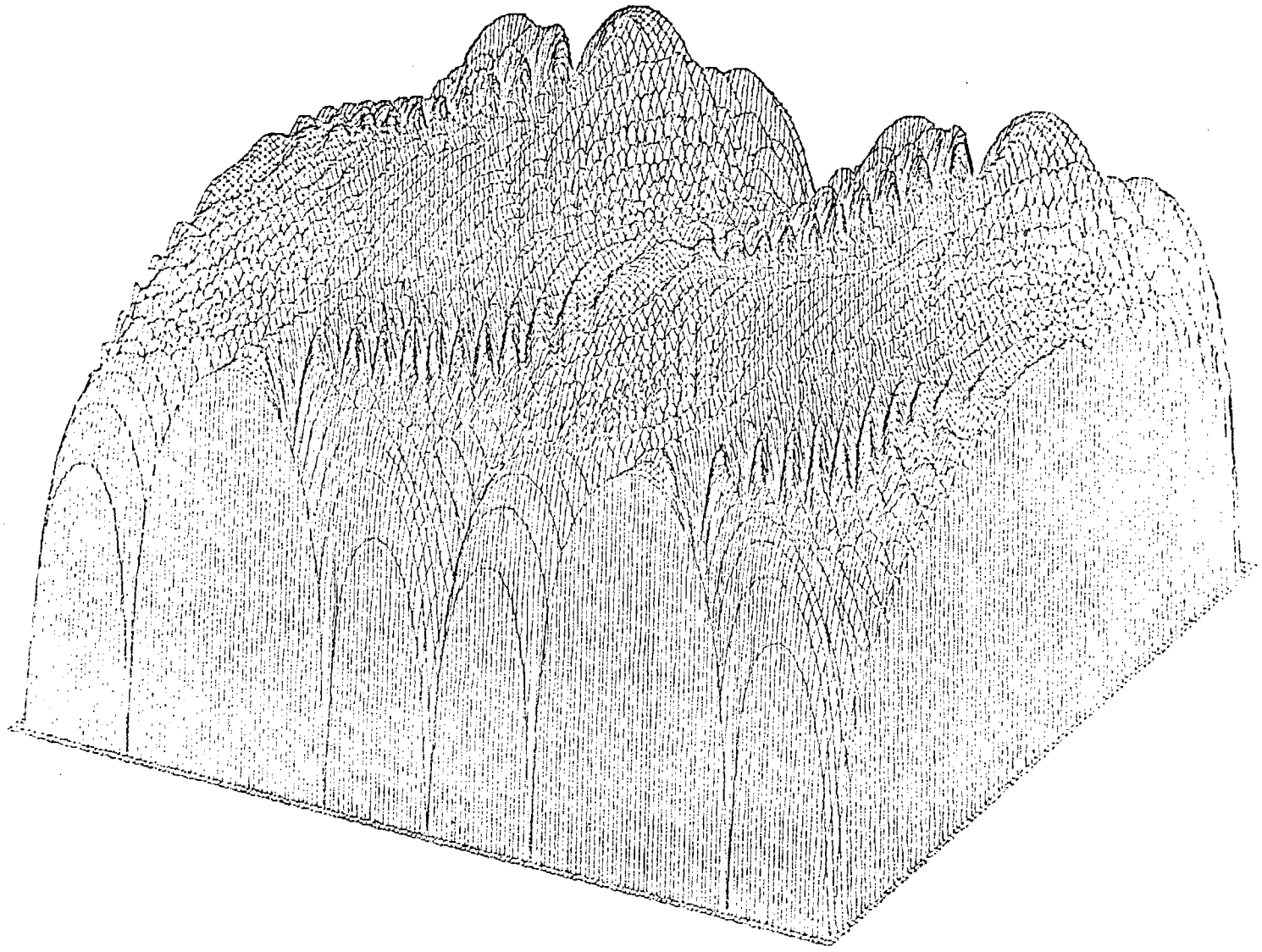

Figure 16. Calculated radiation pattern $(E_\phi)^2$ for two pairs of crossed slots positioned on BOMARC (right and left).

ENGINEERING EXPERIMENT STATION
Georgia Institute of Technology
Atlanta, Georgia 30332

ANTENNA PATTERN ANALYSIS FOR TARGET VEHICLES

Final Report
EES/GIT Project A-1780
TECHNICAL REPORT AFATL-TR-76-63

By
Harold E. Bassett, Charles E. Summers, and
James W. Cofer, Jr.

Prepared for

AIR FORCE ARMAMENT LABORATORY
AFATL/DLMQ
Eglin Air Force Base, Florida

Under
Contract F08635-76-C-0075

June 1976

ENGINEERING EXPERIMENT STATION
Georgia Institute of Technology
Atlanta, Georgia 30332

ANTENNA PATTERN ANALYSIS FOR TARGET VEHICLES

Final Report
EES/GIT Project A-1780
TECHNICAL REPORT AFATL-TR-76-63

By
Harold L. Bassett, Charles E. Summers, and
James W. Cofer, Jr.

Prepared for

AIR FORCE ARMAMENT LABORATORY
AFATL/DLMQ
Eglin Air Force Base, Florida

Under
Contract F08635-76-C-0075

June 1976

UNCLASSIFIED
SECURITY CLASSIFICATION OF THIS PAGE *(When Data Entered)*

REPORT DOCUMENTATION PAGE		READ INSTRUCTIONS BEFORE COMPLETING FORM
1. REPORT NUMBER AFATL-TR-76-63	2. GOVT ACCESSION NO.	3. RECIPIENT'S CATALOG NUMBER
4. TITLE *(and Subtitle)* ANTENNA PATTERN ANALYSIS FOR TARGET VEHICLES		5. TYPE OF REPORT & PERIOD COVERED Final Report 15 Sept. 1975-15 March 1976
		6. PERFORMING ORG. REPORT NUMBER EES/GIT A-1780-F
7. AUTHOR(s) Harold L. Bassett, Charles E. Summers, and James W. Cofer, Jr.		8. CONTRACT OR GRANT NUMBER(s) F08635-76-C-0075
9. PERFORMING ORGANIZATION NAME AND ADDRESS Engineering Experiment Station Georgia Institute of Technology Atlanta, GA 30332		10. PROGRAM ELEMENT, PROJECT, TASK AREA & WORK UNIT NUMBERS
11. CONTROLLING OFFICE NAME AND ADDRESS Air Force Armament Laboratory (DLMQ) ARMAMENT DEVELOPMENT AND TEST CENTER Eglin AFB, Florida 32542		12. REPORT DATE June 1976 13. NUMBER OF PAGES viii + 85
14. MONITORING AGENCY NAME & ADDRESS*(if different from Controlling Office)*		15. SECURITY CLASS. *(of this report)* Unclassified 15a. DECLASSIFICATION/DOWNGRADING SCHEDULE

16. DISTRIBUTION STATEMENT *(of this Report)*

Distribution limited to U. S. Government agencies only; this report documents test and evaluation; distribution limitation applied June 1973. Other requests for this document must be referred to the Air Force Armament Laboratory (DLMQ), Eglin Air Force Base, Florida 32542.

17. DISTRIBUTION STATEMENT *(of the abstract entered in Block 20, if different from Report)*

18. SUPPLEMENTARY NOTES

Available in DDC

19. KEY WORDS *(Continue on reverse side if necessary and identify by block number)*

Target Vehicles	Scoring Antennas	BQM-34A
Antennas	DIGIDOPs	BOMARC
Pattern Analysis	Scale Model	

20. ABSTRACT *(Continue on reverse side if necessary and identify by block number)*

This report contains a description of the boundary value computational method used in predicting the radiation pattern coverage for three target vehicles: TDU-X tow target, BQM-34A drone, and the BOMARC missile. Included are the predicted patterns of the scoring antennas for the three targets and all the antenna systems for the TDU-X tow target.

Scale model radiation patterns were measured and used to verify the computed patterns. It was concluded that the boundary value computational method was an effective method for determining the location of antennas on the targets

DD FORM 1 JAN 73 1473 EDITION OF 1 NOV 65 IS OBSOLETE

UNCLASSIFIED
SECURITY CLASSIFICATION OF THIS PAGE *(When Data Entered)*

Block 20.

and for obtaining an estimate of the percent coverage that will be obtained.

PREFACE

This report was prepared by personnel of the Engineering Experiment Station (EES) of the Georgia Institute of Technology, Atlanta, Georgia, 30332, under Contract F08635-76-C-0075 for the Air Force Armament Laboratory, Eglin Air Force Base, Florida, 32542. This task was under the general supervision of Mr. H. D. Harris, Chief, DLMQ, and Mr. F. Crumly, Group Leader, DLMQ. Mr. Glenn Hatcher, DLMQ, served as the Technical Program Monitor.

Report authors are Messrs. Harold L. Bassett, Charles E. Summers, and James W. Cofer, Jr., who are members of the Systems and Techniques Laboratory, Radar Applications Division of EES. This work was designated as EES Project A-1780 with Messrs. Bassett and Cofer serving as Co-Project Directors. The effective dates of the technical effort were from 15 September 1975 through 15 March 1976.

This technical report has been reviewed and is approved for publication.

FOR THE COMMANDER

TABLE OF CONTENTS

LIST OF FIGURES

LIST OF FIGURES
CONTINUED

LIST OF FIGURES
CONTINUED

LIST OF FIGURES
CONTINUED

LIST OF FIGURES
CONTINUED

LIST OF FIGURES
CONTINUED

SECTION I
INTRODUCTION

1. BACKGROUND

Under Contract F08635-76-C-0075 with the Armament Laboratory at Eglin Air Force Base, Florida, EES personnel undertook a program to analyze the radiation properties of several antenna systems located on three (TDU-X, BQM-34A, and BOMARC) target-type vehicles. Both computational and experimental investigations were conducted. Three basic mathematical approaches were considered: (1) boundary value (2) geometrical theory of diffraction, and (3) moment methods.

It was desired to determine if the boundary value computational method was sufficient for use in locating the antennas on the targets to achieve required antenna pattern coverage characteristics. This technique is simple and inexpensive as compared to the more complex geometrical theory of diffraction technique (G.T.D.) and the moment methods. Scale model measurements were made on each target in order to validate the computer data.

The TDU-X tow target is a large center of gravity towed vehicle that has the payload capacity to carry IRCM/ECM devices for airborne testing. The target has subsystems to support the IRCM/ECM devices. These subsystems are infrared/radar signatures, scoring, command receiver, telemetry and beacons. Those subsystems that radiate or receive a signal have unique antenna pattern requirements.

The major work presented is that of the antenna systems on the TDU-X tow target. Computer techniques were utilized to model the TDU-X tow target and to calculate antenna radiation pattern coverage for the antenna systems. A scale model of the target was fabricated and the computed patterns were verified by actual measurements.

The BQM-34A drone is the utility target for three services. The augmentation and scoring equipment vary according to the user requirements. A recent requirement is to have radar augmentation and scoring co-located on the wing tip. This was one of the driving requirements for this particular contractual effort.

The BOMARC is an interceptor missile that has been converted to a target. The BOMARC is a large target vehicle that has a typical altitude speed range of 72,000 feet at 2.72 Mach. The primary zone of attack is

the frontal zone; thus, the scoring antennas must be located in the forward half of the vehicle.

Only the DIGIDOPS scoring antenna radiation pattern coverage was calculated for the BQM-34A drone and the BOMARC interceptor. These patterns were also verified by scale model measurements.

Of significance is the fact that computer modeling techniques have become sufficiently sophisticated to be used in determining the location of antennas on a target for particular area coverages. Comparsions between the computed data and the scale model measured data bear this out.

2. SUMMARY OF TASKS

The effort was divided into three general tasks, one for each target vehicle. Antenna locations were analyzed by computer and by scale models for the three targets to determine optimum antenna mounting locations for the required pattern coverage.

a. TDU-X Tow Target

Antenna radiation pattern analyses were performed on five antenna systems:

1. DIGIDOPS scoring antennas
2. Command receiver antenna
3. Telemetry antenna
4. X-L Band augmentation antennas
5. and G-Band beacon antenna.

The DIGIDOPS scoring systems operate at 1775 MHz, and although it was desired to have complete spherical coverage for this antenna system, it was required that the antennas should be located to provide complete coverage for the rear hemisphere and for this coverage to extend toward the forward sector as far as possible.

The command receiver operates at 425 MHz, and lower hemisphere pattern coverage was desired. The command receiver antenna is a flush mounted tuned cavity.

The telemetry transmitter operates in the L-Band frequency region and the desired pattern coverage was omni-directional with suggested mounting on the lower part of the center fuselage.

The L-Band system of the X-L Band radar augmentation will be used in tracking the target by ground based radar, and a lower hemisphere omni-directional antenna pattern coverage was required. The X-Band portion of this system provides radar augmentation for airborne tracking radar, and it was required that this antenna system provide coverage toward the stern.

The G-Band beacon is also used to ground track the target, and it was required that the antenna pattern provide lower hemisphere coverage. This system operates at 5650 MHz and at 5720 MHz.

b. BOMARC Missile

Antenna radiation pattern analyses were performed on the DIGIDOPS scoring antenna operating at 1775 MHz. The primary zone of interest was the front hemisphere with total hemispherical coverage desired.

c. BQM-34 Drone Augmentation Pod

The DIGIDOPS scoring and the X-Band augmentation systems will share the same pod. Radiation pattern analyses were performed for antennas mounted on the wing-tip pod. Each pod-mounted scoring antenna was to provide hemispherical radiation pattern coverage toward the side of the drone on which the antenna was mounted.

SECTION II

TECHNICAL APPROACH

This section of the report contains a description of the computer modeling technique and the scale model measurements completed by the Engineering Experiment Station at Georgia Tech on this program for the antenna systems of interest.

1. INITIAL ANTENNA LOCATIONS

Because of the radiation pattern coverage requirements of the TDU-X telemetry, command, radar augmentation and G-Band beacon, these particular antenna systems were located on the target as indicated in Figure 1. Computer analyses and scale model radiation patterns were completed for these particular antenna systems and these data are presented in a later section of this report.

After considerable discussion it was decided to mount one of the scoring antennas on the bottom of the TDU-X fuselage and the other on the fuselage top but slightly offset from the bottom antenna along the fuselage axis. Varying offset distances were then modeled before the final locations were fixed. This is discussed in the following section on computer modeling of two target antenna patterns.

Based on past performance and location of the scoring antennas, these were located on the outboard sides of the BQM-34A wing pods for the computer analysis and scale model measurements. For the BOMARC missile, the scoring antennas were mounted on the right and left side of the fuselage forward of the wings.

The antenna systems were modeled for the locations as described above and the majority of the computed data were verified by scale model measurements.

2. COMPUTER MODELING TECHNIQUES

a. TDU-X DIGIDOPS Scoring Antenna System

(1) Mathematical Model

The computer model adopted was that resulting from a solution to the wave equation (subject to the appropriate boundary conditions) for radiation from rectangular slots on an infinite cylinder. This approach

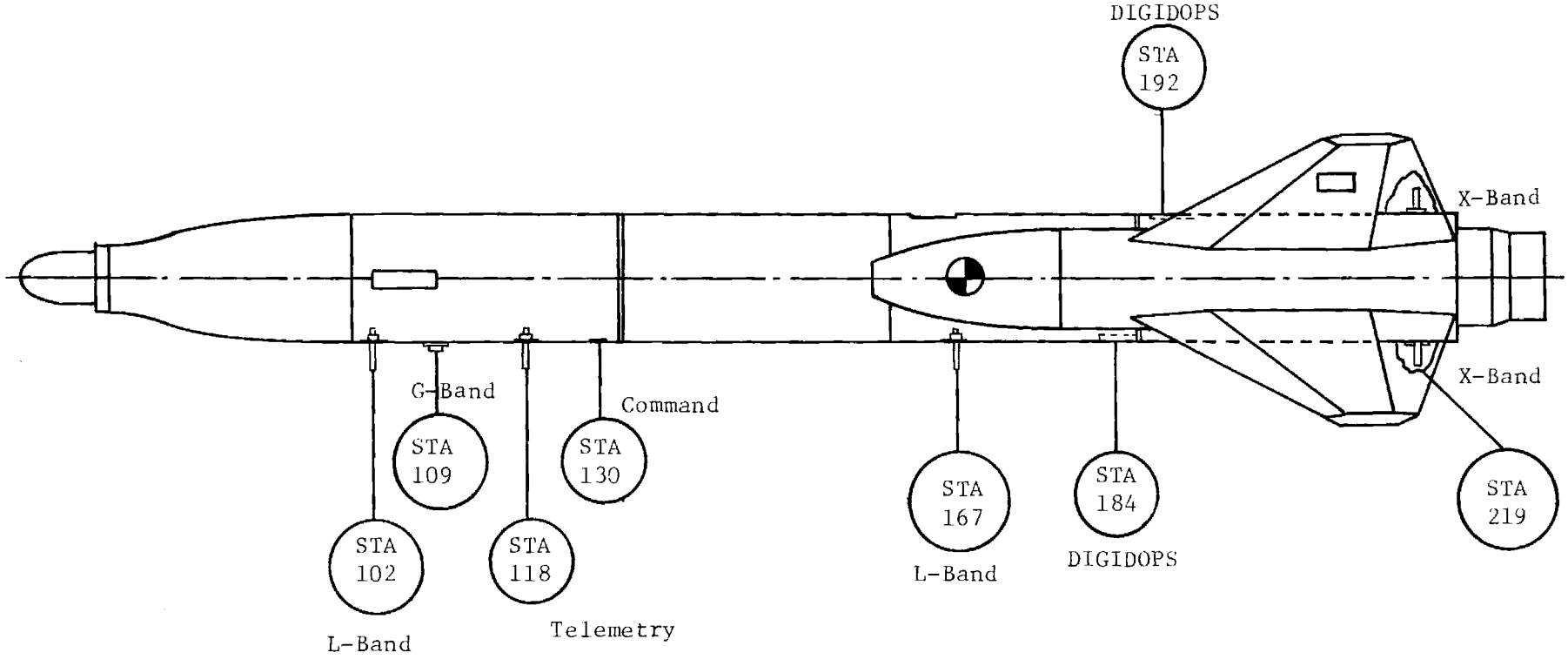

Figure 1. Antenna Locations on TDU-X Tow Target

did not take into account the fact that the cylinders were not infinite (end effects) and the problem of scattering from the wings (wing blockage was considered). The DIGIDOPS antenna consists of two slots, one axial and one circumferential, mounted together in a "T" configuration. The antenna may be considered to be the superposition of two separate antennas (no mutual coupling).

Many authors have discussed the modeling of axial and circumferential slots on cylindrical surfaces. The basic approach used here is that of Silver and Saunders [1],* which is an approximate form of the result obtained by solving the boundary value problem. The far zone fields of the slots can be written for the axial slot as (see Figure 2 for geometric parameters)

$$E_\Phi = \frac{e^{-jkr}}{\pi r} \int_{z_1}^{z_2} G_A(z) e^{jkz \cos\theta} dz \left[\sum_{n=\infty}^{\infty} \frac{j^n e^{-jn\Phi}}{H_n^{(2)'}(ka \sin\theta)} \frac{1}{2\pi} \int_{-\beta/2}^{\beta/2} F_A(\Phi) e^{jn\Phi} d\Phi \right],$$

$$E_\theta = 0, \qquad (1)$$

where the electric field across the slot is characterized by,

$$G_A(z) = \cos\left(\frac{\pi z}{a}\right), \qquad (2)$$

$$F_A(\phi) = 1 .$$

Integrating the equations where necessary the Φ-component of the axial slot becomes,

$$E_\Phi = \frac{e^{-jkr}}{r} \frac{\cos\left(\frac{\pi}{2} \cos\theta\right)}{\sin\theta} \frac{1}{\frac{\pi}{2} x} \sum_{n=0}^{\infty} \frac{e_n j^n \cos n\Phi}{H_n^{(2)'}(ka \sin\theta)} \frac{\sin\left(\frac{n\beta}{2}\right)}{\left(\frac{n\beta}{2}\right)}, \qquad (3)$$

$e_n = 1, \quad n = 0,$

$e_n = 2, \quad n \neq 0, \quad x = ka \sin\theta.$

*References are indicated by [] and are included as Section V.

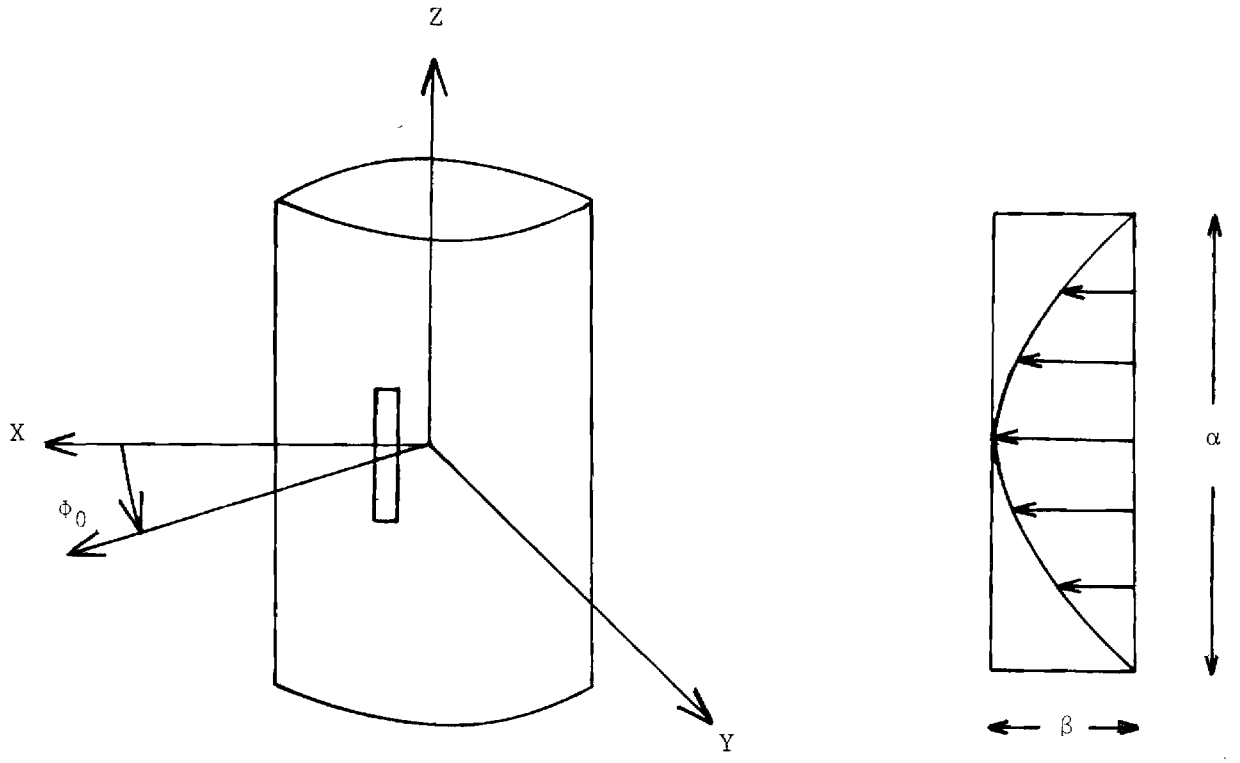

Figure 2. Geometry for Axial Slot on a Cylinder

Patterns were generated for one axial slot located at $\theta = 90^{o}$, $\Phi = 90^{o}$ on a 7-inch radius cylinder. The pattern for this slot is shown in Figure 3. The slot dimensions used were 1.0-inch by 3.327-inch. This plot is a three dimensional one with the power pattern shown as a function of the variables θ and Φ. The height of the surface above the floor is an indication of the power intensity along a particular direction θ, Φ. Care should be exercised when interpreting such plots since this coordinate transformation implies equal weighting of the pole and equator regions of the farfield sphere; however, plots of this type are useful for locating regions of low coverage.

The circumferential slot, unlike the axial, has both a θ and a ϕ component. The equations describing the two components for a circumferential slot are [2],

$$E_{\theta} = \frac{-je^{-jkr}}{\pi r} \int_{z_1}^{z_2} G_c(z) e^{jkz \cos\theta} dz \left[\sum_{n=-\infty}^{\infty} \frac{j^n e^{-jn\Phi}}{\sin\theta \, H_n^{(2)}(ka \sin\theta)} \frac{1}{2\pi} \int_{\beta_1}^{\beta_2} F_c(\beta) e^{jn\beta} d\beta \right], \tag{4}$$

$$E_{\Phi} = \frac{e^{-jkr}}{\pi r} \int_{z_1}^{z_2} G_c(z) e^{jkz \cos\theta} dz \frac{\cot\theta}{ka \sin\theta} \left[\sum_{n=-\infty}^{\infty} \frac{nj^n e^{-jn\Phi}}{H_n^{(2)'}(ka \sin\theta)} \frac{1}{2\pi} \int_{\beta_1}^{\beta_2} F_c(\beta) e^{jn\beta} d\beta \right], \tag{5}$$

where the electric field across the slot is given by

$$G_c(z) = 1,$$

$$F_c(\Phi) = \cos\left(\frac{\pi\Phi}{\beta}\right), \tag{6}$$

and the geometric parameters are defined in Figure 4.

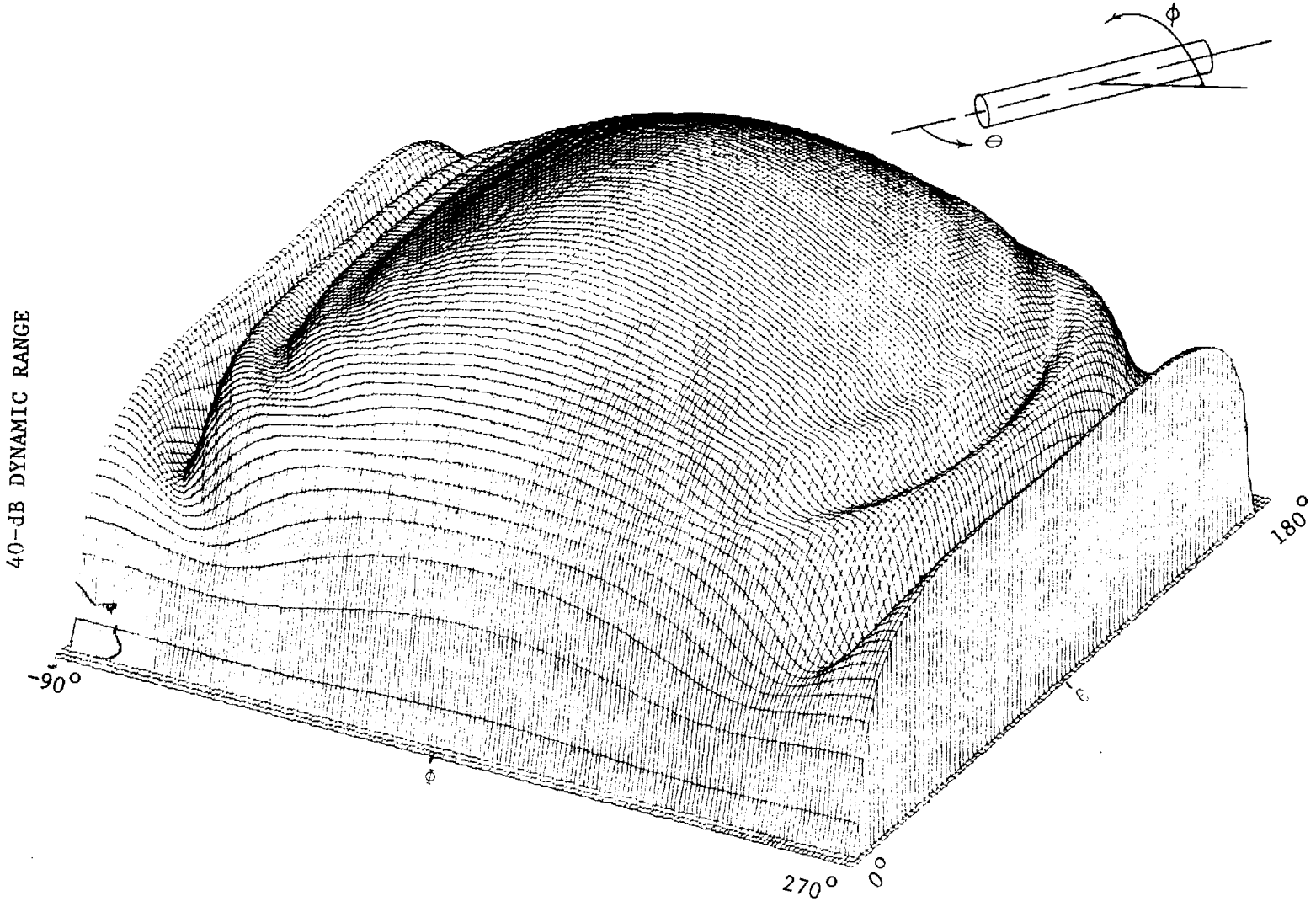

Figure 3. Calculated Radiation Pattern (E_{ϕ}^{2}) for a Single Axial Slot on a Conducting Right Circular Cylinder Having the Same Diameter as the TDU-X Target. Wing and Pod Blockage Was Not Included

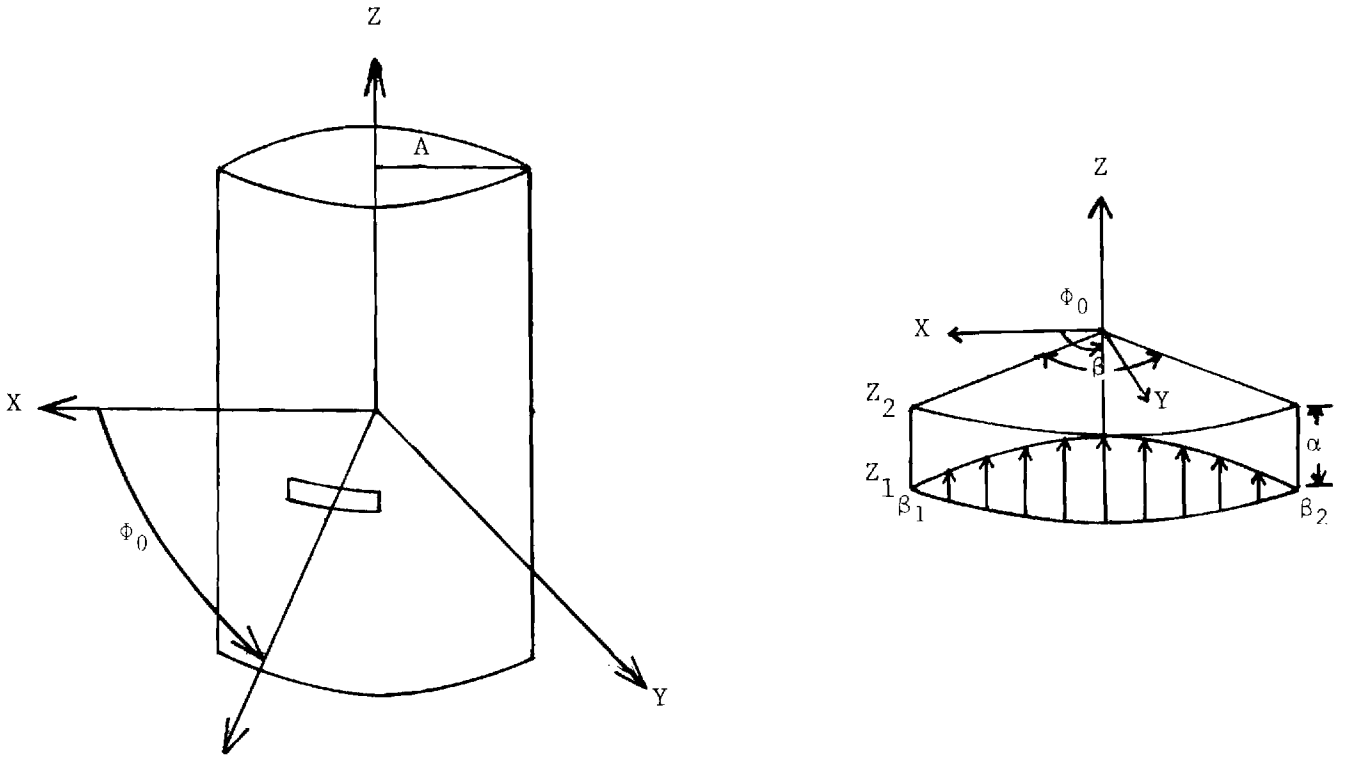

Figure 4. Geometry for Circumferential Slot on a Cylinder

Performing the integration as before, the following useful equations are obtained.

$$E_\theta = \frac{-je^{-jkr}}{\pi r} \left(\frac{a \sin [k(\frac{a}{2})\cos\theta]}{[k(\frac{a}{2})\cos\theta]} \right) \sum_{n=0}^{\infty} \frac{e_n j^n \cos n\Phi}{\sin\theta \, H_n^{(2)}(ka \sin\theta)} \left(\frac{1}{\beta} \frac{\cos(\frac{n\beta}{2})}{(\frac{\pi}{\beta})^2 - n^2} \right) \quad (7)$$

$$E_\Phi = \frac{-2je^{-jkr}}{\pi r} \left(\frac{a \sin[k(\frac{a}{2})\cos\theta]}{[k(\frac{a}{2})\cos\theta]} \right) \frac{\cot\theta}{ka \sin\theta} \sum_{n=0}^{\infty} \frac{nj^n \sin n\Phi}{Hn^{(2)'}(ka \sin\theta)} \left(\frac{1}{\beta} \frac{\cos(\frac{n\beta}{2})}{(\frac{\pi}{\beta})^2 - n^2} \right) \quad (8)$$

These equations were programmed on a digital computer to generate the pattern of a circumferential slot (see Figures 5,6). For small values of θ, the above equations for E are invalid; therefore, for $\theta = 0^o$, the pattern was assumed to have the same value as for $\theta = 2^o$. The same dimensions were used for the circumferential slots as for the axial.

The complete DIGIDOPS antenna pattern was produced by a superposition of the axial and circumferential patterns. The basic equation used to add the two patterns was

$$E_t(\theta,\Phi) = E_a(\theta,\Phi)e^{-j\Psi_1} + E_c(\theta,\Phi)e^{-j\Psi_2} \quad (9)$$

where a and c denote axial and circumferential patterns, respectively, and Ψ_1 and Ψ_2 are the absolute phases of the two slot patterns at the farfield point (i.e., total phase equal to initial phase plus path length dependence.

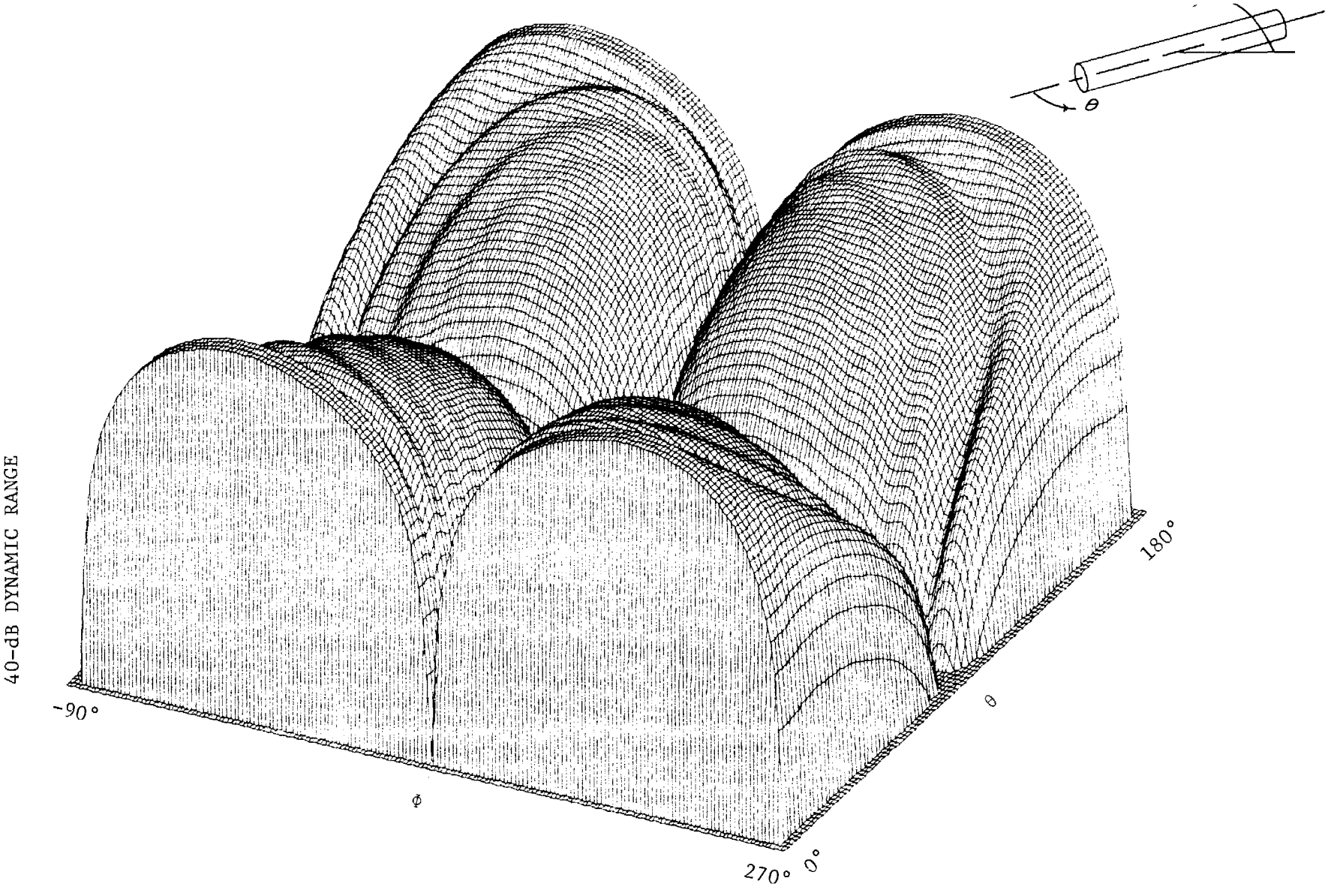

Figure 5. Calculated Radiation Pattern (E_{Φ}^{2}) for one Circumferential Slot (Positioned on Top) on a Conducting Right Circular Cylinder Having the Same Diameter as the TDU-X Target. Wing and Pod Blockage Was Not Included

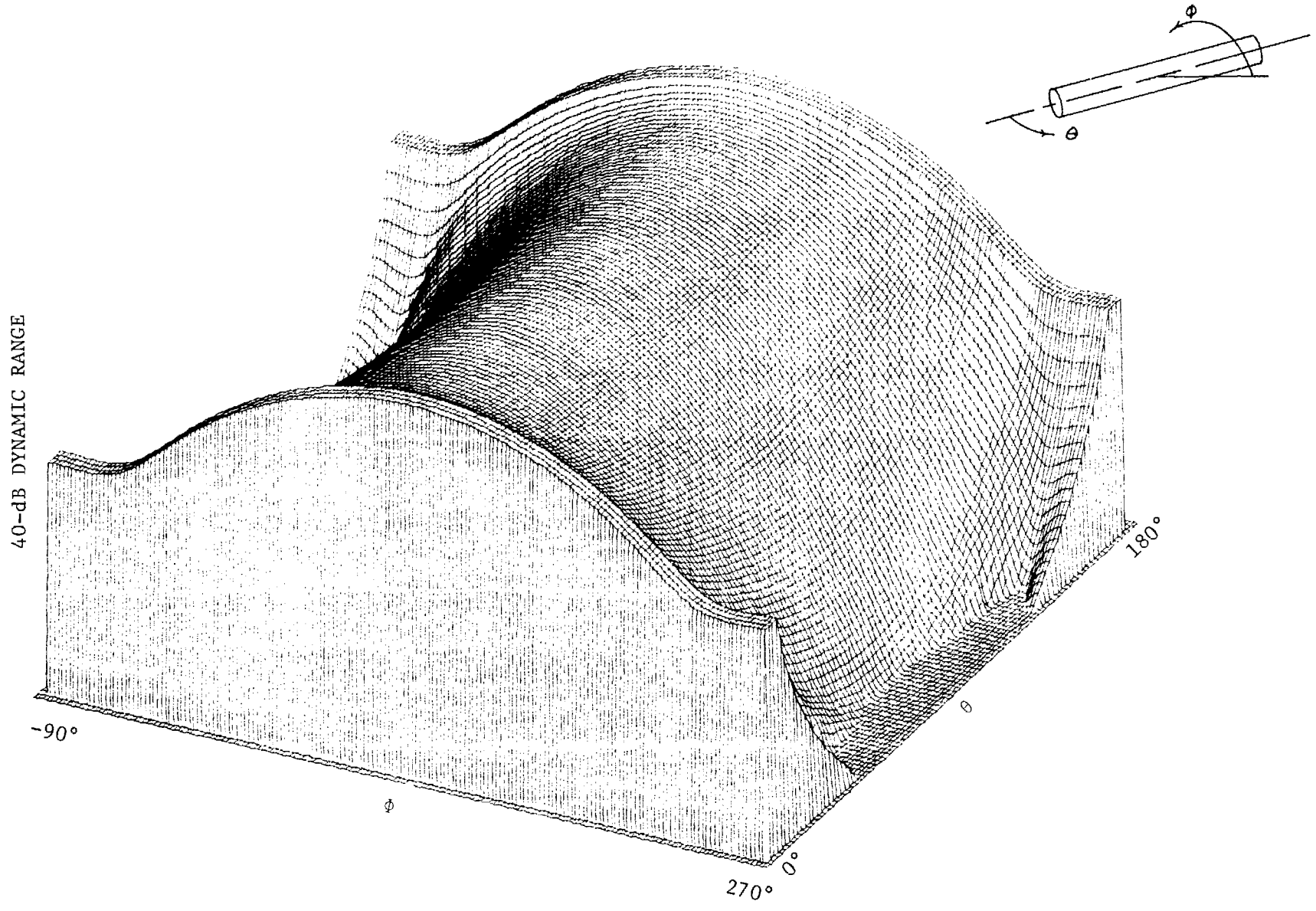

Figure 6. Calculated Radiation Pattern (E_0^2) for One Circumferential Slot (Positioned on Top) on a Conducting Right Circular Cylinder Having the Same Diameter as the TDU-X Target. Wing and Pod Blockage Was Not Included

The current configuration (for the models seen at Tyndall Air Force Base) for the two DIGIDOPS antennas is shown in Figures 7 and 8. The spacing along the z-axis between the center of the two antennas in 8 inches. Patterns were calculated for the case of two axial antennas, one on top of the cylinder ($\Phi = 90^{o}$) and one on the bottom ($\Phi = -90^{o}$) with the spacing along the z-axis as 7.0 inches. This pattern is demonstrated three dimensionally in Figure 9. The E_{ϕ}^{2} pattern for one crossed pair of slots on the cylinder was calculated and shown in Figure 10. The total power pattern for the complete system with two DIGIDOPS antennas is given in Figure 11.

The spacing between the DIGIDOPS antennas was varied in steps of $\lambda/4$ from 0 to $\lambda/2$ along the z-axis. The patterns for the antennas spaced zero are given in Figures 12, 13, and 14. The patterns for the antennas spaced $\lambda/4$ are given in Figures 15, 16, and 17. The patterns for the antennas spaced $\lambda/2$ are given in Figures 18, 19, and 20. The first of the set of three patterns in each group is the E_{θ}^{2} component. The second is the E_{ϕ}^{2} component, while the third is the total power ($E_{\theta}^{2} + E_{\phi}^{2}$). The plots show that there was no significant change in the coverage for the three spacings.

(2) Wing Effects

Blockage for the TDU-X DIGIDOPS antennas was taken into account by deriving an angular mask behind which the antenna patterns were set to zero. This model assumes no forward or back scattering from the wings and is sufficient to show the effect of the wings in coverage.

A blockage matrix was drawn up so that the blockage as a function of θ and ϕ could be entered into the computer analysis. This matrix was specified in 2-degree increments in θ and ϕ.

The blockage matrix for an antenna located above the wings ($\Phi = 90^{o}$) is given in Figure 21. The shaded areas indicate the angles at which the pattern is set to zero. An example of the effect of the blockage on a single axial slot located at $\Phi = 90^{o}$ is given in Figure 22.

The blockage matrix for an antenna located below the wings ($\Phi = -90^{o}$) is given in Figure 23. In this figure, as in the previous matrix diagram, the shaded areas indicate the angles at which the pattern is set to zero. An example of the effect of this blockage on a single axial slot at $\Phi = -90^{o}$ is given in Figure 24.

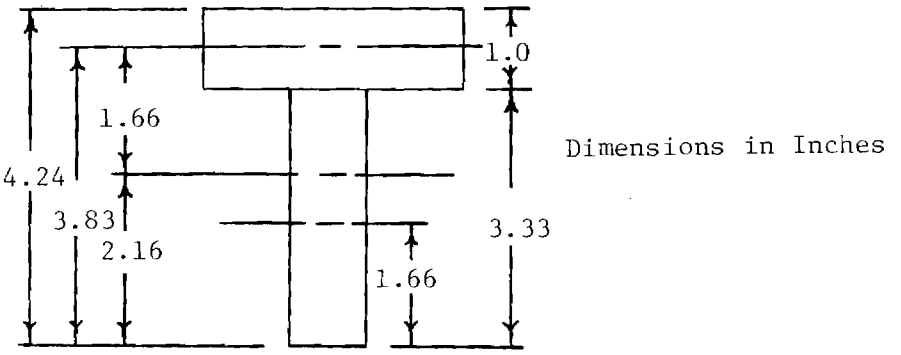

Figure 7. DIGIDOPS Scoring Antenna Dual Cavity-Backed Slot Configuration

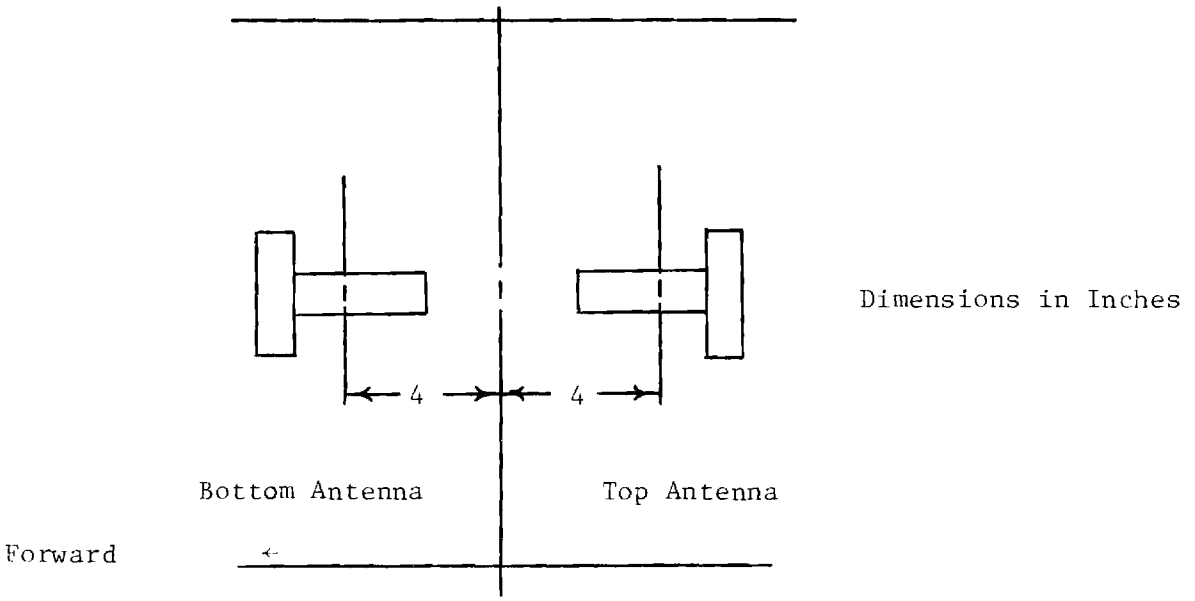

Figure 8. Displacement Between Top and Bottom TDU-X Scoring Antennas

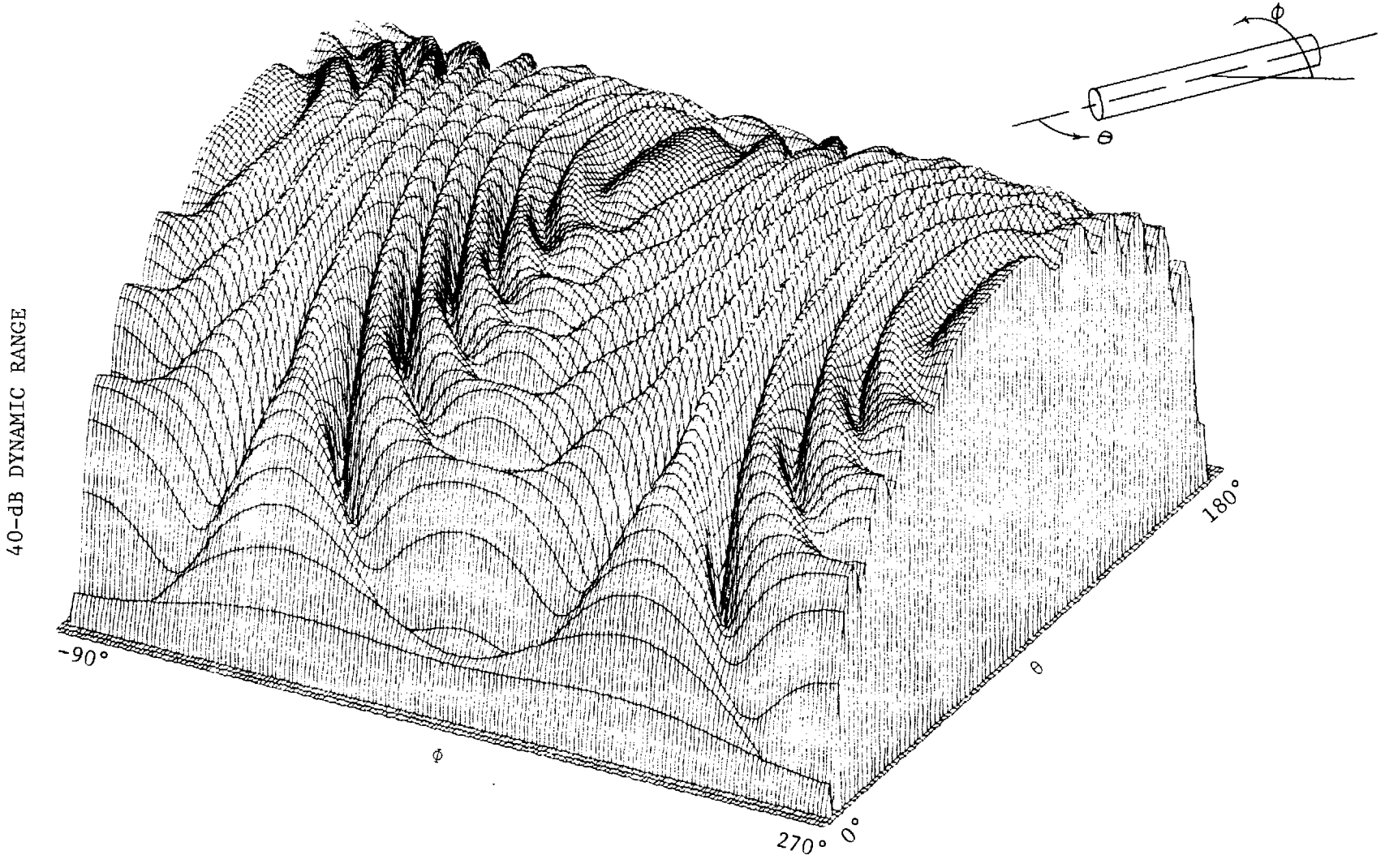

Figure 9. Calculated Radiation Pattern (E_{ϕ}^{2}) for Two Axial Slots (Positioned on Top and Bottom as Indicated by AFATL) on a Conducting Right Circular Cylinder Having the Same Diameter as the TDU-X Target. Wing and Pod Blockage Was Not Included

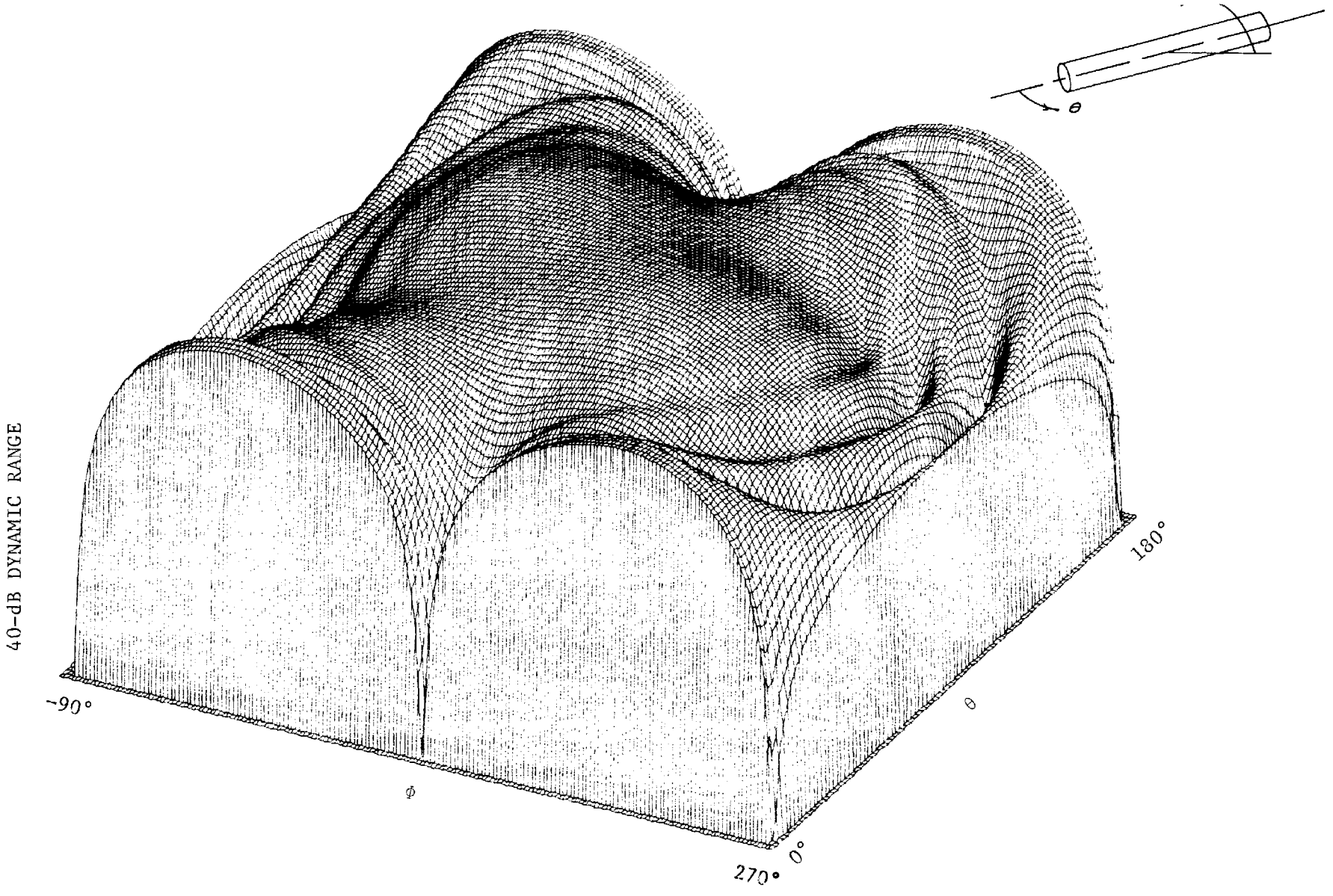

Figure 10. Calculated Radiation Pattern (E_Φ^2) for One Pair of Crossed Slots (Positioned on Top) on a Conducting Right Circular Cylinder Having the Same Diameter as the TDU-X Target. Wing and Pod Blockage Was Not Included

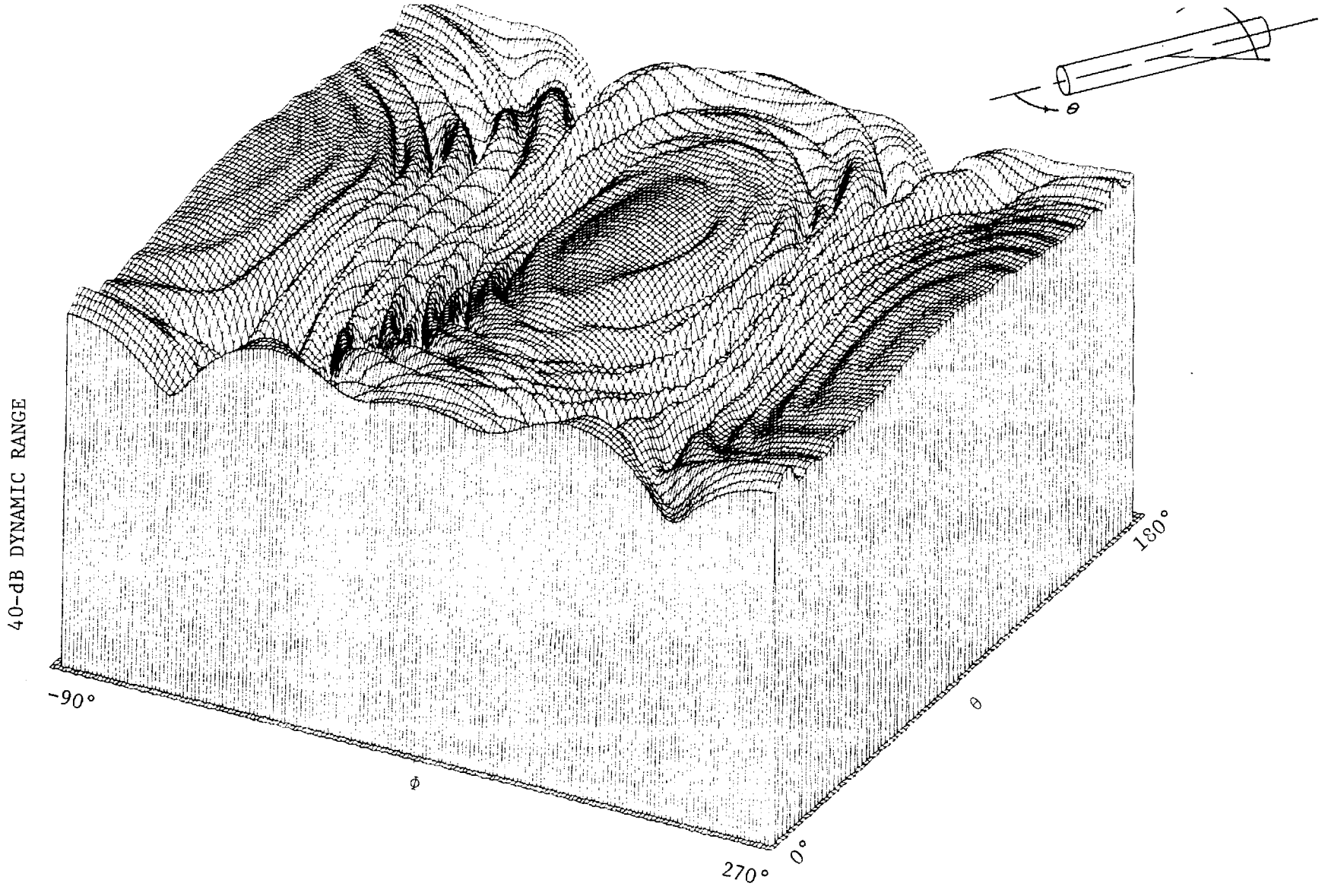

Figure 11. Calculated Radiation Pattern ($E_\theta^2 + E_\phi^2$) for Two Pairs of Crossed Slots (Positioned on Top and Bottom as Indicated by AFATL) on a Conducting Right Circular Cylinder Having the Same Diameter as the TDU-X Target. Wing and Pod Blockage Was Not Included

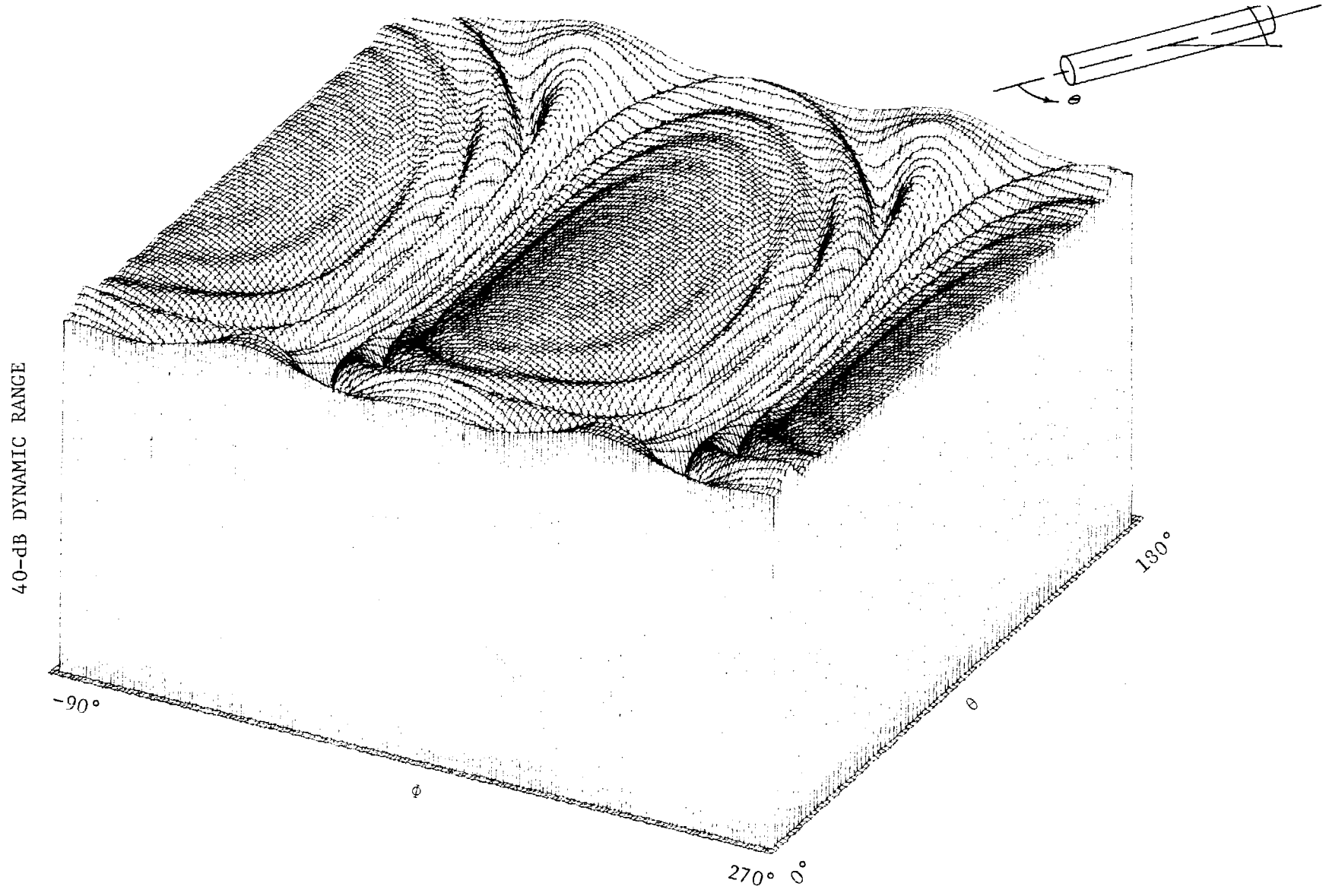

Figure 12. Calculated Radiation Pattern (E_θ^2) for Two Pairs of Crossed Slots (Positioned on Top and Bottom as Indicated by AFATL) on a Conducting Right Circular Cylinder Having the Same Diameter as the TDU-X Target. Wing and Pod Blockage Was Not Included. (Zero Spacing Between Top and Bottom Antennas)

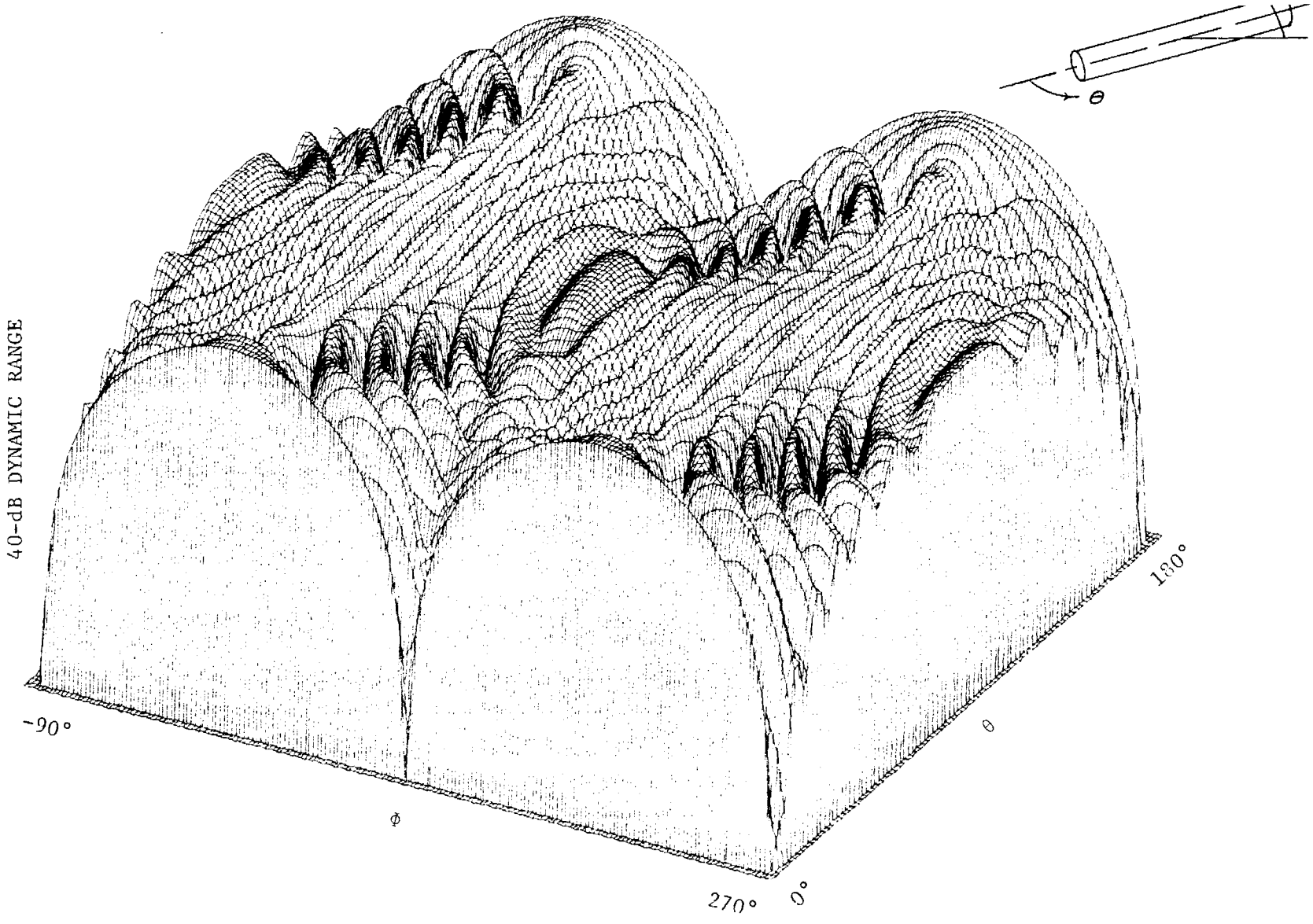

Figure 13. Calculated Radiation Pattern (E_{Φ}^2) for Two Pairs of Crossed Slots (Positioned on Top and Bottom as Indicated by AFATL) on a Conducting Right Circular Cylinder Having the Same Diameter as the TDU-X Target. Wing and Pod Blockage Was Not Included. (Zero Spacing Between Top and Bottom Antennas)

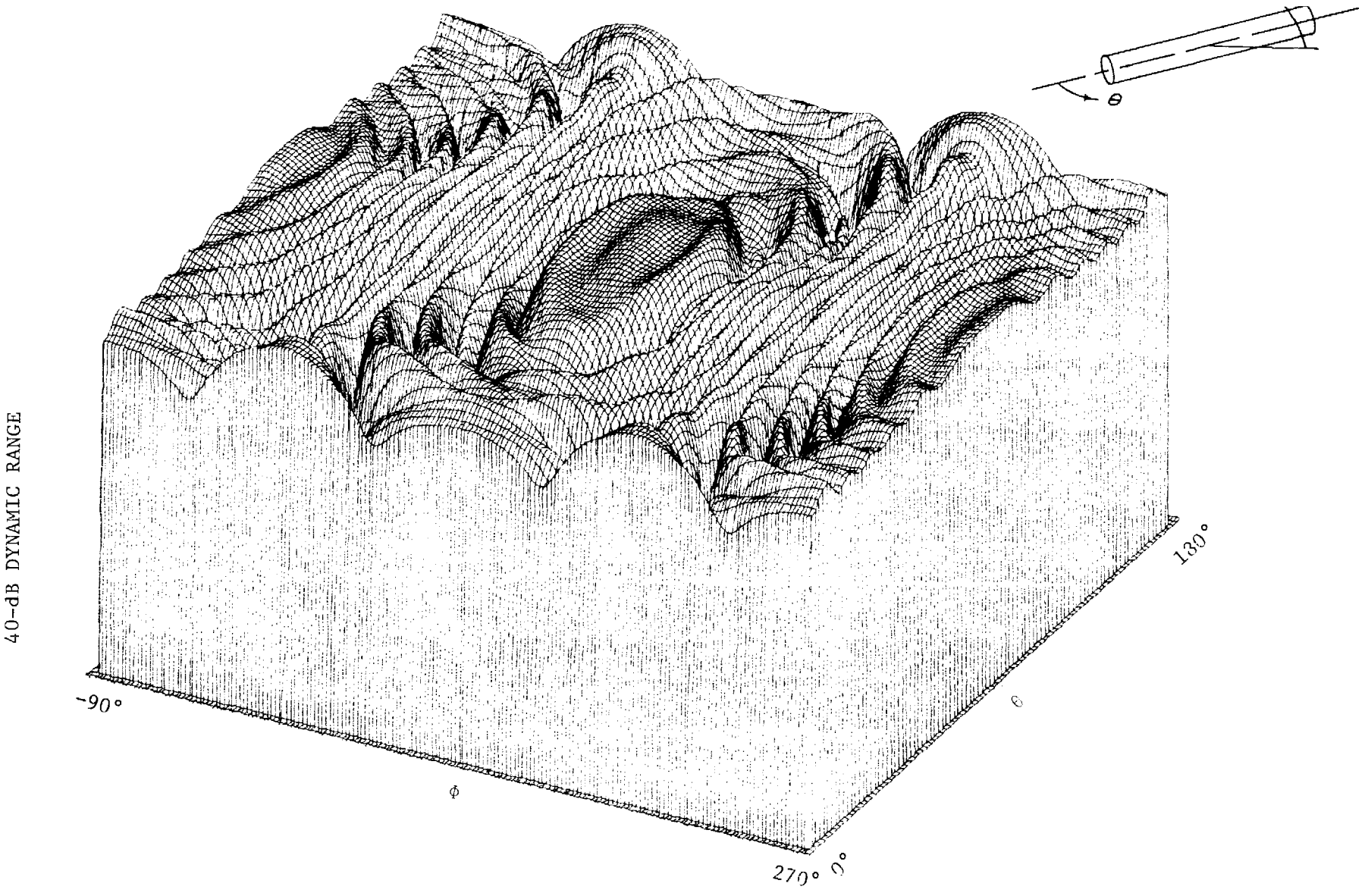

Figure 14. Calculated Radiation Pattern ($E_\theta^2 + E_\phi^2$) for Two Pairs of Crossed Slots (Positioned on Top and Bottom as Indicated by AFATL) on a Conducting Right Circular Cylinder Having the Same Diameter as the TDU-X Target. Wing and Pod Blockage Was Not Included. (Zero Spacing Between Top and Bottom Antennas)

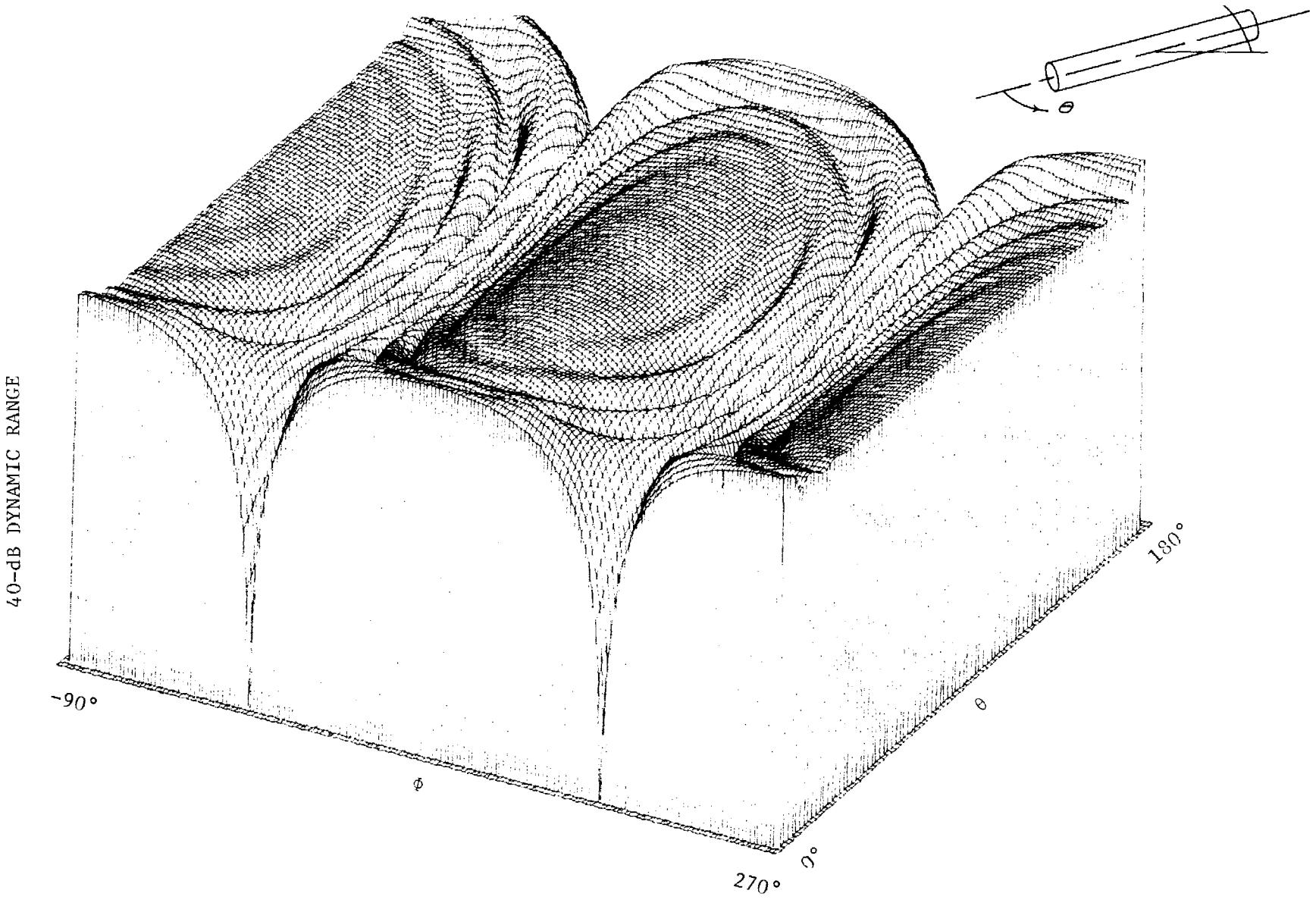

Figure 15. Calculated Radiation Pattern (E_θ^2) for Two Pairs of Crossed Slots (Positioned on Top and Bottom as Indicated by AFATL) on a Conducting Right Circular Cylinder Having the Same Diameter as the TDU-X Target. Wing and Pod Blockage Was Not Included ($\lambda/4$ Spacing Between Top and Bottom Antennas)

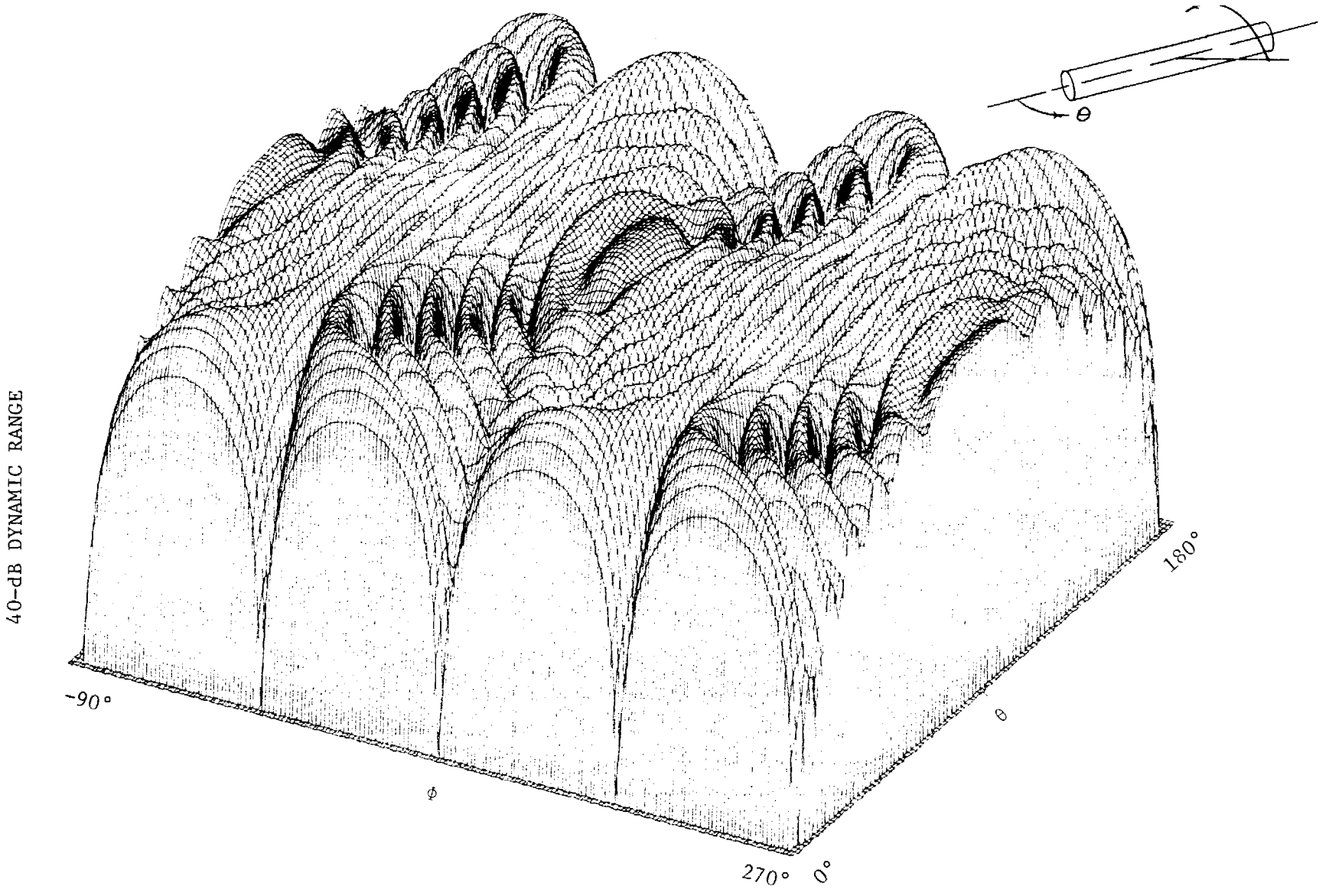

Figure 16. Calculated Radiation Pattern (E_{ϕ}^{2}) for Two Pairs of Crossed Slots (Positioned on Top and Bottom as Indicated by AFATL) on a Conducting Right Circular Cylinder Having the Same Diameter as the TDU-X Target. Wing and Pod Blockage Was Not Included. ($\lambda/4$ Spacing Between Top and Bottom Antennas)

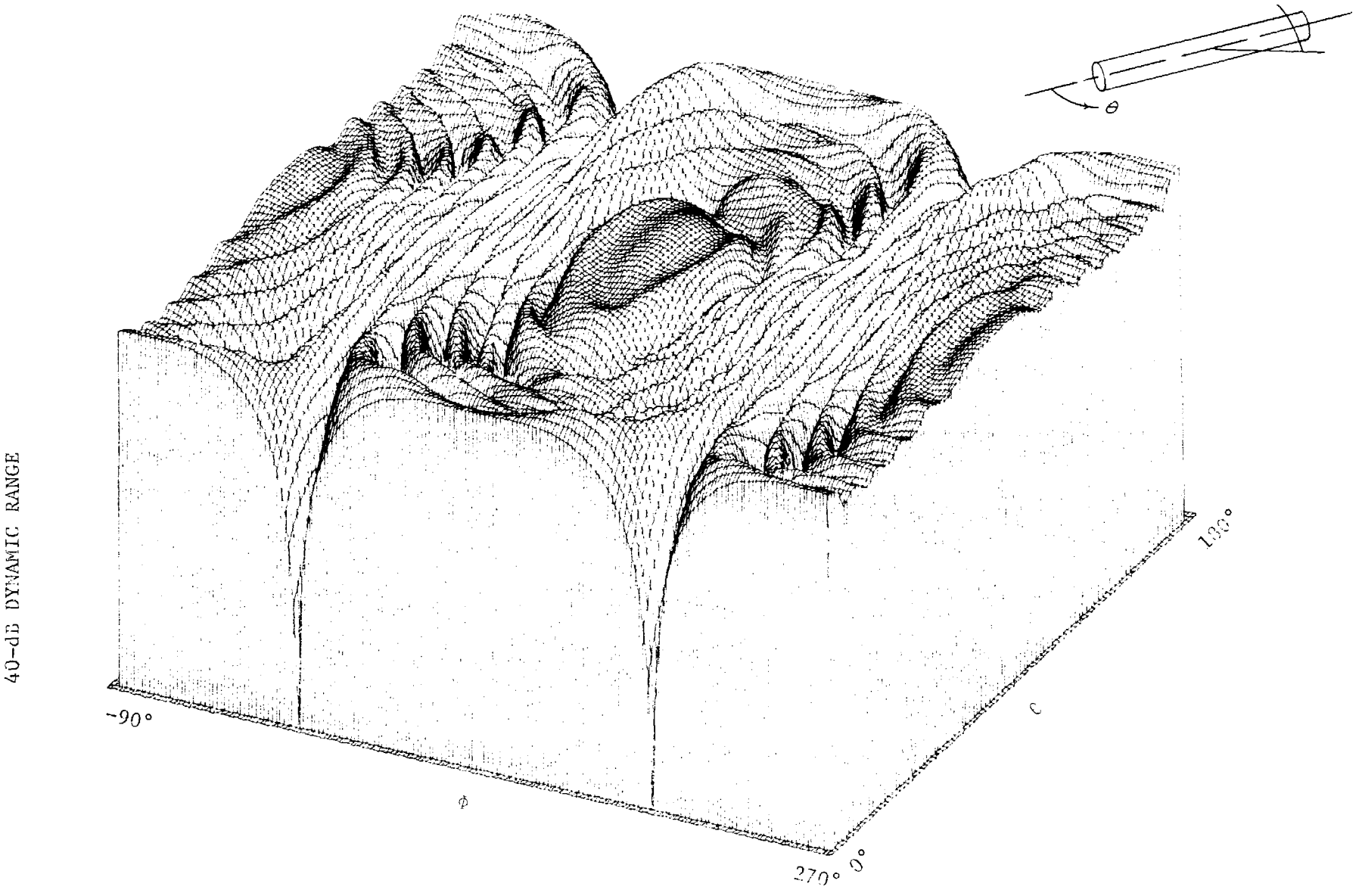

Figure 17. Calculated Radiation Pattern ($E_\theta^2 + E_\Phi^2$) for Two Pairs of Crossed Slots (Positioned on Top and Bottom as Indicated by AFATL) on a Conducting Right Circular Cylinder Having the Same Diameter as the TDU-X Target. Wing and Pod Blockage Was Not Included. ($\lambda/4$ Spacing Between Top and Bottom Antennas)

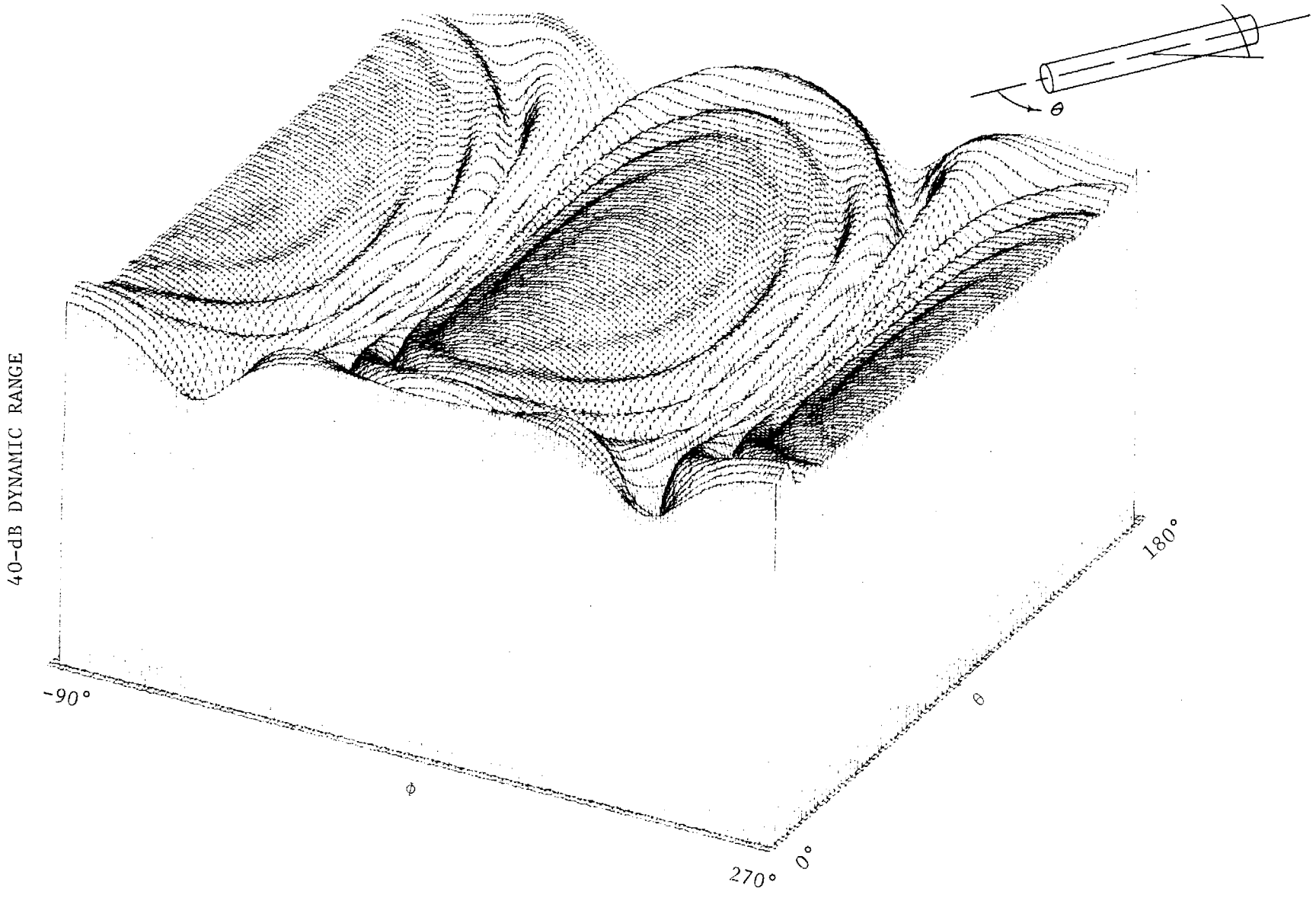

Figure 18. Calculated Radiation Pattern (E_θ^2) for Two Pairs of Crossed Slots (Positioned on Top and Bottom as Indicated by AFATL) on a Conducting Right Circular Cylinder Having the Same Diameter as the TDU-X Target. Wing and Pod Blockage Was Not Included. ($\lambda/2$ Spacing Between Top and Bottom Antennas)

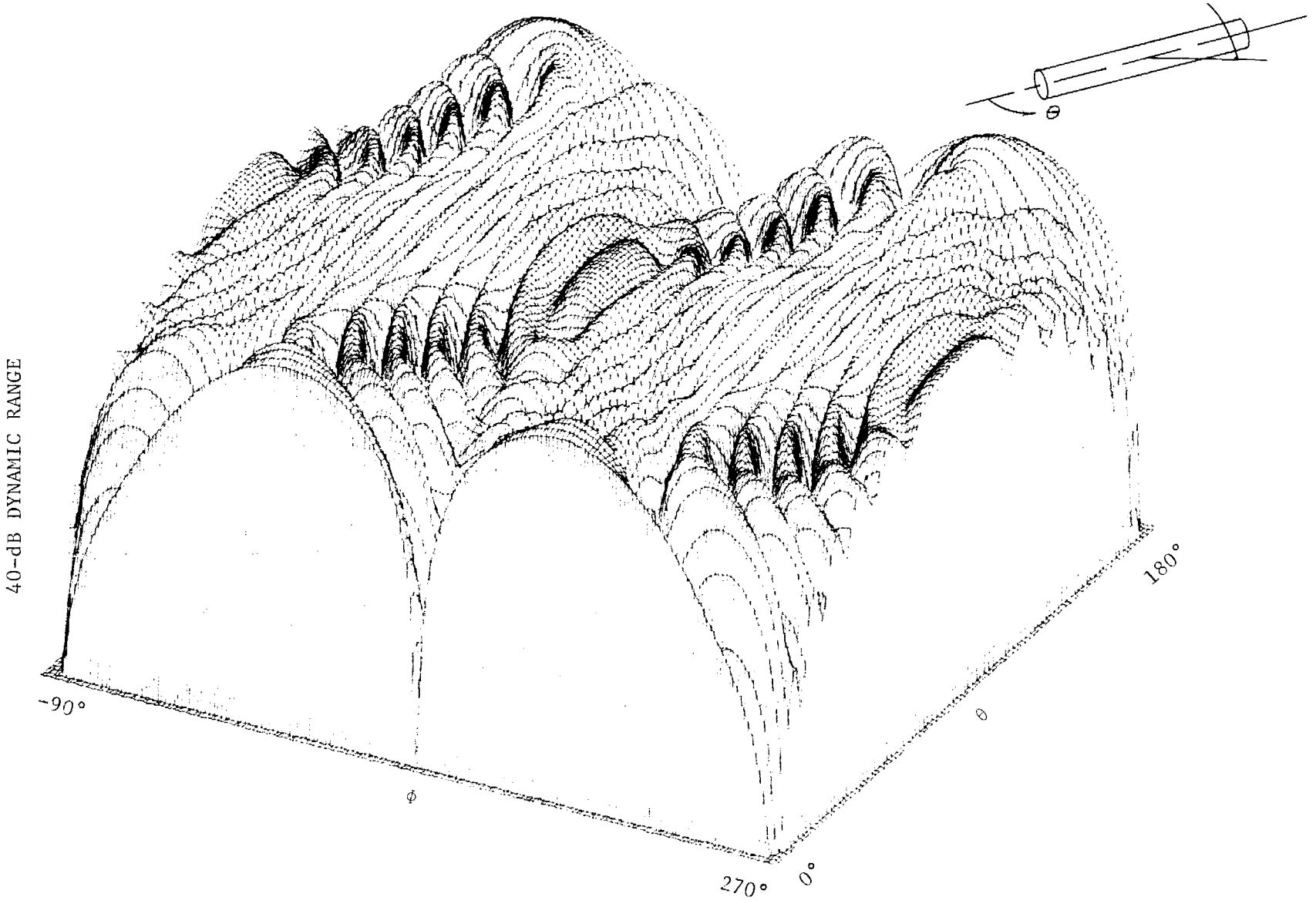

Figure 19. Calculated Radiation Pattern (E_{Φ}^2) for Two Pairs of Crossed Slots (Positioned on Top and Bottom as Indicated by AFATL) on a Conducting Right Cylinder Having the Same Diameter as the TDU-X Target. Wing and Pod Blockage Was Not Included. ($\lambda/2$ Spacing Between Top and Bottom Antennas)

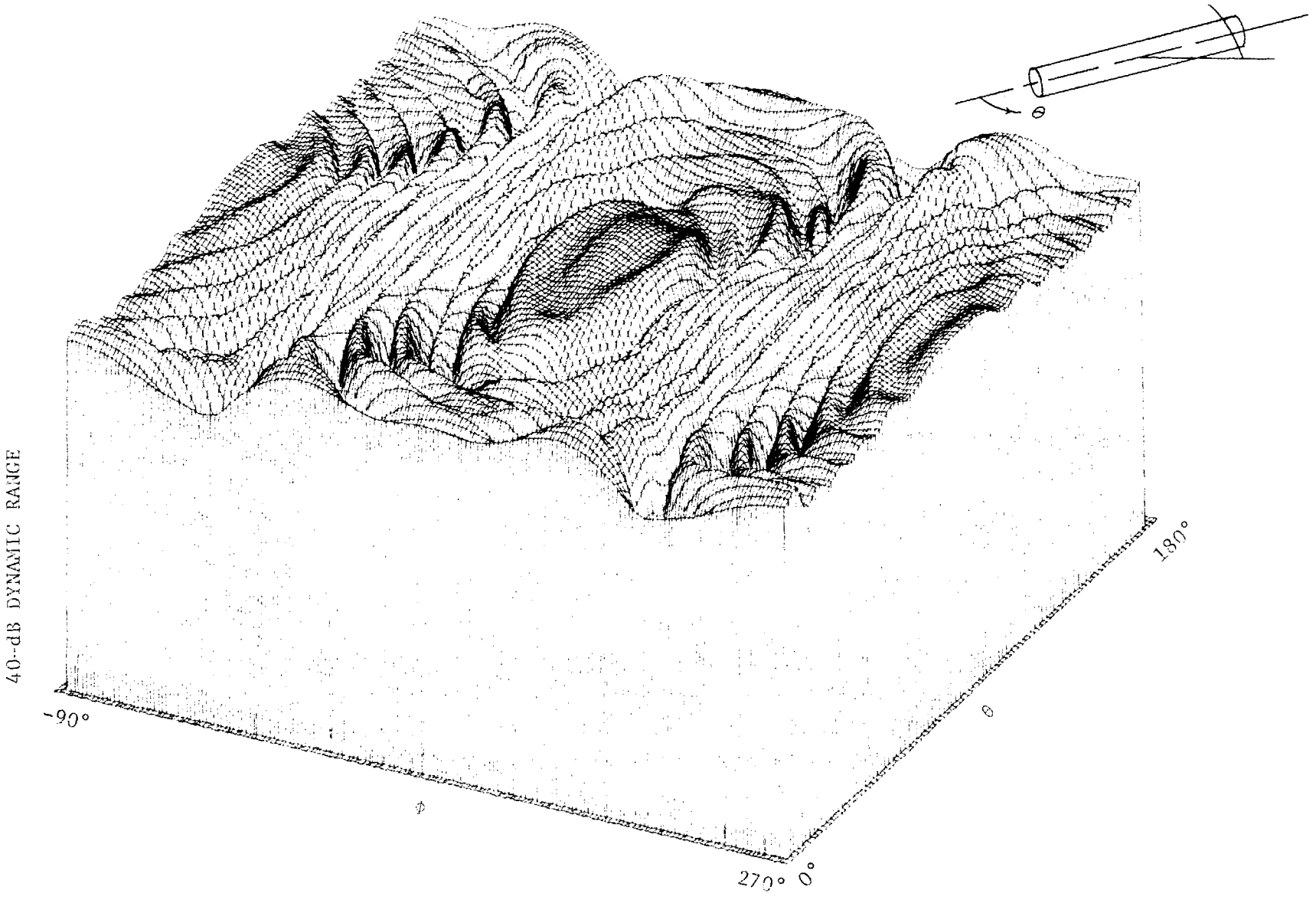

Figure 20. Calculated Radiation Pattern ($E_\theta^2 + E_\Phi^2$) for Two Pairs of Crossed Slots (Positioned on Top and Bottom as Indicated by AFATL) on a Conducting Right Circular Cylinder having the Same Diameter as the TDU-X Target. Wing and Pod Blockage Was Not Included. ($\lambda/2$ Spacing Between Top and Bottom Antennas)

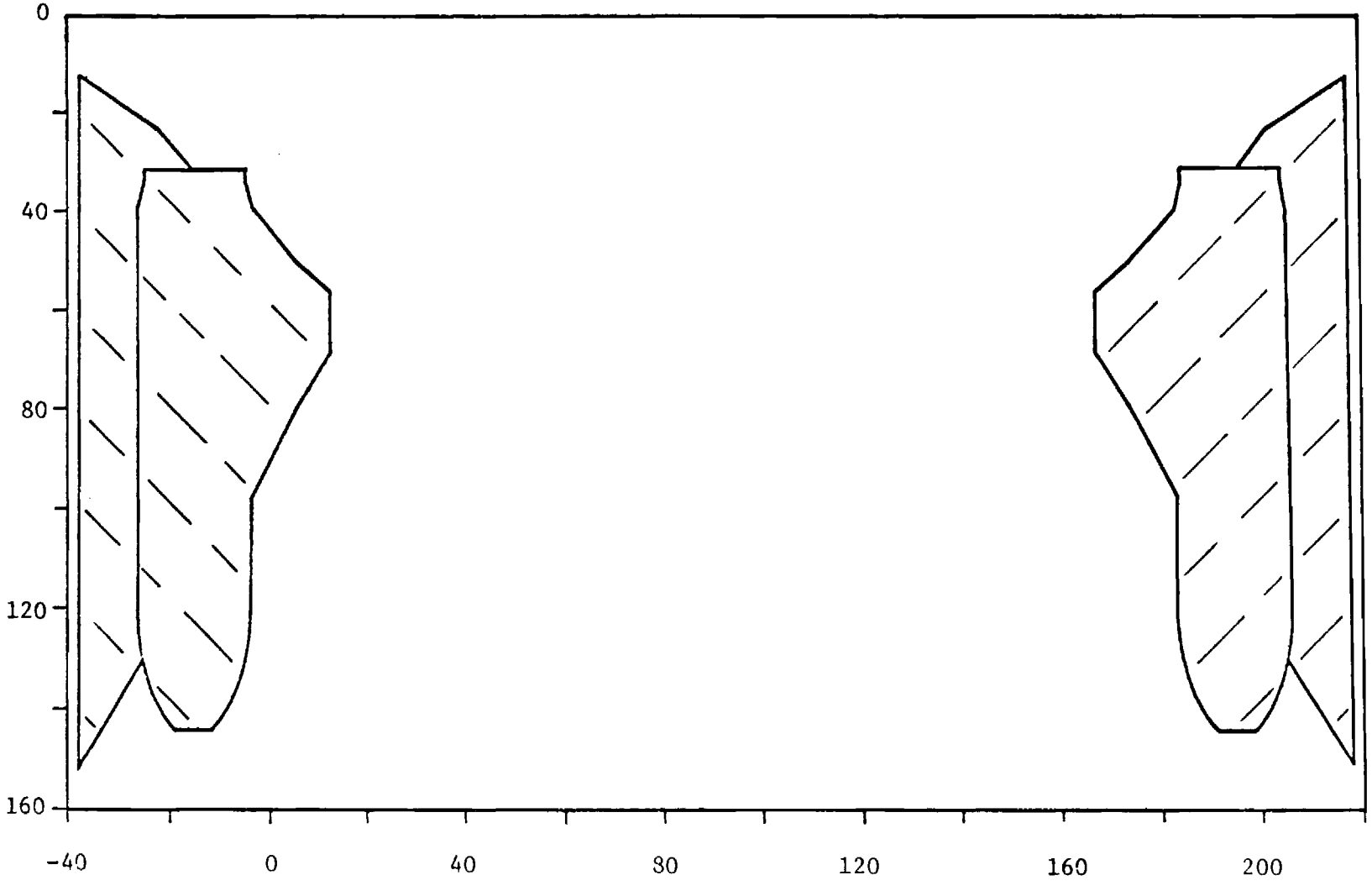

Figure 21. Blockage Matrix For Antenna Located on Top of TDU-X

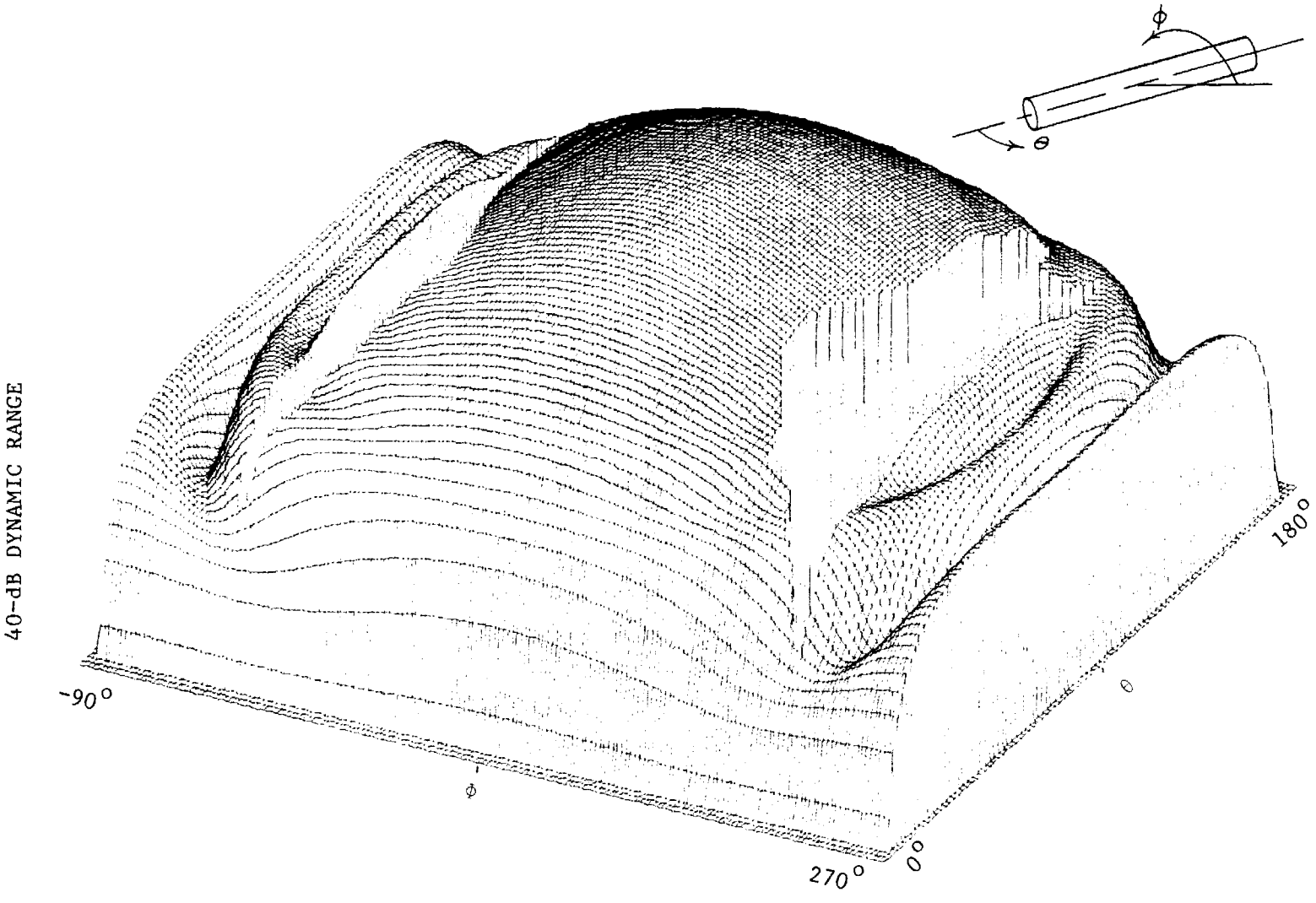

Figure 22. Calculated Radiation Pattern (E_{ϕ}^{2}) for a Single Axial Slot on a Conducting Right Circular Cylinder Having the Same Diameter as the TDU-X Target. Wing and Pod BLockage Was Included

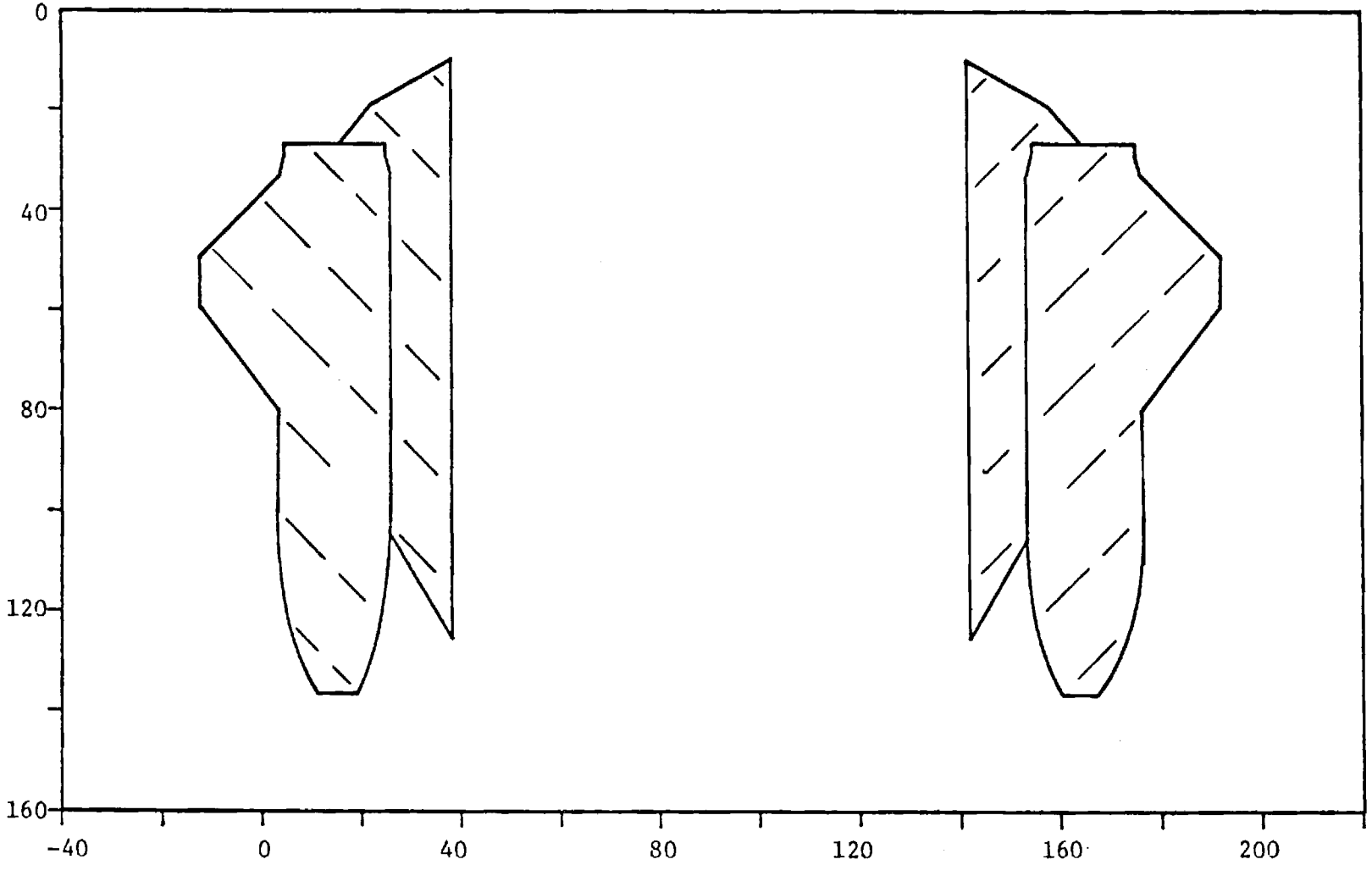

Figure 23. Blockage Matrix For Antenna Located on Bottom of TDU-X

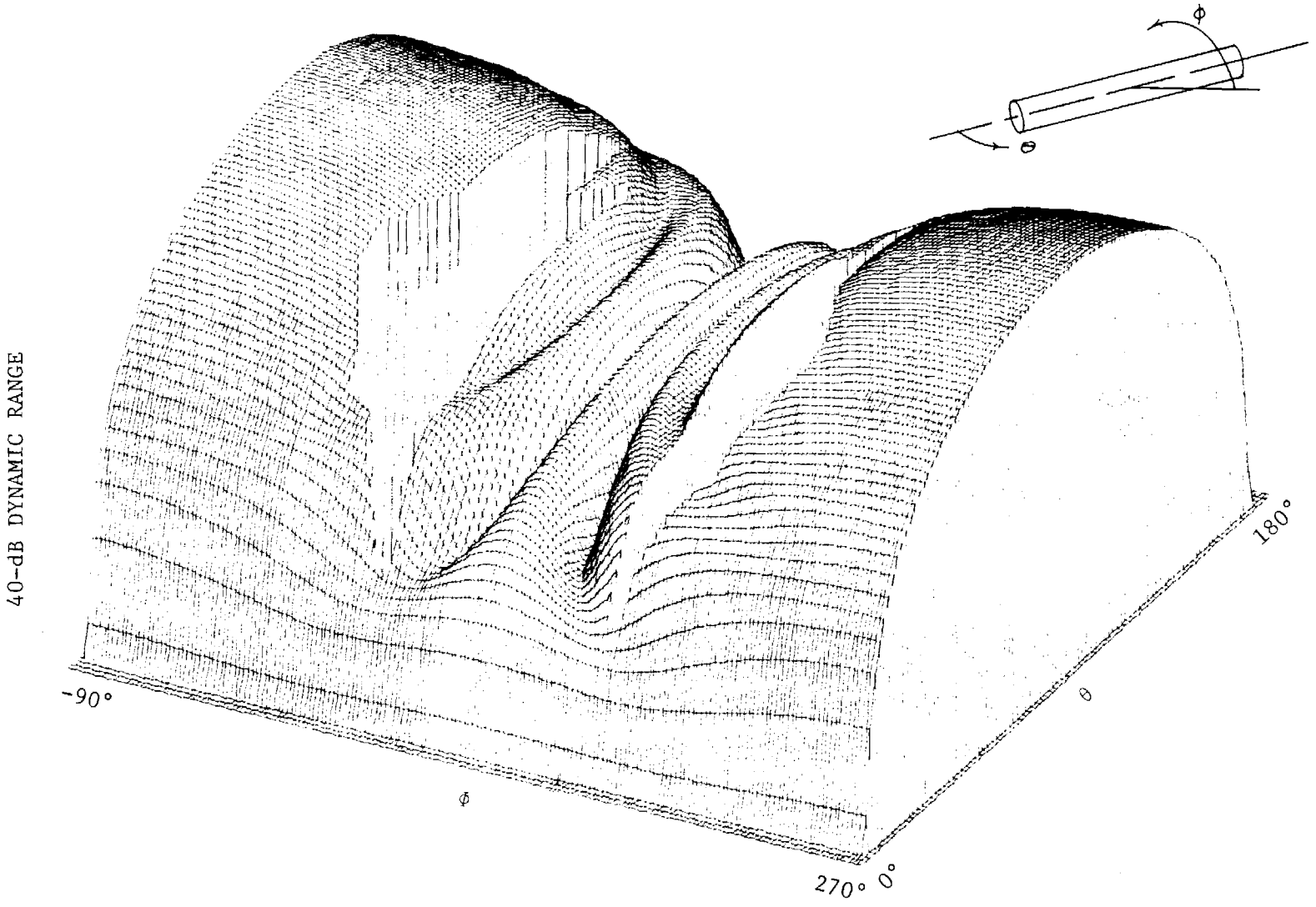

Figure 24. Calculated Radiation Pattern (E_{ϕ}^{2}) for One Axial Slot (positioned on Bottom) on a Conducting Right Circular Cylinder Having the Same Diameter as the TDU-X Target. Wing and Pod Blockage Was Included

The effect of the total wing blockage for the actual configuration of DIGIDOPS antennas is given in Figure 25. Where there is blockage, there is a tendency for the other antenna to fill it. This is a pattern showing total power $(E_\theta^2 + E_\phi^2)$. If the effect of scattering were to be included the blockage would be filled in even more.

(3) Pattern Gain

The gains for these antenna patterns were calculated using the basic equation

$$G = 10 \log_{10} \left[\frac{4\pi E^2_{max}}{\Delta\theta \Delta\Phi \sum_i \sin \theta_i \left[\sum_j E^2(\theta_i, \phi_j) \right]} \right] , \qquad (10)$$

Note that this calculation actually yields directivity since element efficiency is not included. True gain is found by subtracting element losses from directivity values.

The gains calculated for a single axial slot at $\Phi = 90^o$ was 5.35 dB. The gain calculated for the total power $(E_\theta^2 + E_\phi^2)$ of a pair of DIGIDOPS antennas mounted in the present configuration was 4.1 dB. The gain for the single slot with blockage was 5.9 dB and for the DIGIDOPS with blockage was 4.5 dB.

(4) Power Coverage Functions

Power coverage functions are very similar to probability distribution functions in that they depict the relative area of the farfield sphere over which the power is below a certain level versus the level. This is accomplished by numerically stepping through the data at one power level at a time and adding up the spherical surface areas over which the power is below the subject level. Such a plot shows at a glance the amount of the pattern that is below any given power level. The plot is a good method for comparing coverage for different antenna configurations. A composite plot of the coverage functions was made for the four different DIGIDOPS positions examined earlier to compare the coverage. There were three different cases plotted, Figures 26, 27, and 28, which show the coverage for E_θ^2, E_ϕ^2, and the total power

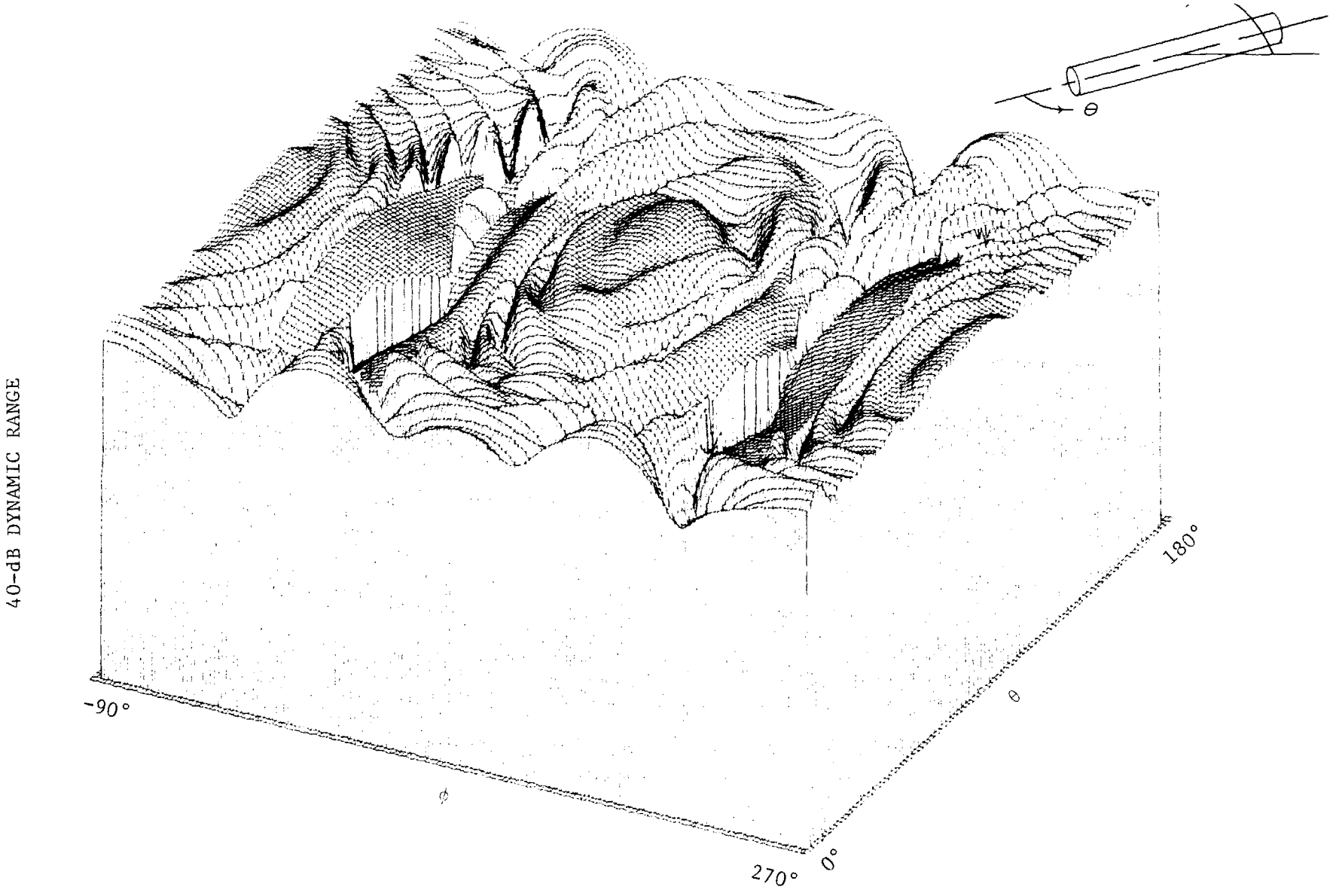

Figure 25. Calculated Radiation Pattern ($E_\theta^2 + E_\phi^2$) for Two Pairs of Crossed Slots (Positioned on Top and Bottom as Indicated by AFATL) on a Conducting Right Circular Cylinder Having the Same Diameter as the TDU-X Target. Wing and Pod Blockage Was Included

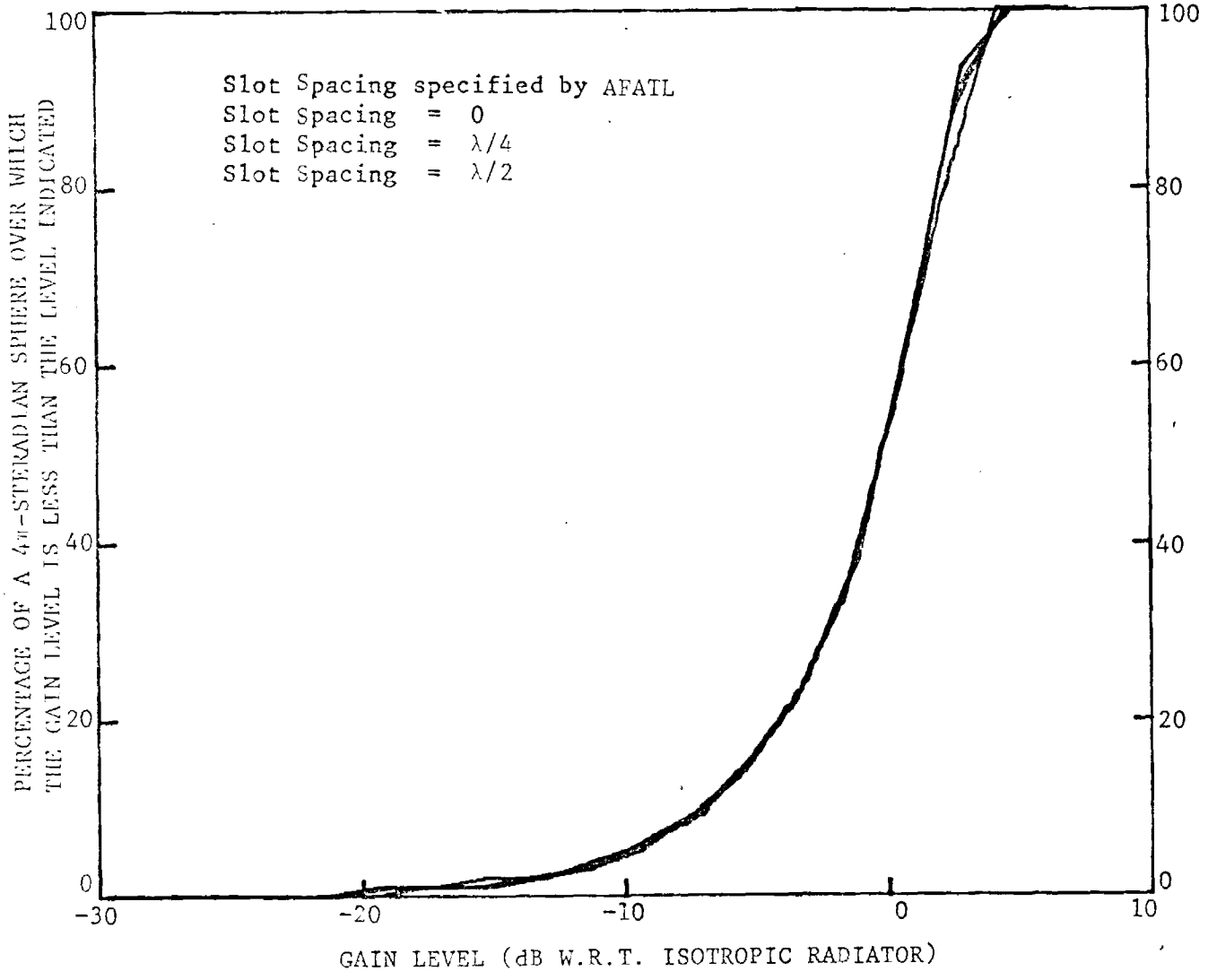

Figure 26. Power Distribution Function (E_θ^2) for Two Pairs of Crossed Slots (One Pair Each on Top and Bottom) on the TDU-X Target. Slot Positions are Indicated. No Wing and Pod Blockage Included

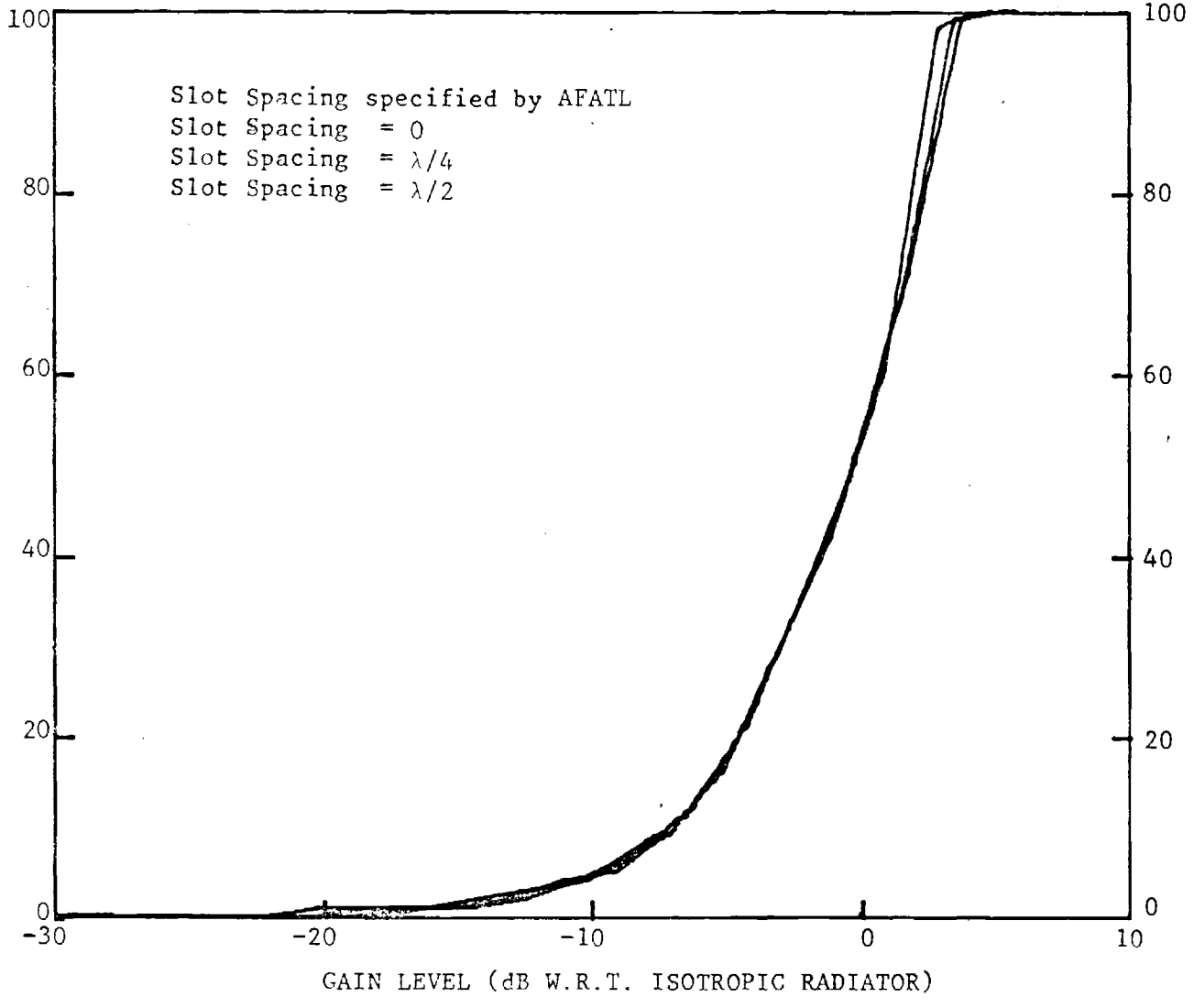

Figure 27. Power Distribution Function (L_0^2) for Two Pairs of Crossed Slots (One Pair Each on Top and Bottom) on the TDU-X Target. Slot Positions are Indicated. No Wing and Pod Blockage Included

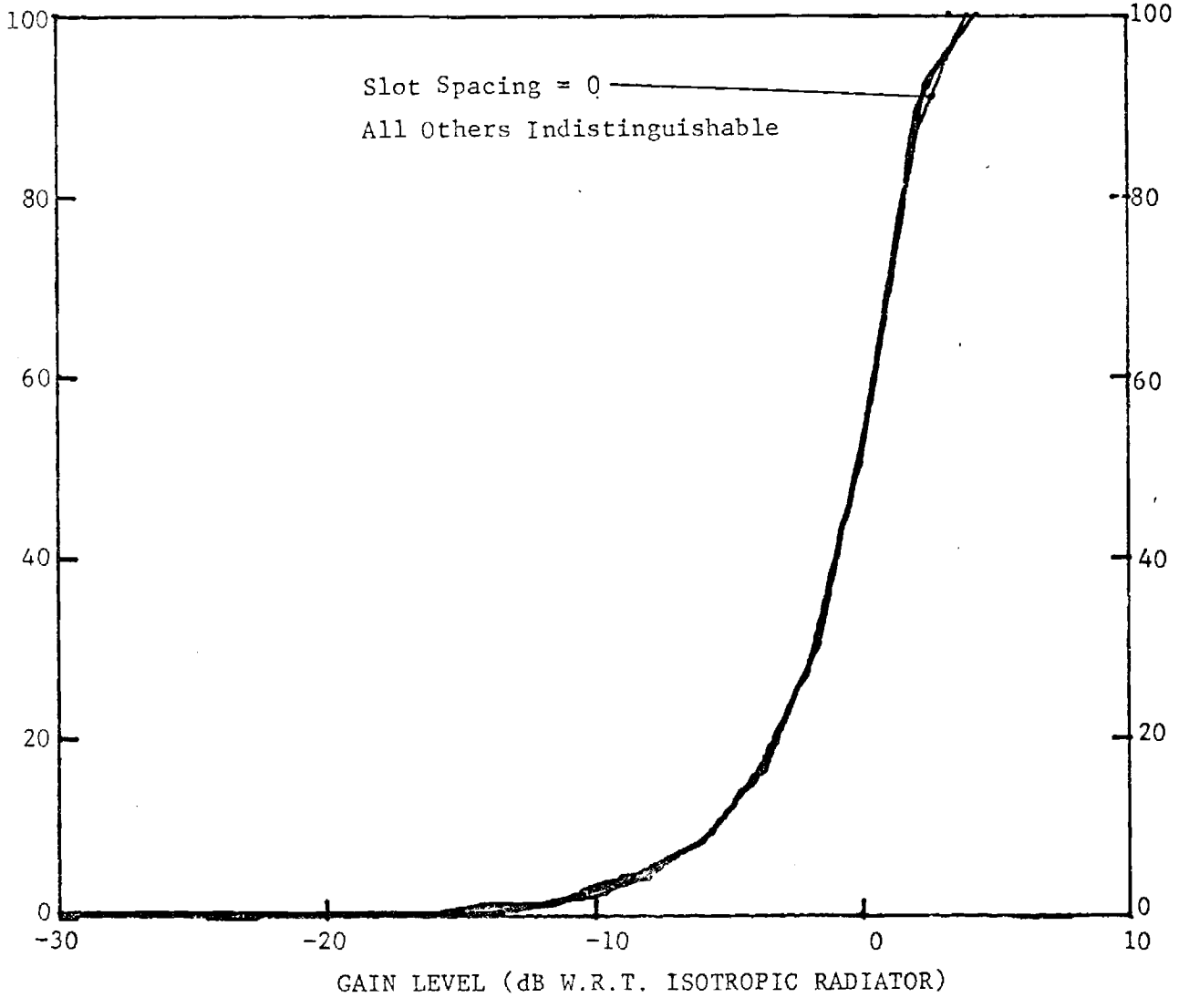

Figure 28. Power Distribution Function (Total Power, $(E_\theta^2 + E_\phi^2)$ for Two Pairs of Crossed Slots (One Pair Each on Top and Bottom) on the TDU-X Target. Slot Positions are Indicated. No Wing and Pod Blockage Included

$(E_\theta^2 + E_\phi^2)$, respectively. The plots show that for this antenna configuration the coverage does not change significantly with variations in antenna location. The power coverage function for the total power $(E_\theta^2 + E_\phi^2)$ for the original position with blockage included is shown in Figure 29 for comparison.

(5) Summary of Computed Results

The analysis of the DIGIDOPS system on the TDU-X showed that typically good coverage was attained for the antennas used. The blockage included did not affect the coverage in the areas needed because of the tendency of the antennas to fill in the gaps. The location of the DIGIDOPS antennas on the TDU-X for the positions that were modeled was not found to affect the antenna pattern nor the coverage significantly.

The principal plane patterns of the final configuration of the TDU-X scoring antennas are presented in Figures 30 through 35. The antenna gain is approximately 0 dBi. These patterns can be compared with the scale model radiation patterns of Figures 41 through 46. This comparison will be discussed in the data summary section of the TDU-X later in this report.

b. TDU-X Command Receiver Antenna

The computer analysis for the command receiver antenna utilized a slot on a cylinder and the equation presented previously. This pattern is shown in Figure 36.

c. Telemetry Transmitter Antenna and L-Band Augmentation Antenna

The computer analysis for the TDU-X tow target Telemetry Transmitting stub and L-Band Augmentation Antenna was accomplished by modeling the antenna as a dipole on the surface of an infinite cylinder in a manner similar to the DIGIDOP's antenna. As with the DIGIDOP's analysis, this method does not consider the effect of the finite extent of the tow target but is sufficient for modeling purposes.

The mathematical model used is that discussed by Carter [3]. The basic equations used for the θ and ϕ components of the electric field are

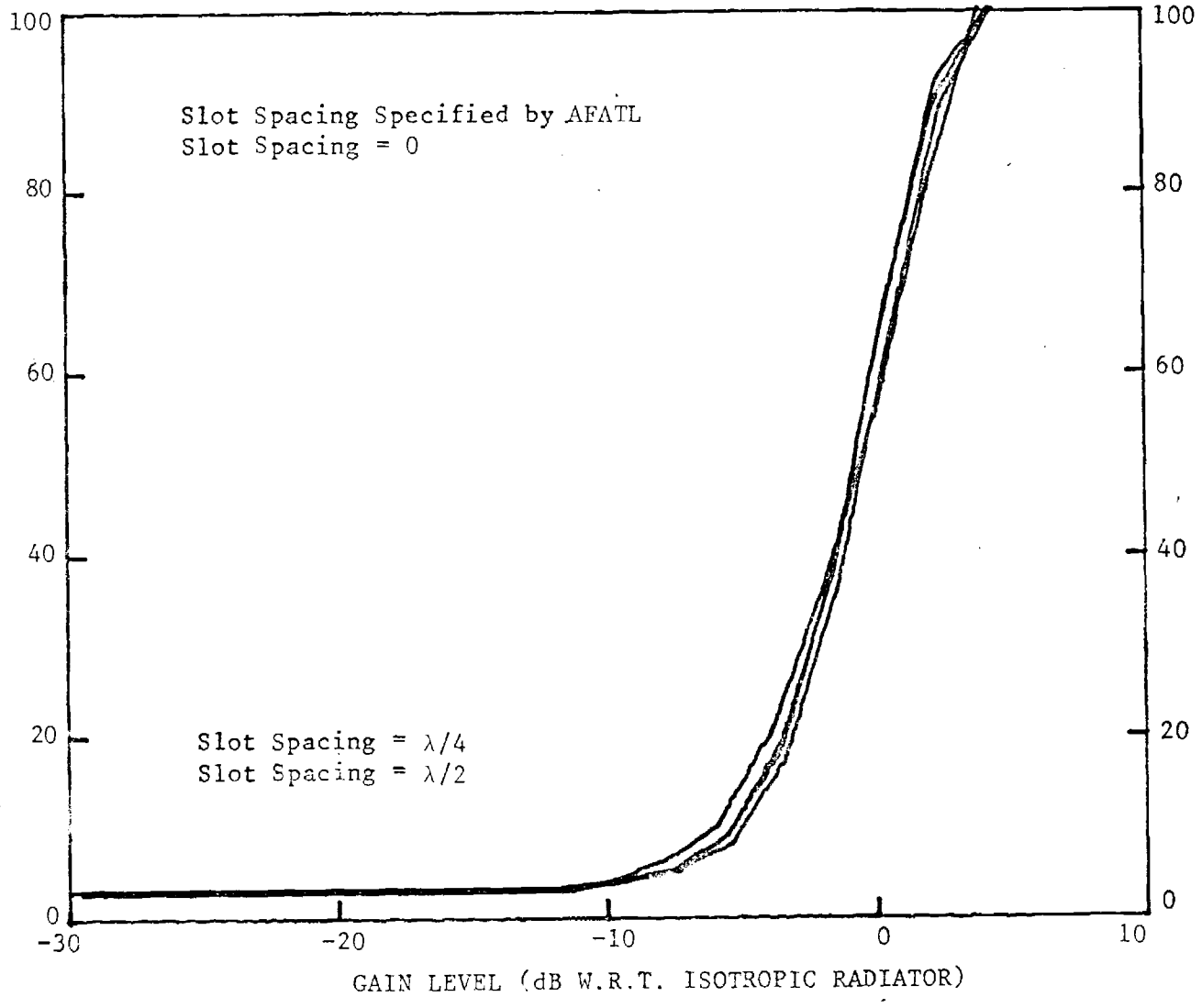

Figure 29. Power Distribution Function (Total Power, $E_\theta^2 + E_\phi^2$) for Two Pairs of Crossed Slots (One Pair Each on Top and Bottom) on the TDU-X Target. Slot Positions are Indicated. Wing and Pod Blockage Included

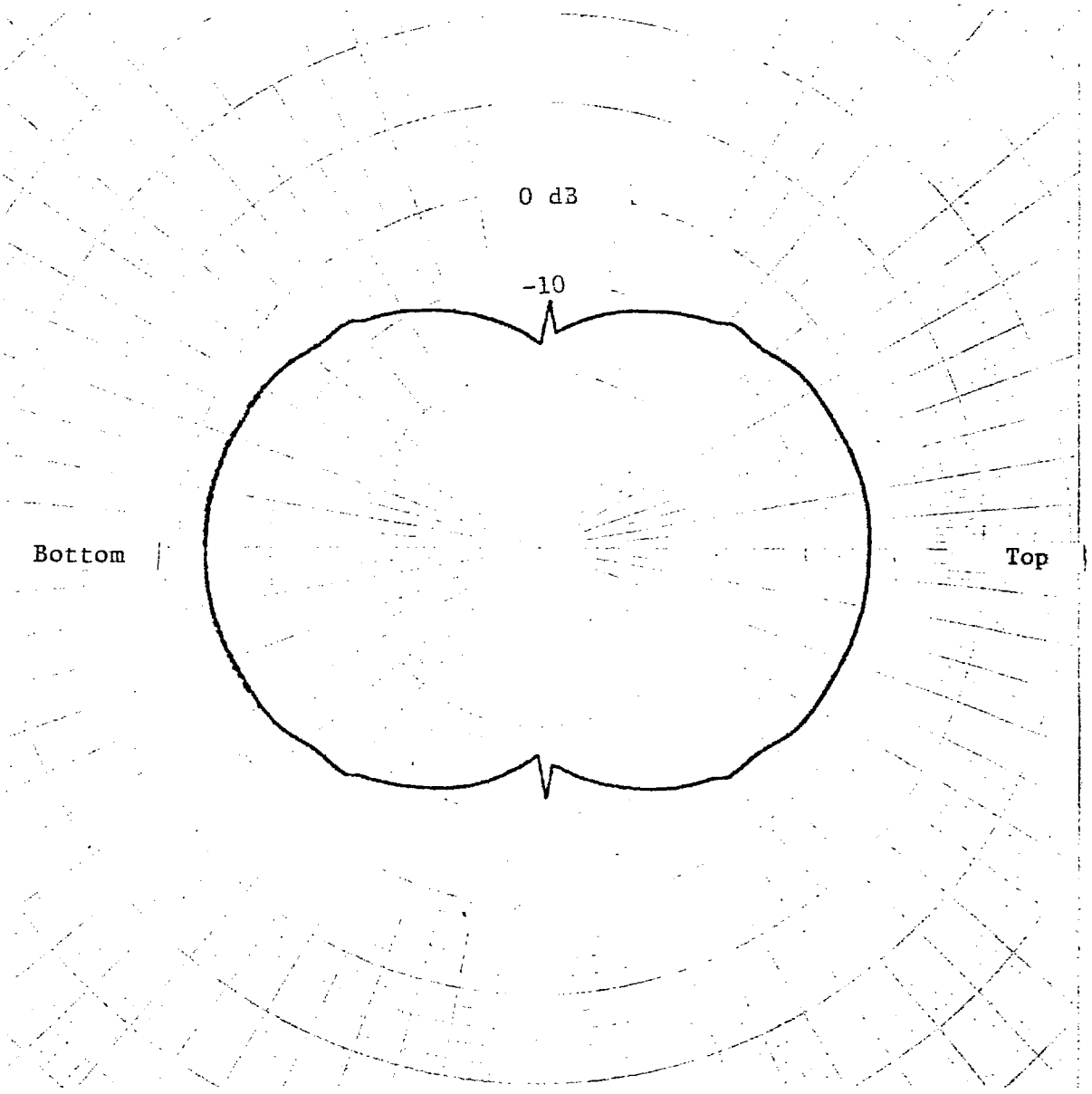

Figure 30. Principal Plane Plot, Eϑ, TDU-X Scoring Antennas, Pitch Ange 90°, Variable Roll Angle

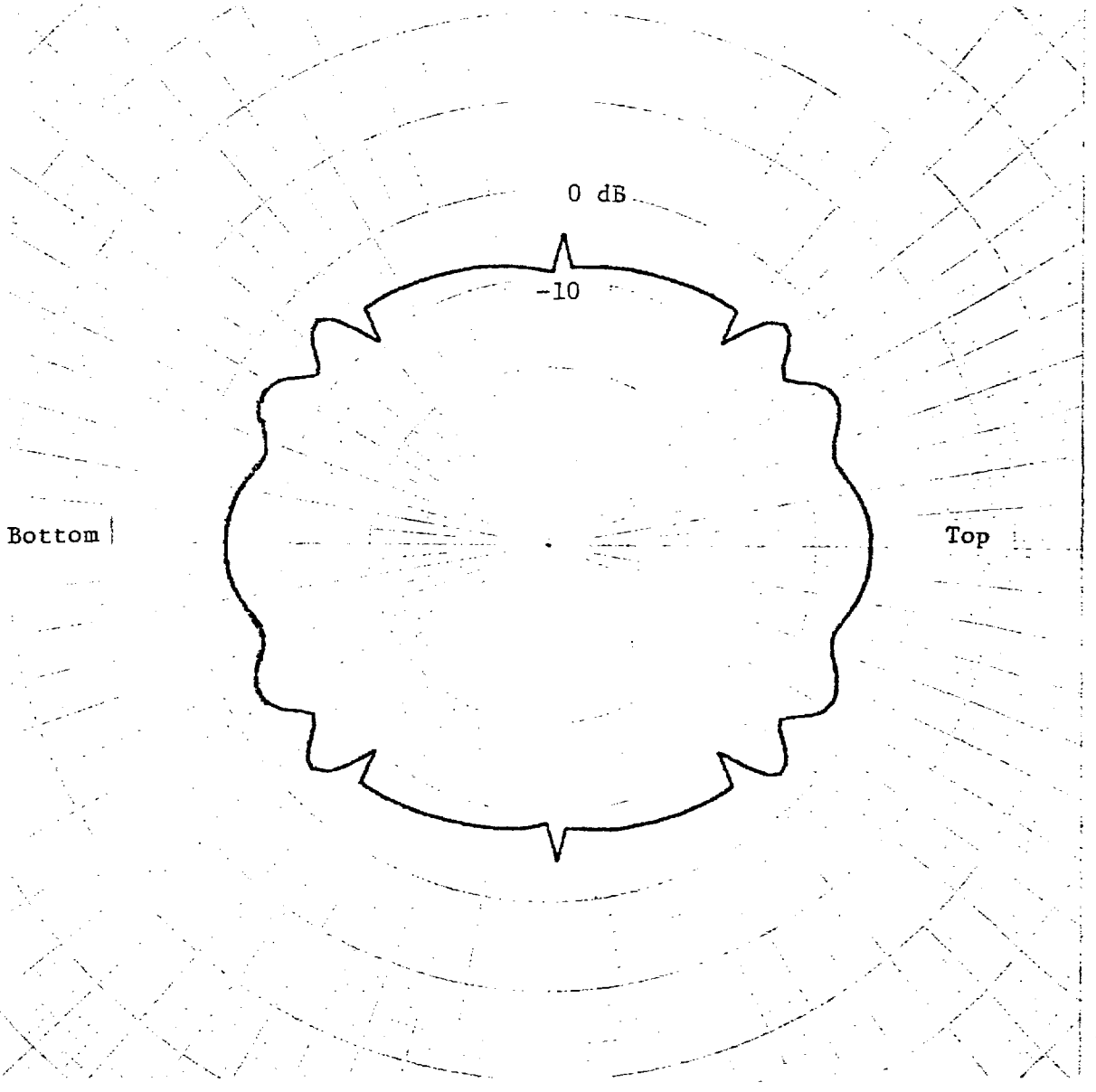

Figure 31. Principal Plane Plot, Eθ, TDU-X Scoring Antennas, Pitch Angle 90°, Variable Roll Angle

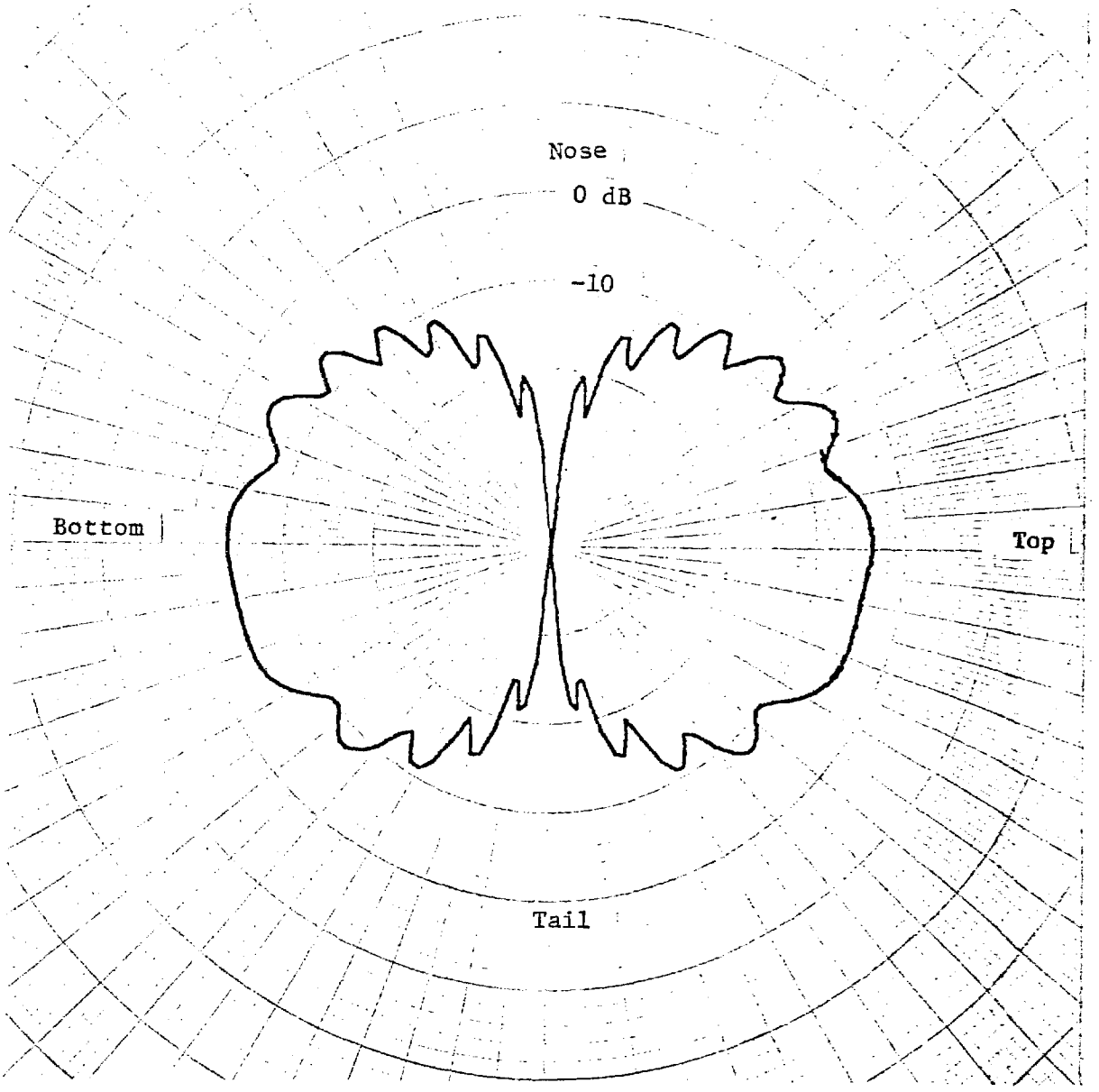

Figure 32. Principal Plane Pattern, Eϕ, TDU-X Scoring Antennas, Roll Angle 90°, Variable Pitch Angle

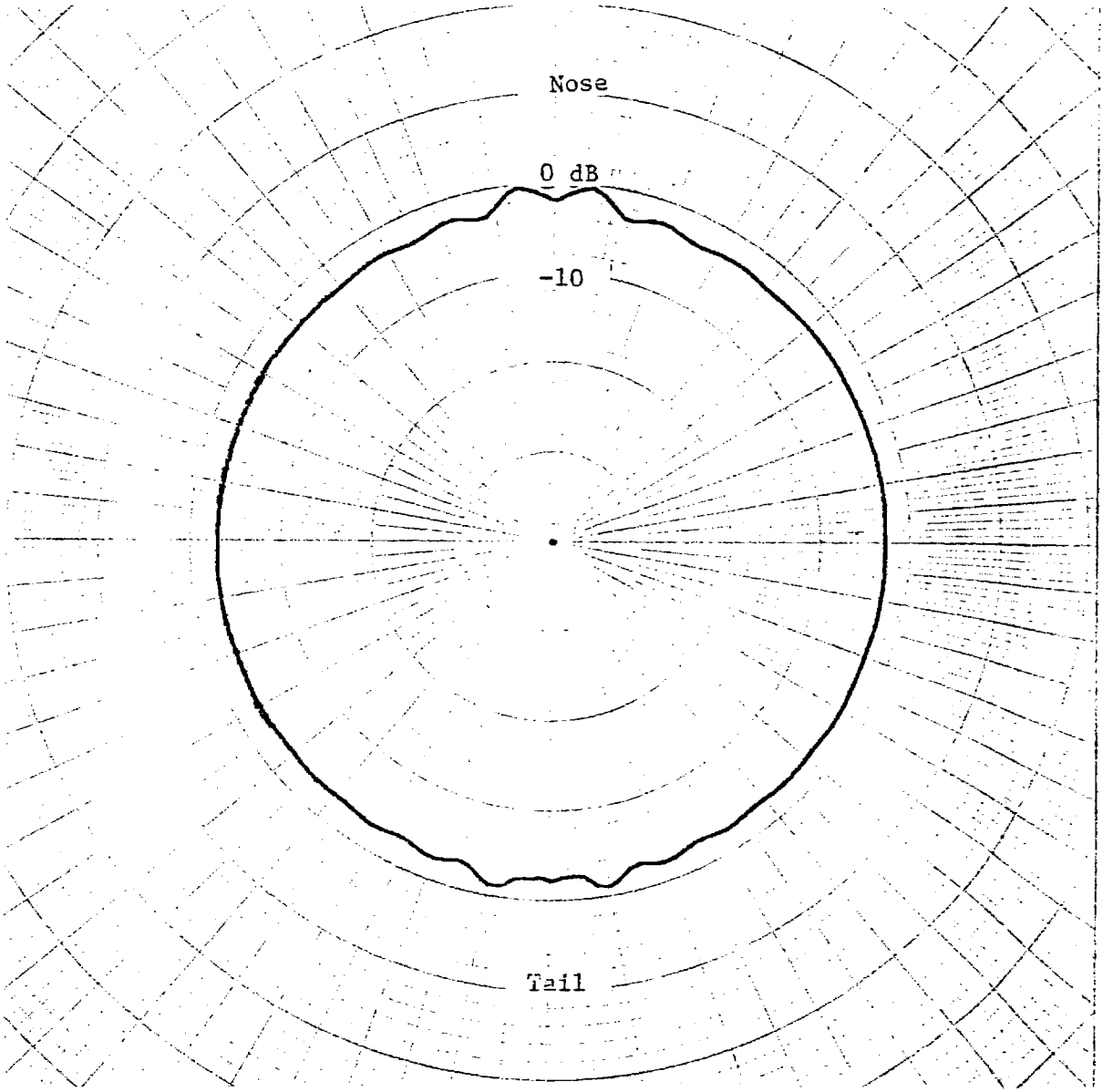

Figure 33. Principal Plane Pattern, Eθ, TDU-X Scoring Antennas, Roll Angle 90°, Variable Pitch Angle

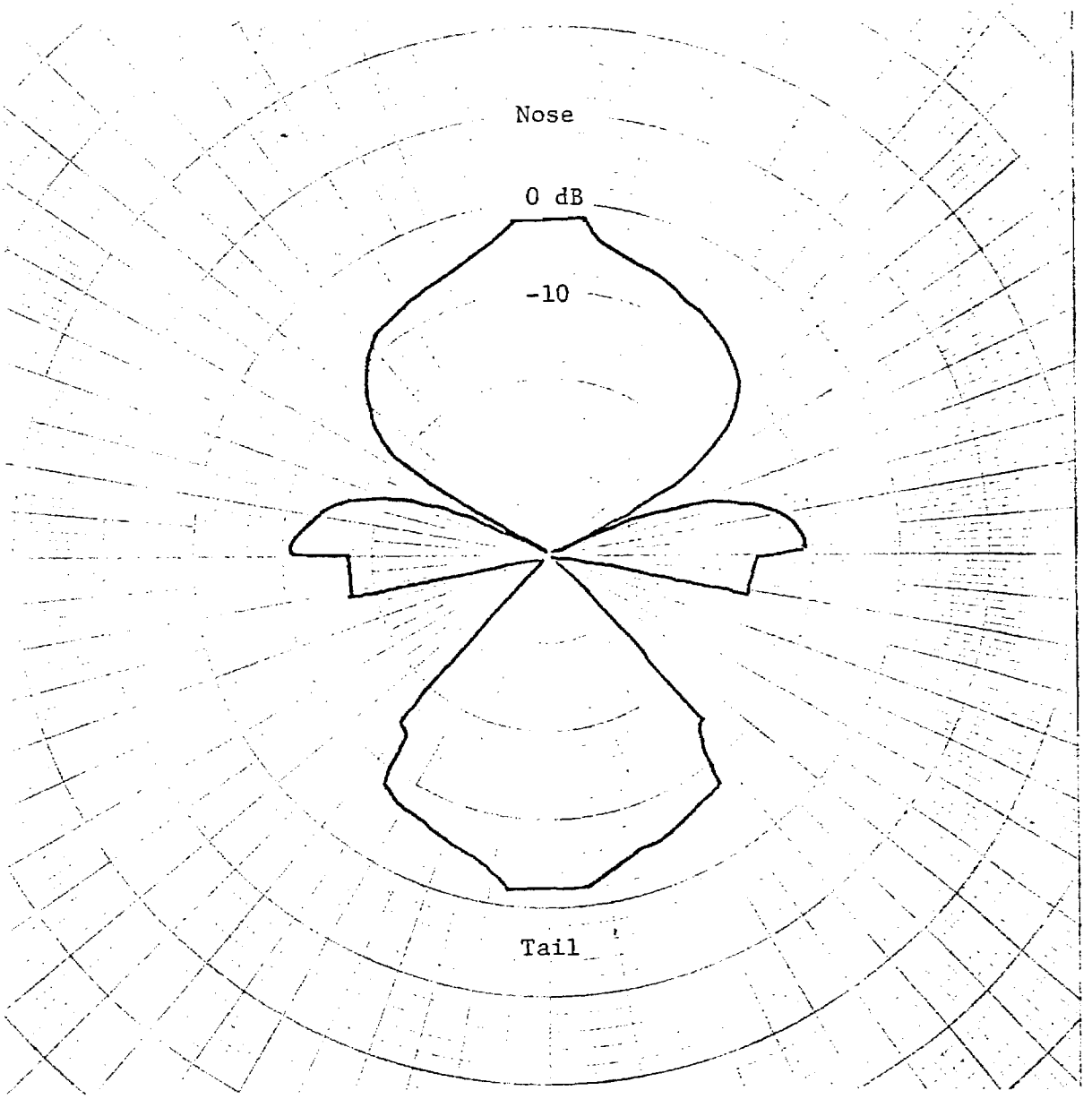

Figure 34. Principal Plane Pattern, Eϕ, TDU-X Scoring Antennas, Pitch and Roll Angles 0°, Variable Yaw Angle

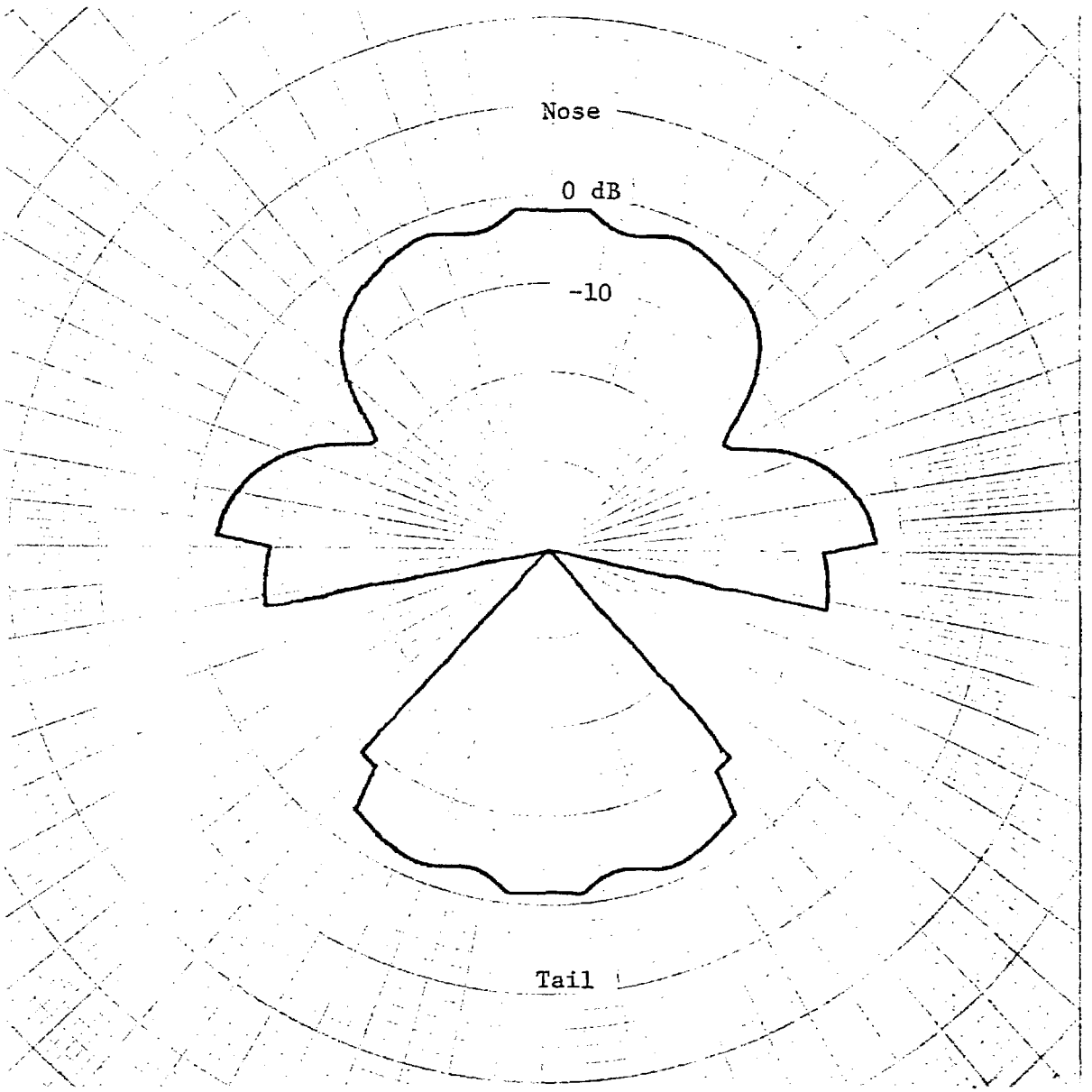

Figure 35. Principal Plane Pattern, Eθ, TDU-X Scoring Antennas, Roll and Pitch Angles 0^{o}, Variable Yaw Angle

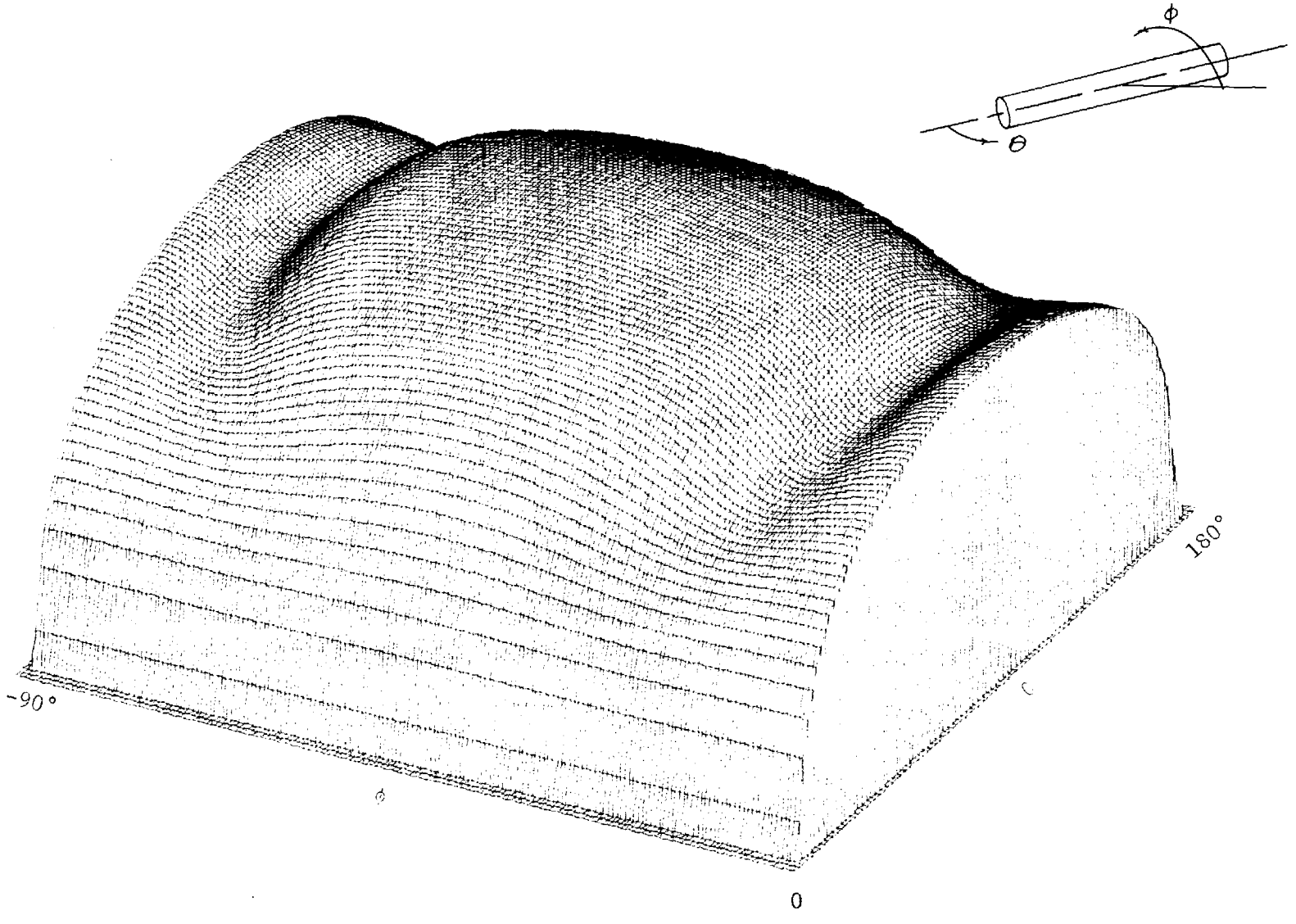

Figure 36. Calculated Radiation Pattern for a Slot Antenna Positioned on Bottom of a Conducting Right Cylinder Having the Same Diameter as the TDU-X Target

$$E_{\theta} = j \cos\theta \left[D_o + 2 \sum_{n=1}^{\infty} j^n D_n \cos n\phi\right] , \qquad (11)$$

$$E_{\phi} = \left(-j \frac{2}{ka} \sin\theta\right) \sum_{n=1}^{\infty} J^n n B_n \sin n\phi , \qquad (12)$$

where,

$$D_n = Jn'(ka \sin\theta) - \left[\frac{J_n(ka \sin\theta)}{H^{(2)}{}_n(ka \sin\theta)}\right] Hn'^{(2)}(ka \sin\theta) , \qquad (13)$$

and

$$B_n = Jn(ka \sin\theta) - \left[\frac{J'(ka \sin\theta)}{H'n^{(2)}(ka \sin\theta)}\right] Hn(ka \sin\theta) , \qquad (14)$$

where a is the radius of the cylinder.

The stub antenna was located at ϕ = -90 degrees and the θ and ϕ components were calculated separately, and the three dimensional patterns plotted (Figure 37, 38).

3. MEASURED DATA - SCALE MODEL AND FULL SCALE PATTERNS

Scale models of the TDU-X tow target and the BQM-34A wing pod were fabricated and used in obtaining measured antenna radiation pattern data. A scale model BOMARC was obtained from Eglin AFB and was used to model the DIGIDOPS scoring antenna system. Most of the measured data were obtained on the TDU-X scale model. It should be noted that this particular effort was done to verify the computed data.

a. TDU-X Tow Target

A one-fifth scale model of the TDU-X tow target was fabricated for use in the measurement program. A photograph of this model is presented in Figure 39. The antennas tested with the model were DIGIDOPS, Telemetry, and L-Band Augmentation.

(1) Scoring Antennas

A photograph of one of the scale model DIGIDOPS scoring antennas is presented in Figure 40. This antenna was fabricated from sections of K_u-Band waveguide. Teflon plugs were used to load the cavity-backed slots in a manner similar to the full scale antennas.

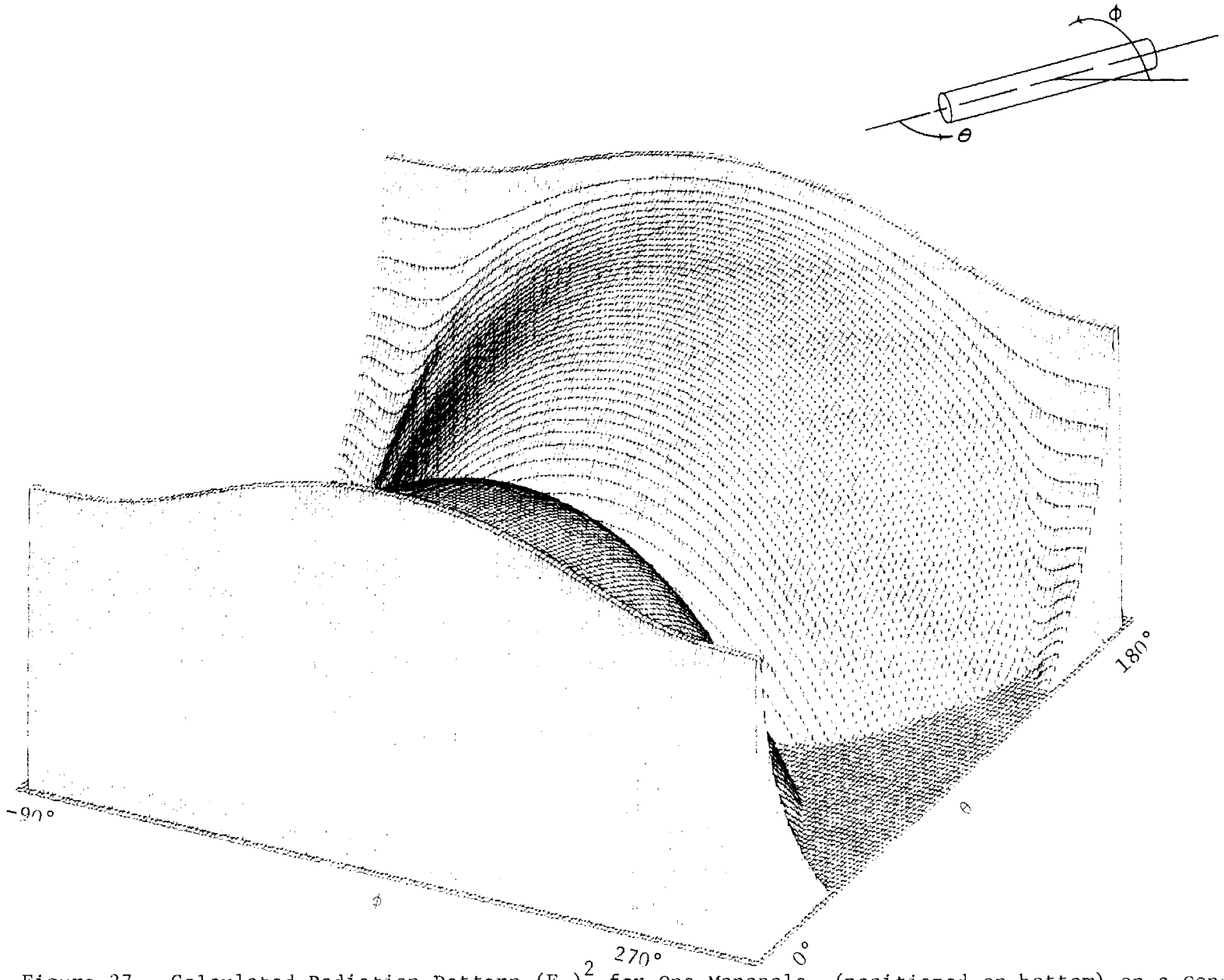

Figure 37. Calculated Radiation Pattern $(E_\theta)^2$ for One Monopole (positioned on bottom) on a Conducting Right Cylinder Having the Same Dimensions as the TDU-X Target

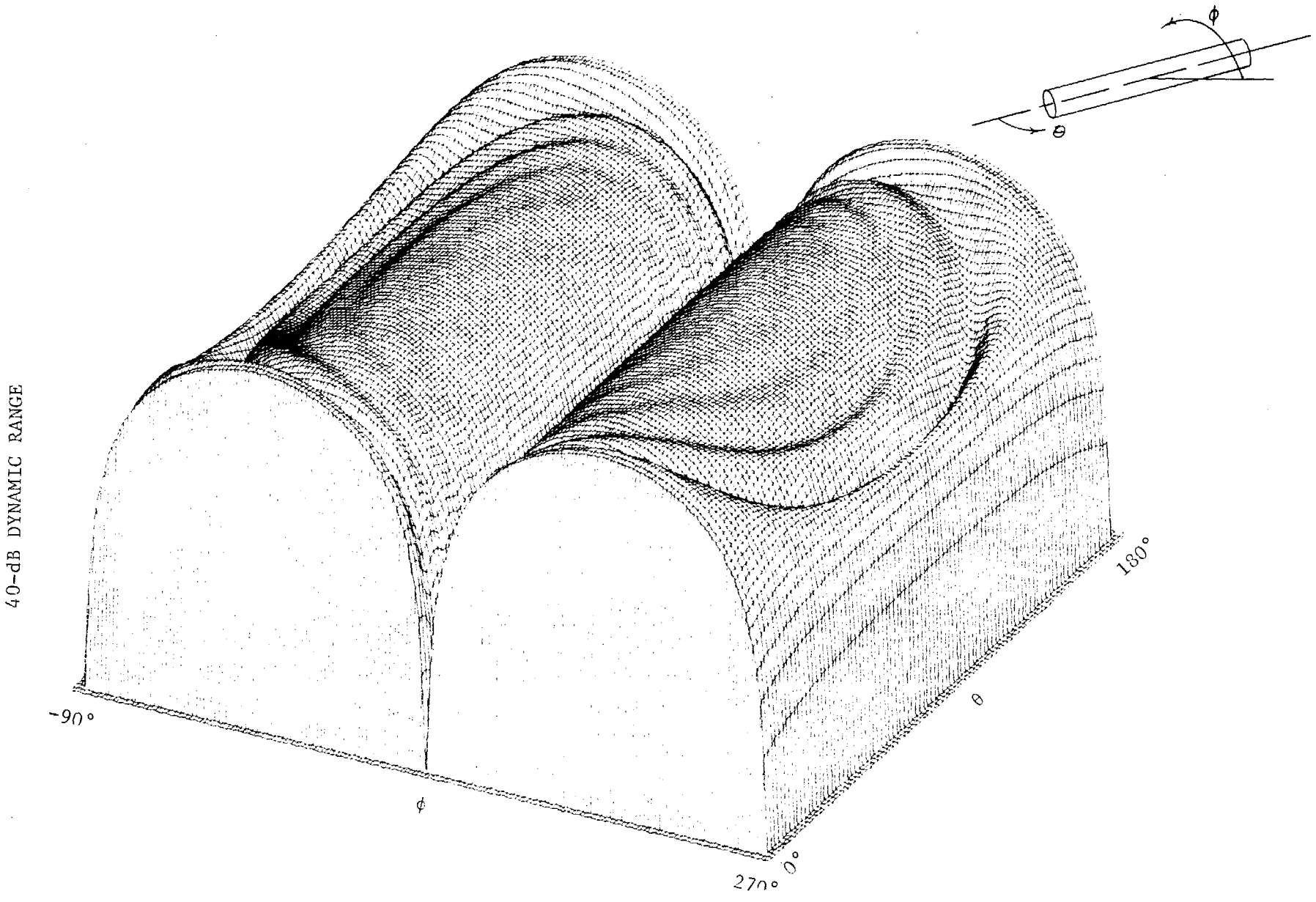

Figure 38. Calculated Radiation Pattern for One Monopole (positioned on bottom) on a Conducting Right Circular Cylinder Having the Same Diameter as the TDU-X Target

Figure 39. TDU-X Scale Model on Antenna Range

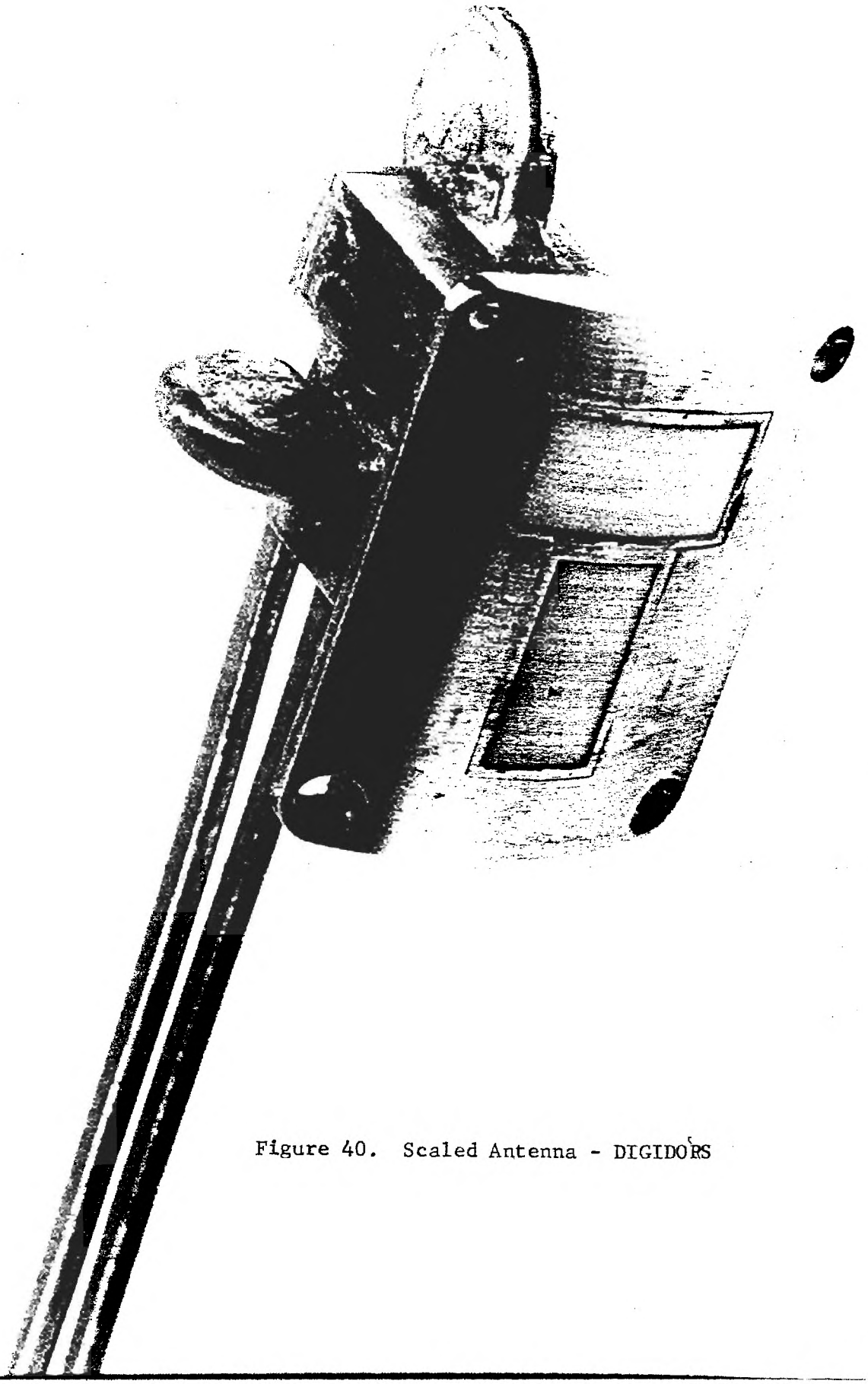

Figure 40. Scaled Antenna - DIGIDORS

Only the primary radiation patterns will be presented herein. A number of patterns were run with a single antenna and were used to verify computer input data. In addition, some radiation patterns were made without the target fins to determine the effect on the patterns. The principal plane plots for the two polarizations are plotted in Figures 41 through 46. A comparison of these data to that of Figures 30 through 35 reveals that the computer modeling, although not exact, is a sufficient means of determining the coverage characteristics of two target antenna systems.

Figure 41 shows a principal plane pattern of the TDU-X scoring antennas in the roll plane with the target at a 90-degree pitch angle. Since the antennas are mounted on the top and bottom of the vehicle, good pattern coverage is provided in these areas. As a comparison, the computed pattern is presented in Figure 30. Although the right and left side coverage is predicted to be lower than the measured coverage, the comparison is favorable.

The horizontal polarization roll plane pattern is presented in Figure 42 and the expected coverage was obtained. The vertical polarization pitch plane pattern is shown in Figure 43. The predicted pattern of Figure 32 indicates deep nulls on the nose and tail of the target, whereas the measured pattern indicates good tail coverage. This difference is caused by two factors: (1) the reflections from the fins and the pods enhance the tail coverage and (2) the measured antennas do not possess the ideal cross polarization characteristics of the antennas utilized in the pattern predictions. The horizontally polarized pitch plane pattern is presented in Figure 44. Good agreement exists between these pattern cuts.

The yaw plane cuts are shown in Figures 45 and 46 for the TDU-X scoring antennas. Note the blockage effects of the fins in Figures 34 and 35. Although the measured patterns indicate that the blockage is not as severe as predicted, they do serve as good indicators of the areas where coverage problems will arise.

The remaining individual θ , ϕ pattern cuts are not included in this report. These data have been analyzed and summarized and are

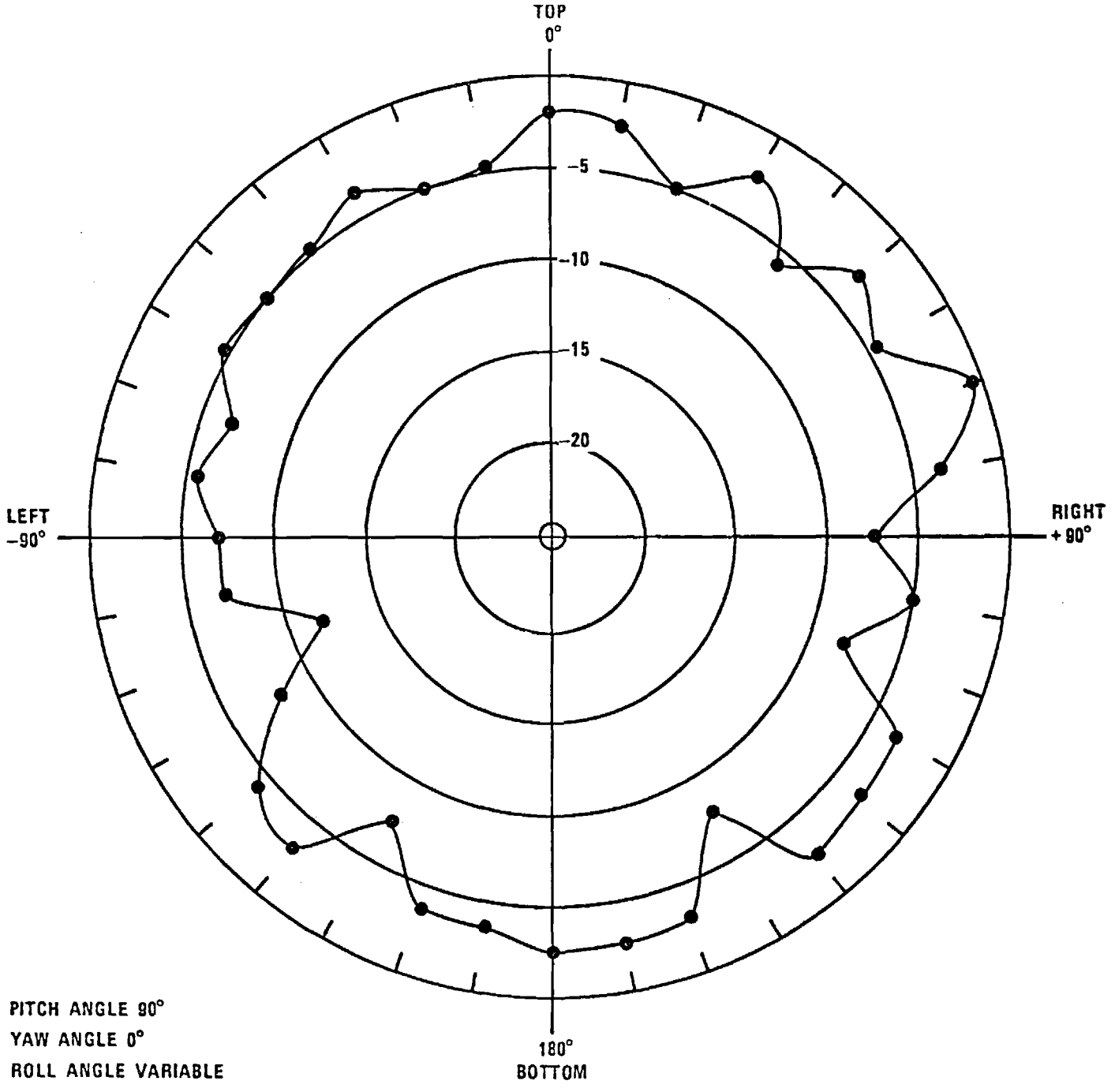

Figure 41. Principal Plane Plot, TDU-X Scoring Antennas, Vertical Polarization, Two Antennas at Top and Bottom

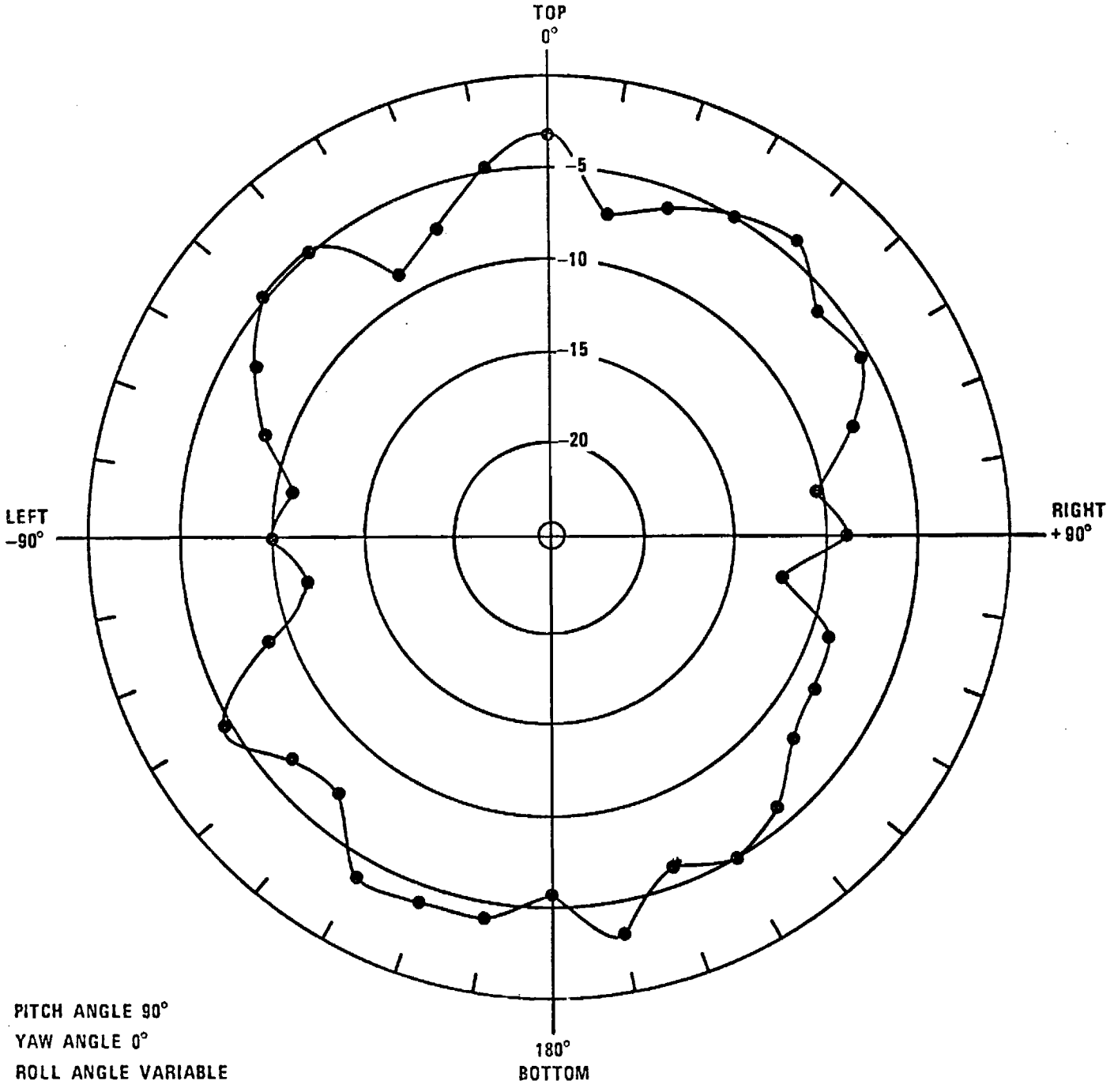

Figure 42. Principal Plane Plot, TDU-X Scoring Antennas, Horizontal Polarization, Two Antennas Located at Top and Bottom

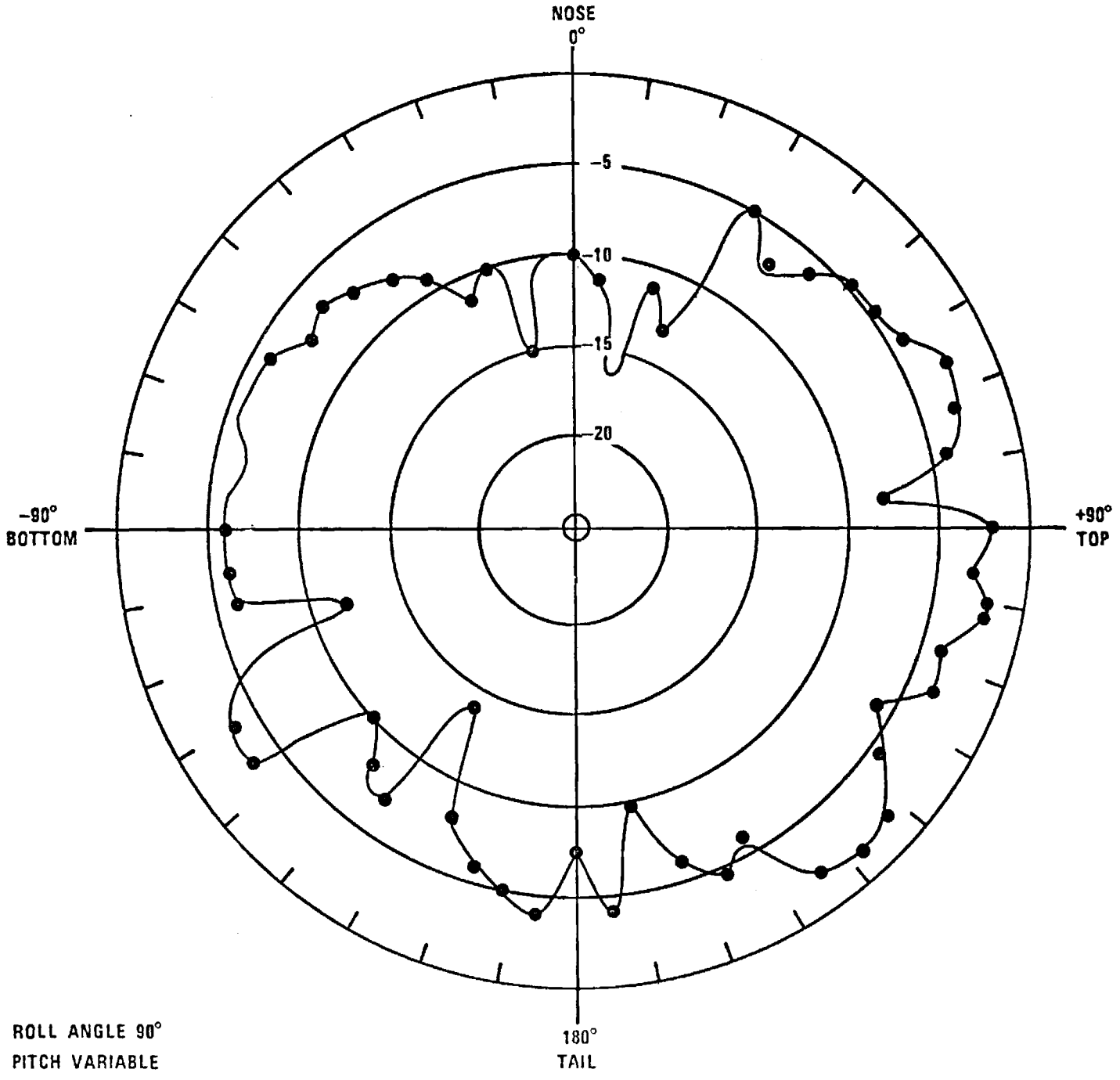

Figure 43. Principal Plane Plot, TDU-X Scoring Antennas, Vertical Polarization, Two Antennas at Top and Bottom

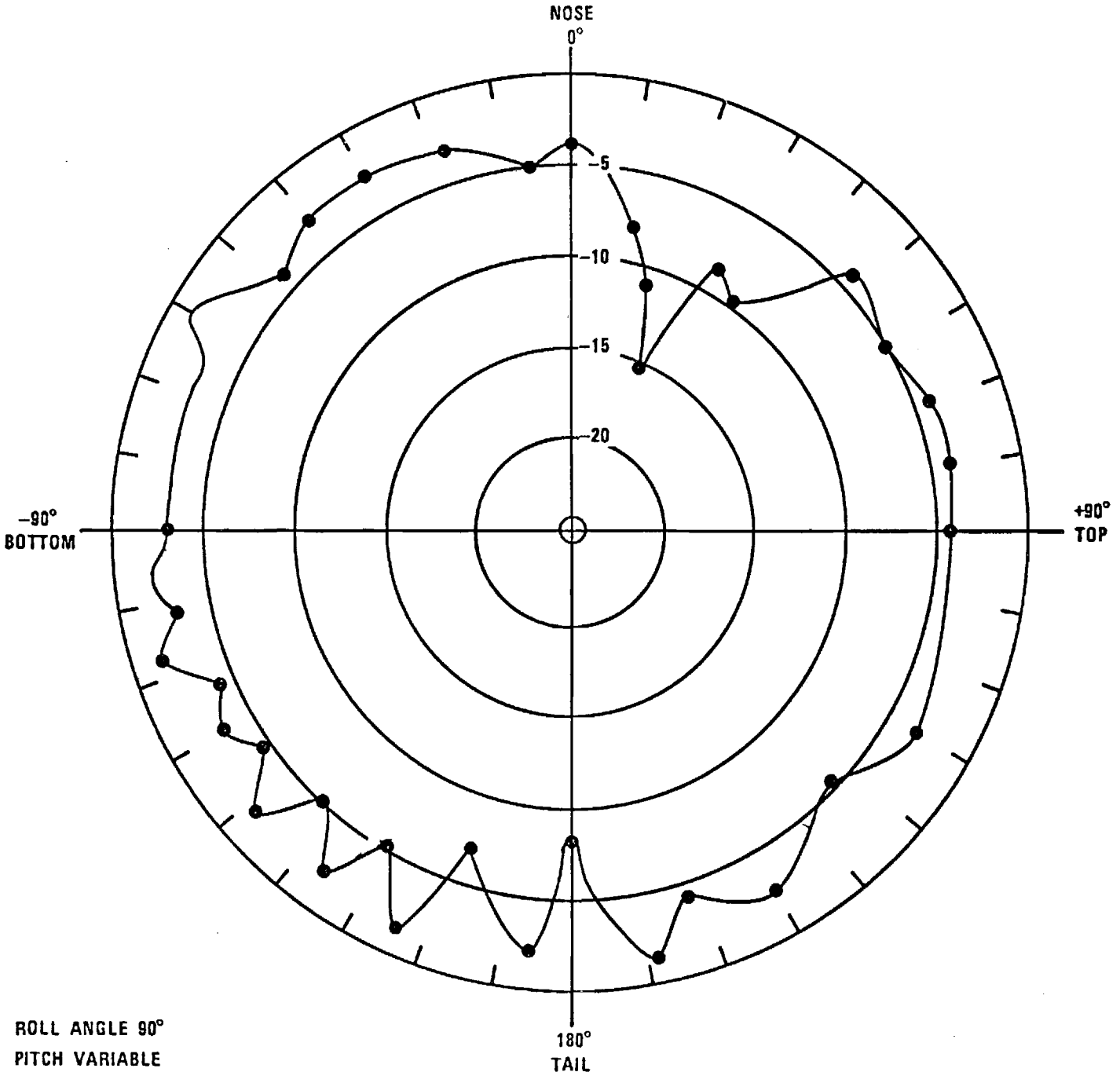

Figure 44. Principal Plane Plot, TDU-X Scoring Antennas, Horizontal Polarization, Two Antennas at Top and Bottom

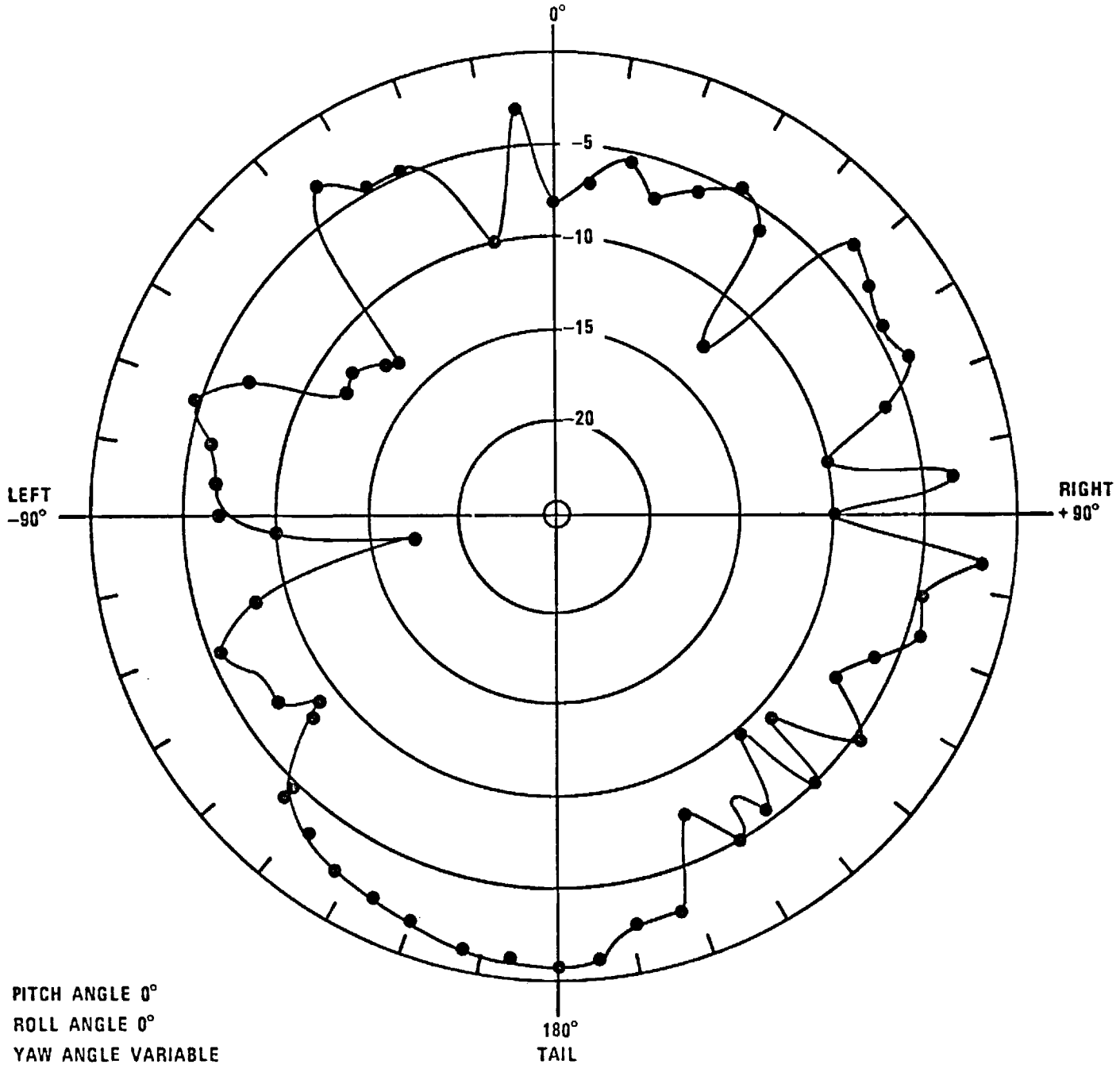

Figure 45. Principal Plane Plot, TDU-X Scoring Antennas, Vertical Polarization, Two Antennas Located at Top and Bottom

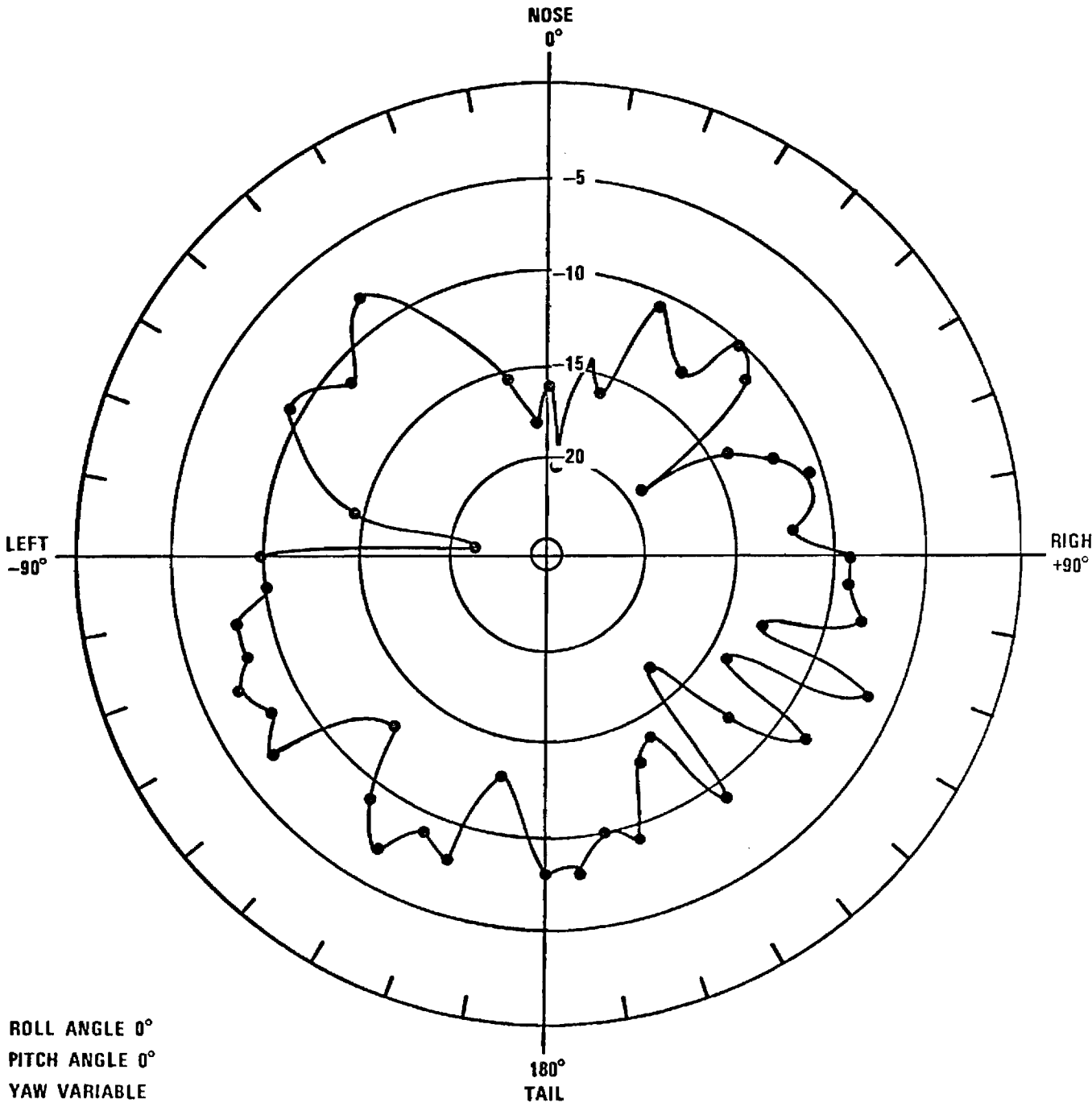

Figure 46. Principal Plane Plot, TDU-X Scoring Antennas, Horizontal Polarization, Two Antennas Located at Top and Bottom

presented herein in two ways. First, the data have been plotted in contours as presented in Figures 47 and 48. These two plots are cylindrical equal spaced projections. The equal spaced projections distort the pattern contours, but the areas near the nose and tail (poles) have been expanded. Since tail coverage was of keen interest, it was felt that this presentation would be best. The plots of Figures 47 and 48 should not be used to determine percentage of total spherical area covered by certain gain contours. The contour plots are based on the measured pattern in the coordinate system of Figure 49.

These contour plots of measured data were graphed in another form as shown in Figures 50 and 51. The second method of presenting the overall data is the 3-D antenna pattern plots as previously presented (see Figure 25).

In all of the scoring antenna plots presented herein, the gain of the antenna (i.e., the gain at the maximum power level) is 0 dB.

(2) Telemetry Antenna - TDU-X

The principal plane scale model radiation patterns of the telemetry antenna are shown in Figures 52 through 55. Both horizontal and vertical polarization are included.

Lower hemispherical coverage was desired and was obtained except for the null directly beneath the antenna, which was expected.

(3) L-Band Augmentation Antenna - TDU-X

The principal plane plots of the forward L-Band antenna are presented in Figures 56 and 57. These patterns are almost identical to those of the telemetry antenna.

Isolation measurements between the telemetry antenna and the L-Band augmentation antenna were made over the L-Band frequency range. Typically, an isolation of 30 dB between these two antenna terminals is maintained over this frequency range.

b. BQM-34A Drone

The DIGIDOPS scoring antennas were mounted on the outer edge of the wing-tip pods as indicated in Figure 58. Scale model antenna

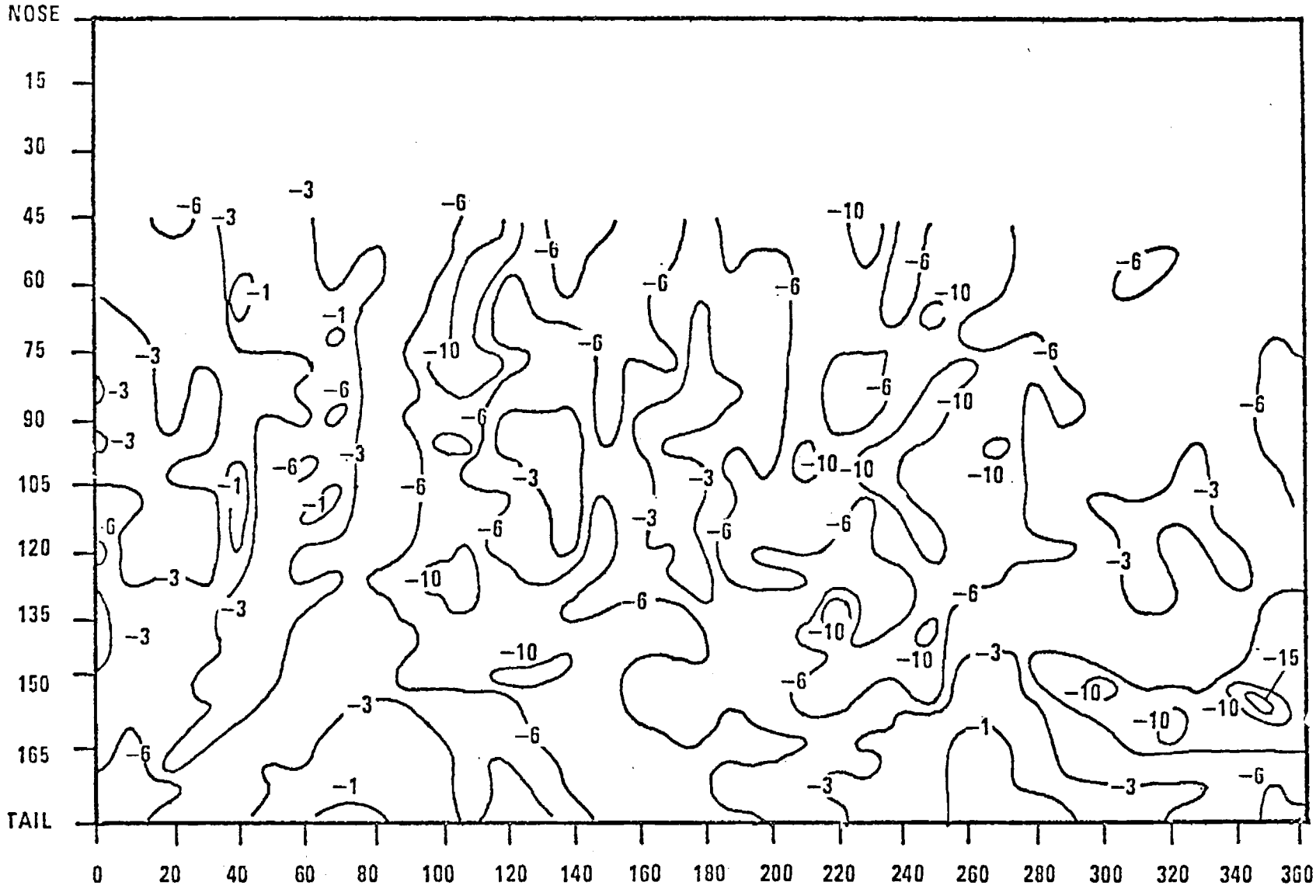

Figure 47. Radiation Pattern Contour Plot, TDU-X Scoring Antennas, Vertical Polarization

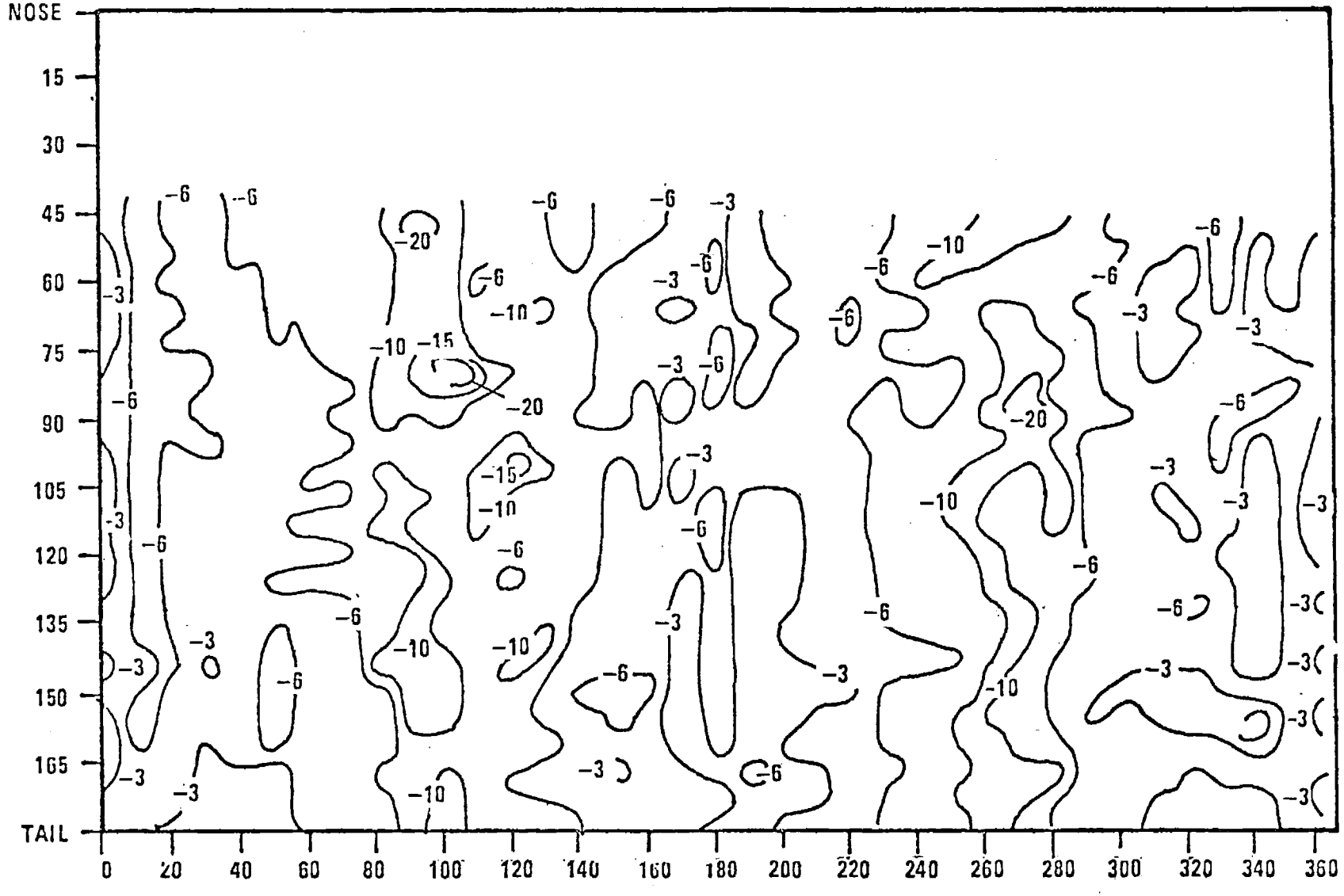

Figure 48. Radiation Pattern Contour Plot, TDU-X Scoring Antennas, Horizontal Polarization

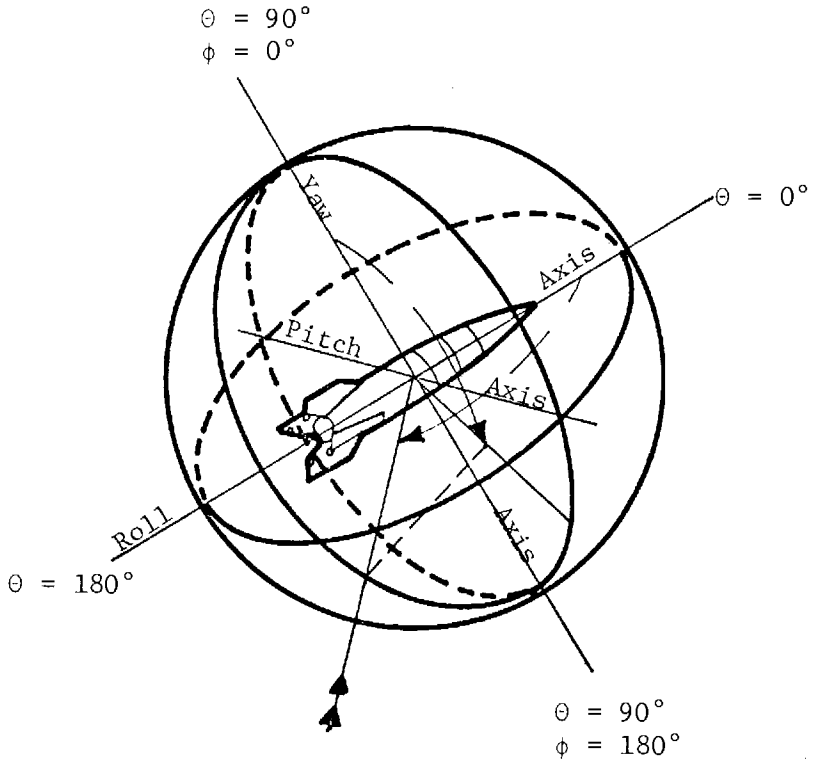

Figure 49. Coordinate System to Interpret Radiation Pattern Contour Plots

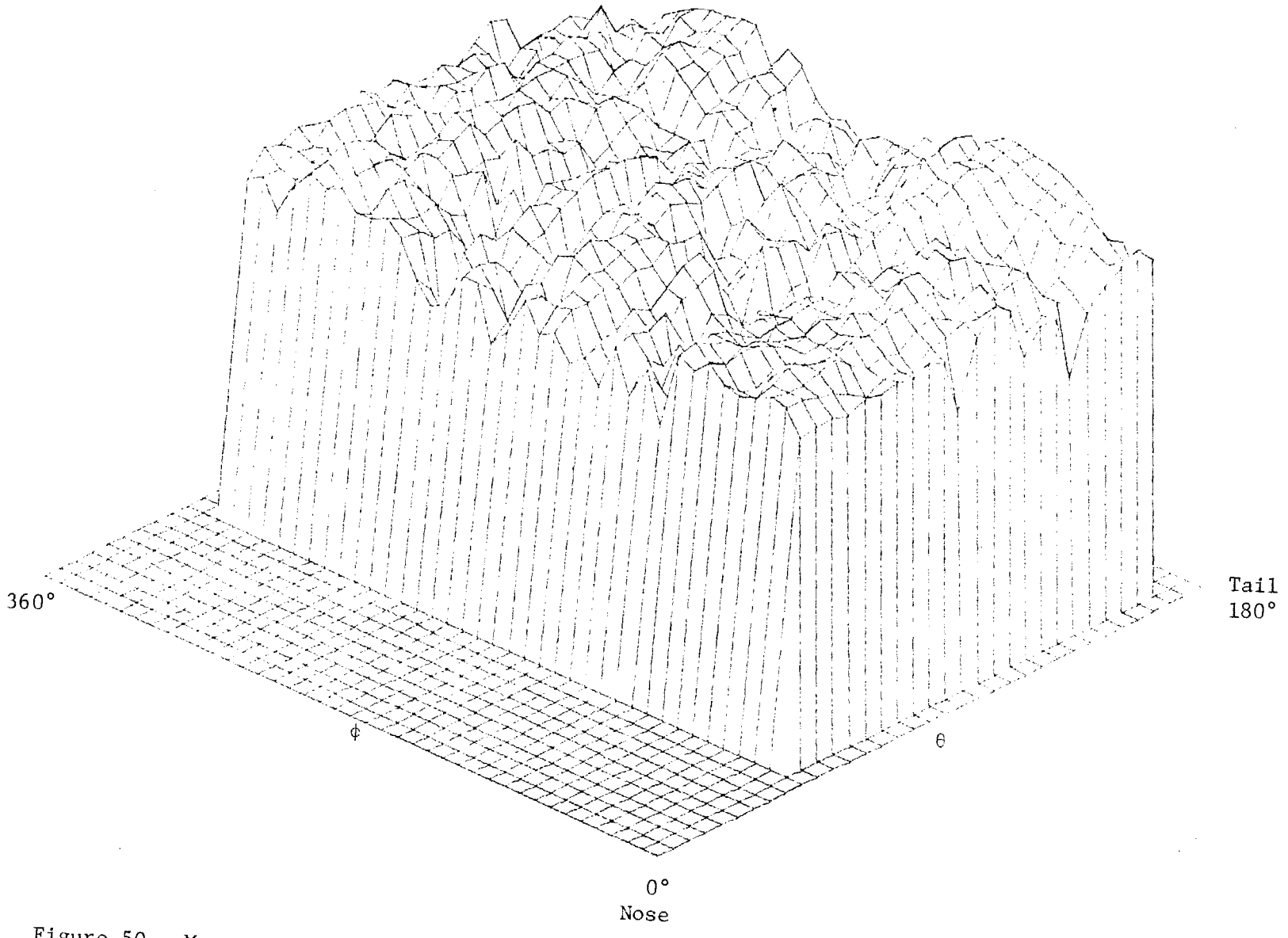

Figure 50. Measured Radiation Pattern Data for TDU-X Scoring Antennas (E_θ). Two Antennas Located at Top and Bottom

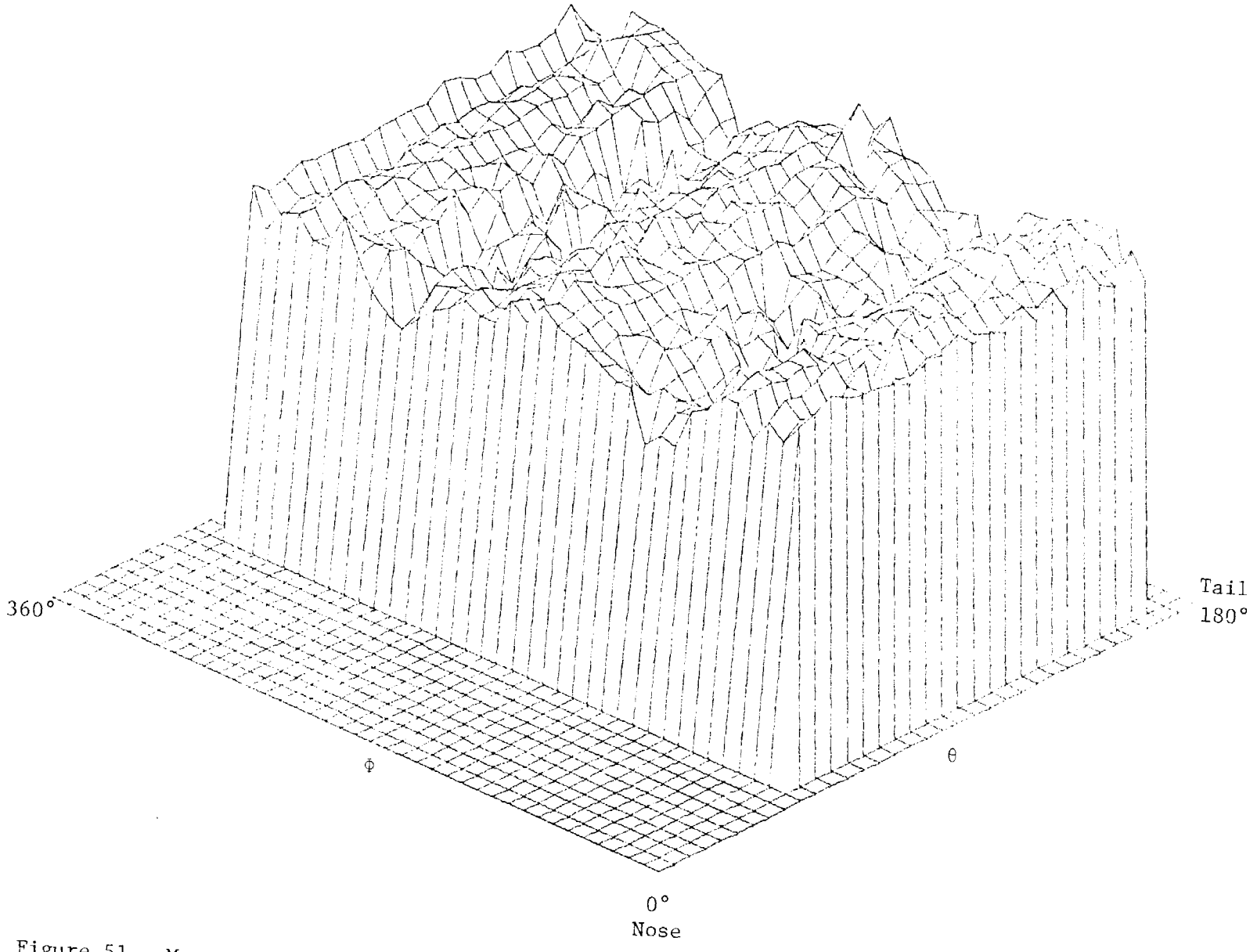

Figure 51. Measured Radiation Pattern Data for TDU-X Scoring Antenna (E_ϕ). Two Antennas Located at Top and Bottom

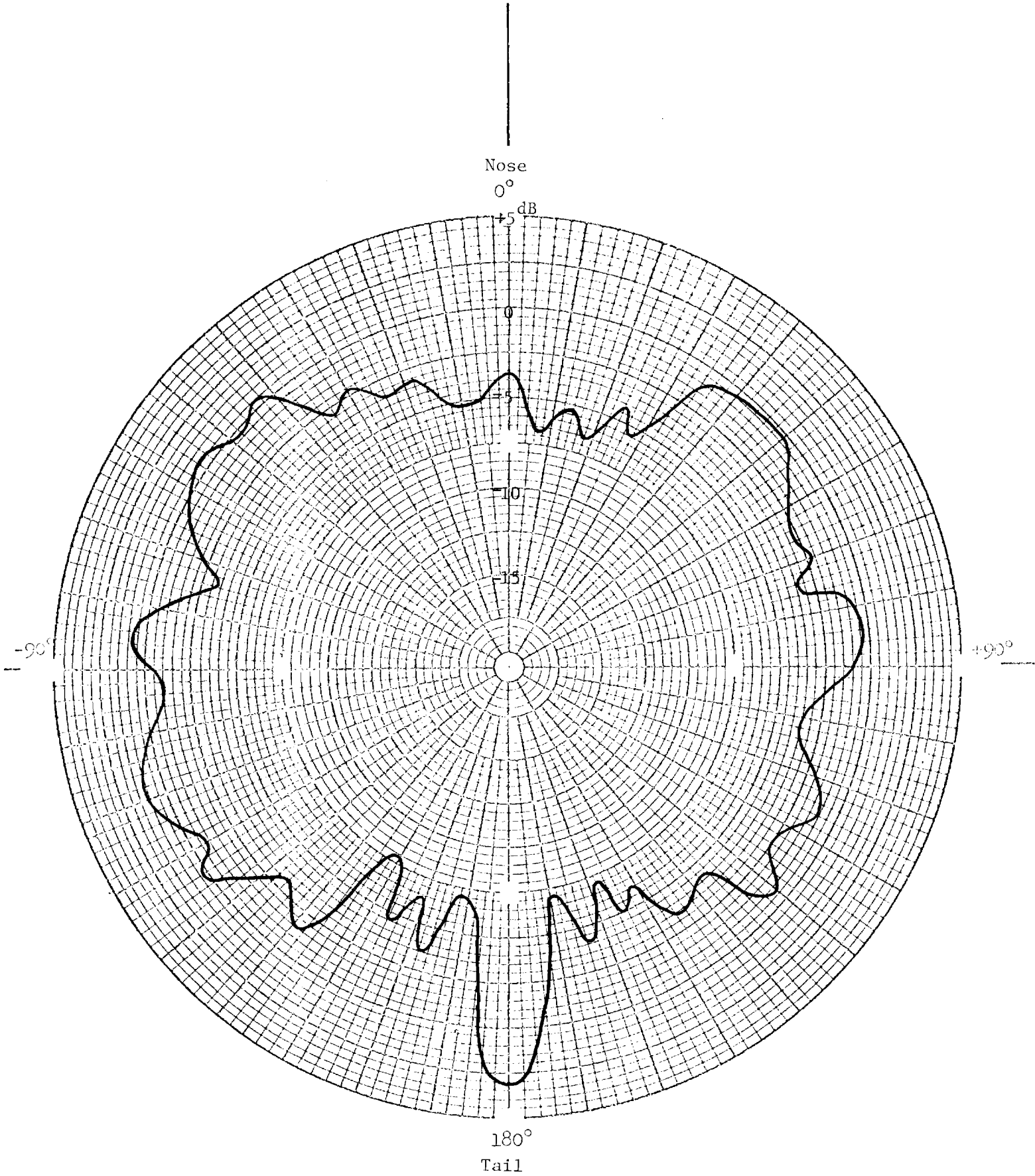

Figure 52. TDU-X Telemetry Antenna Radiation Pattern, Vertical Polarization, Roll and Pitch Angle 0°, Yaw Angle Variable

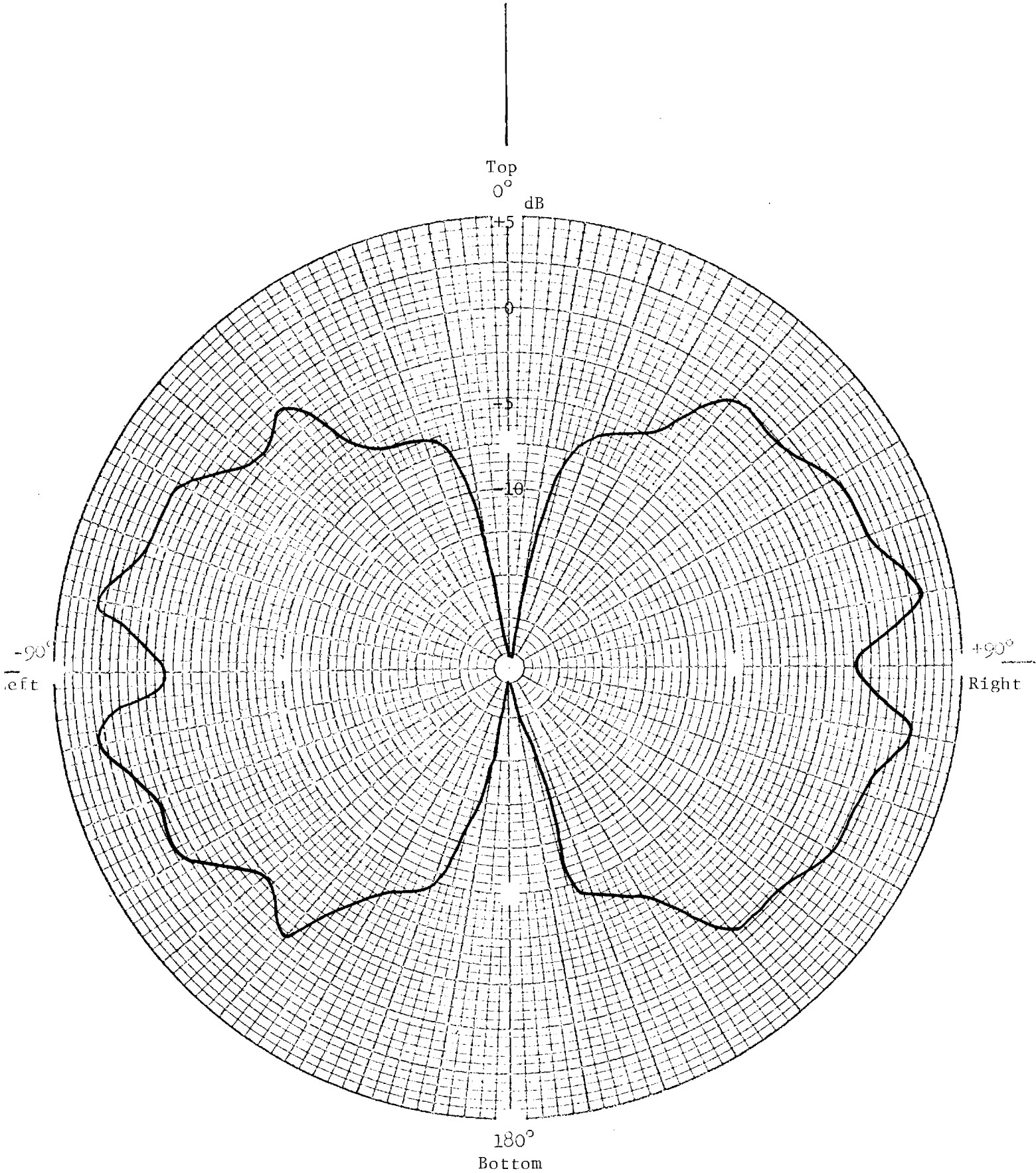

Figure 53. TDU-X Telemetry Antenna Radiation Pattern, Vertical Polarization, Pitch and Yaw Angles 0°, Roll Angle Variable

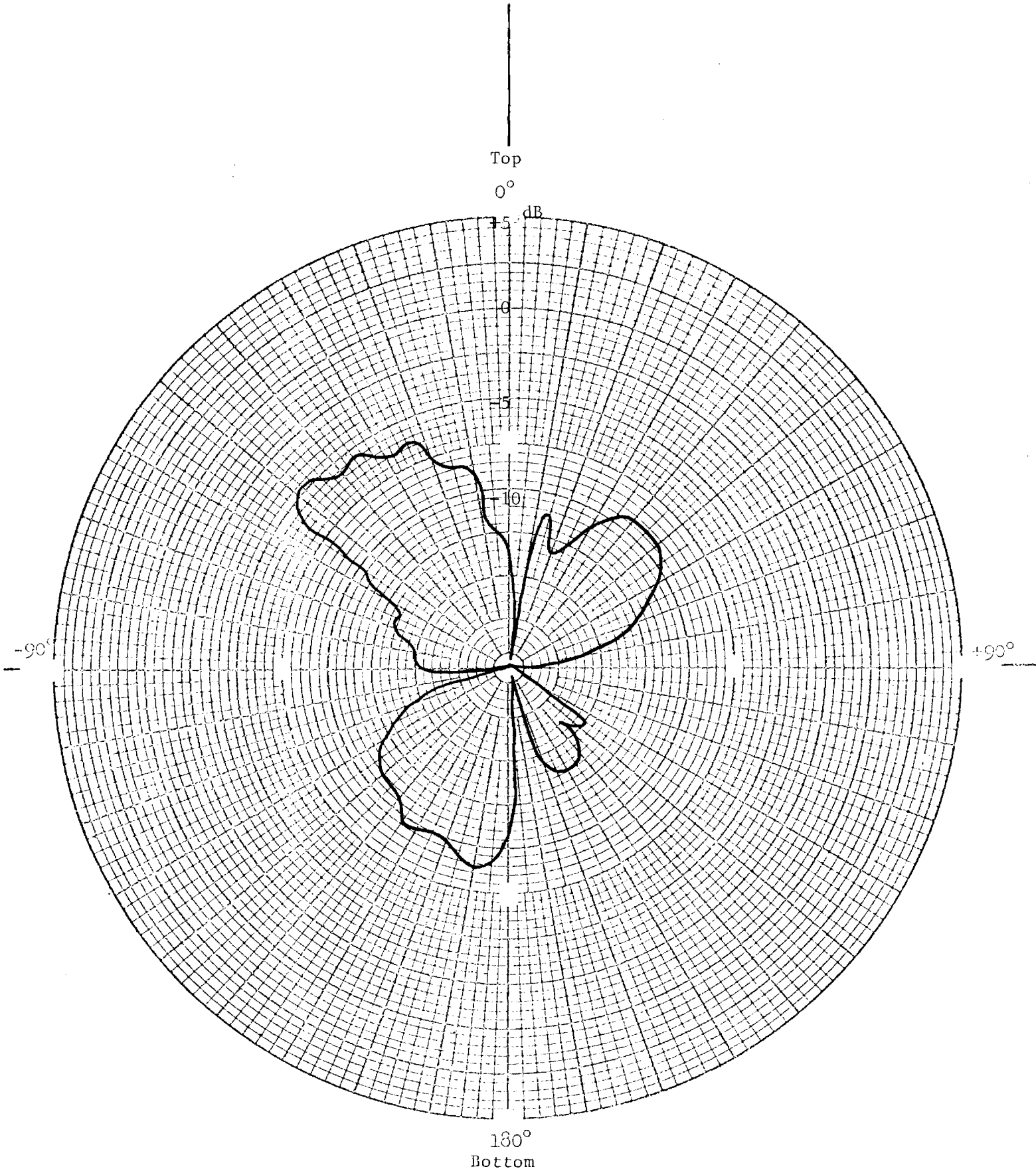

Figure 54. TDU-X Telemetry Antenna Radiation Pattern, Horizontal Polarization, Variable Yaw Angle

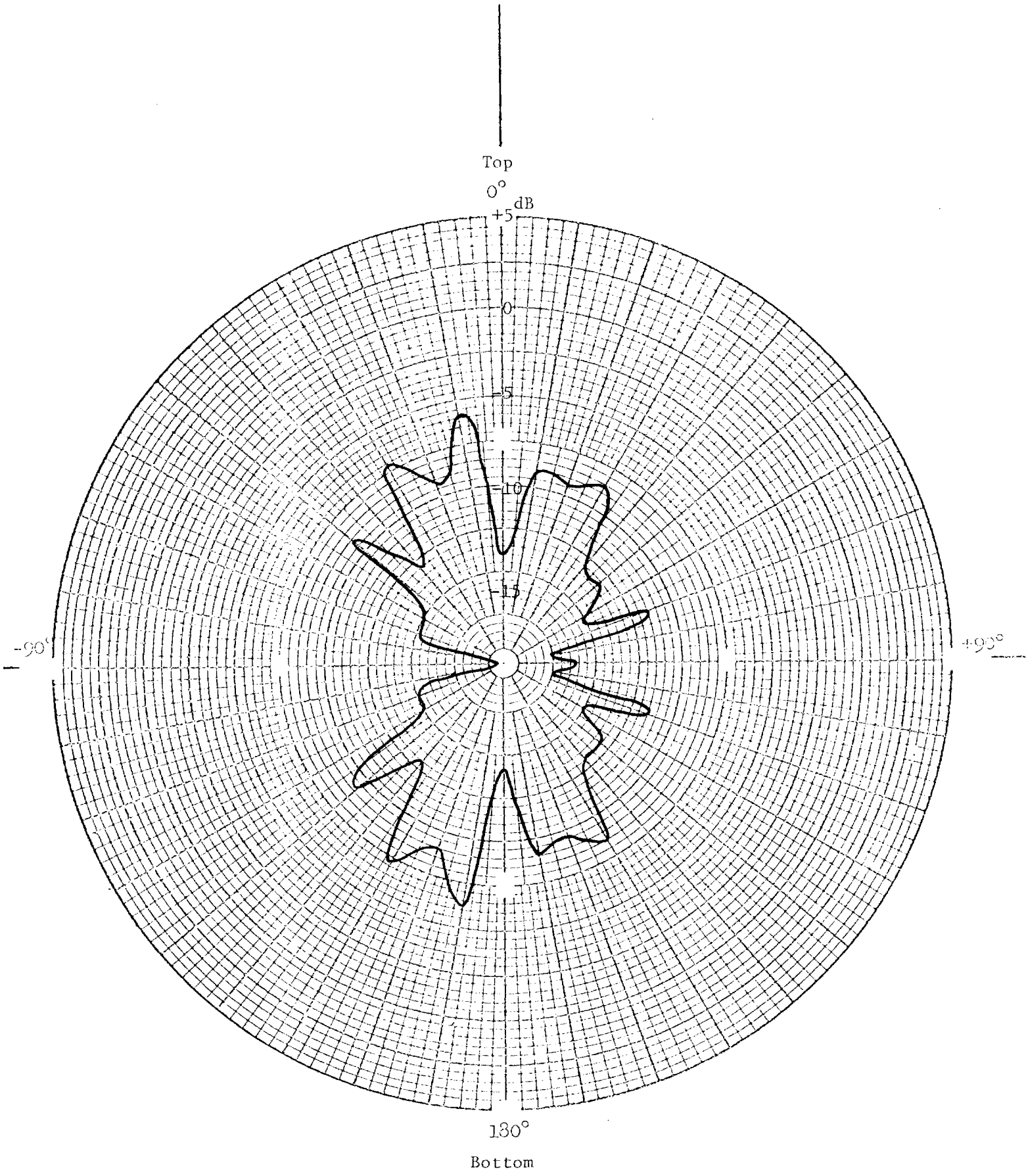

Figure 55. TDU-X Telemetry Antenna Radiation Pattern, Horizontal Polarization, Variable Roll Angle

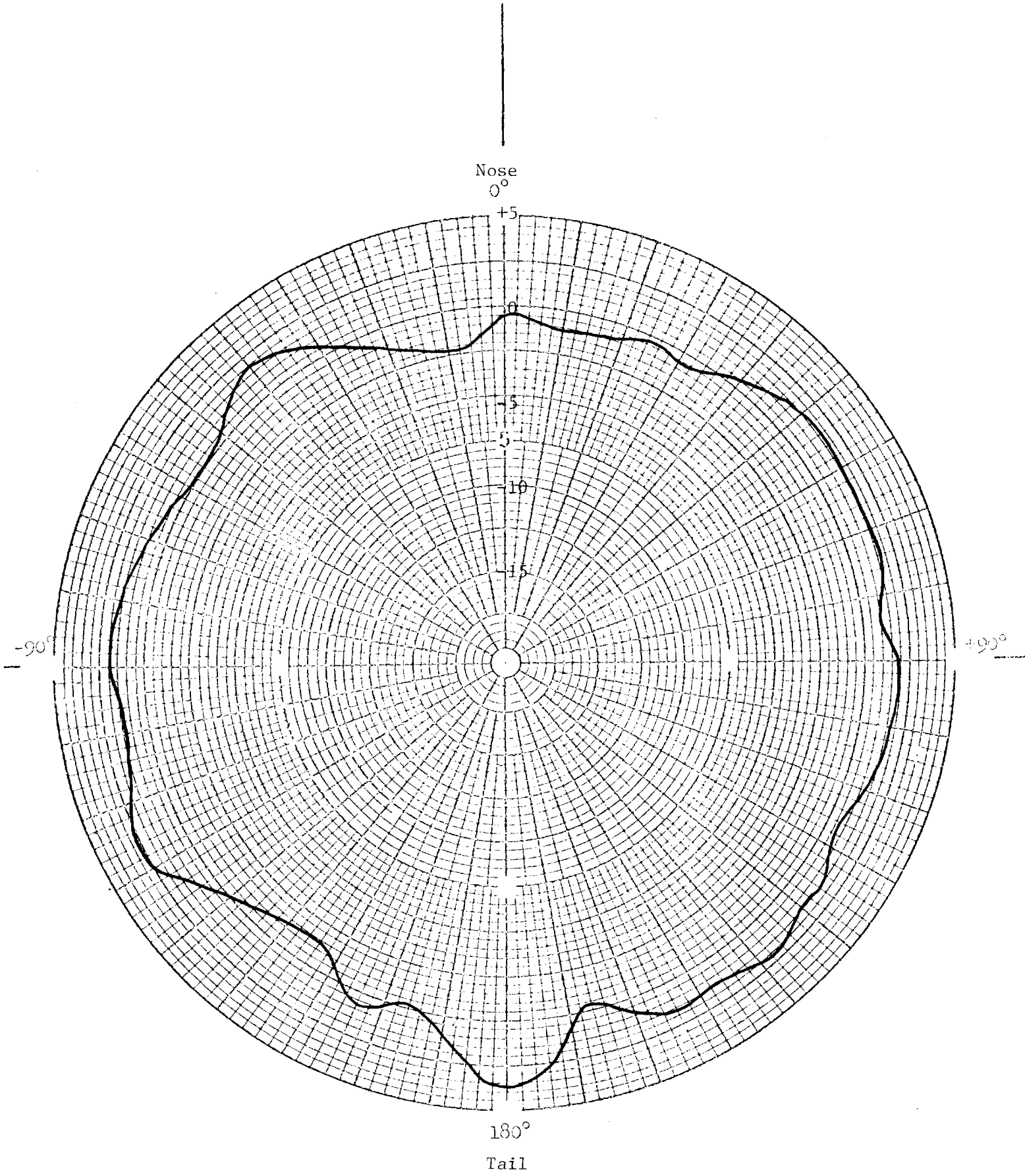

Figure 56. TDU-X L-Band Augmentation Antenna Radiation Pattern, Vertical Polarization, Variable Yaw Angle

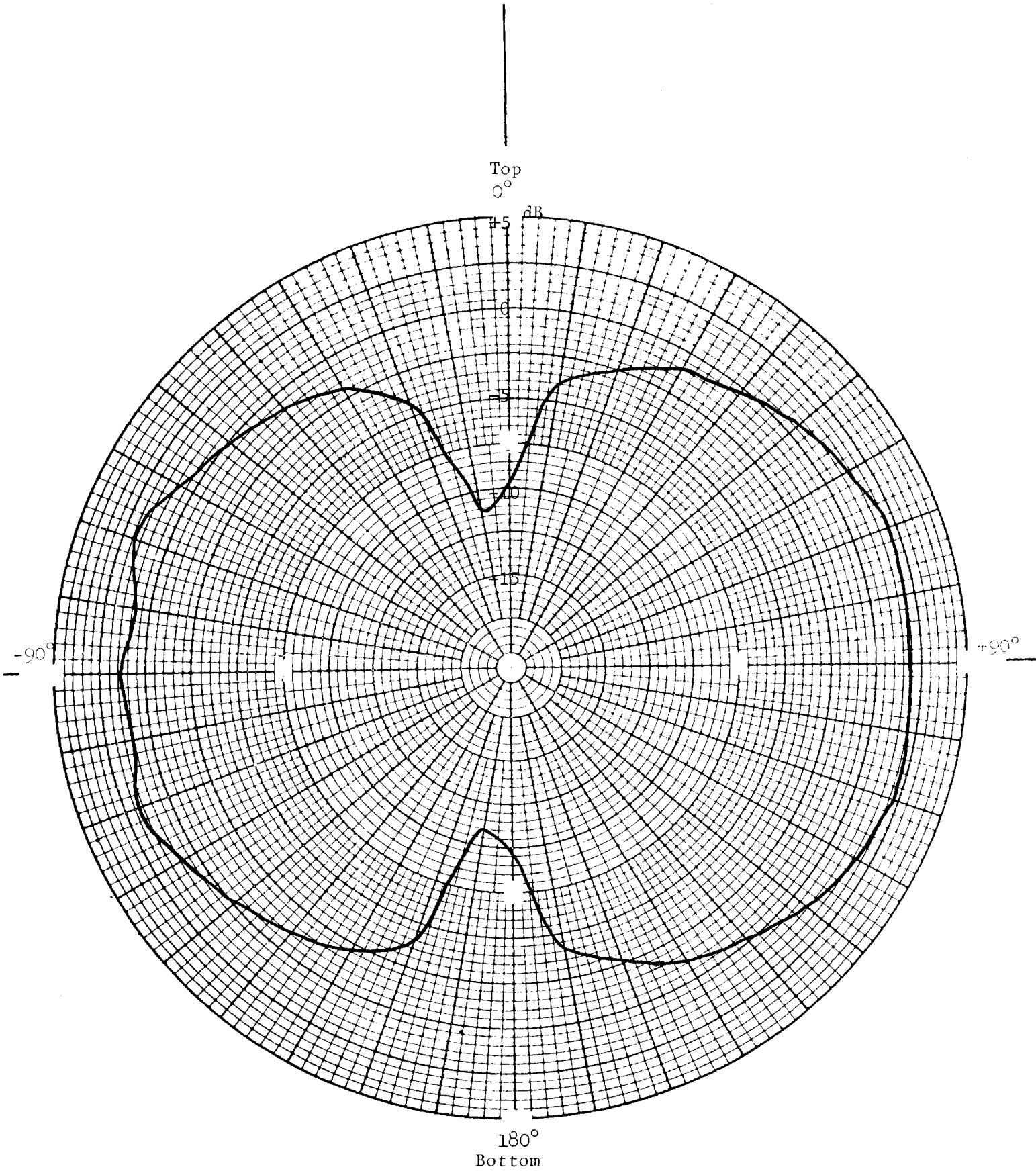

Figure 57. TDU-X L-Band Augmentation Antenna Radiation Pattern, Vertical Polarization, Variable Roll Angle

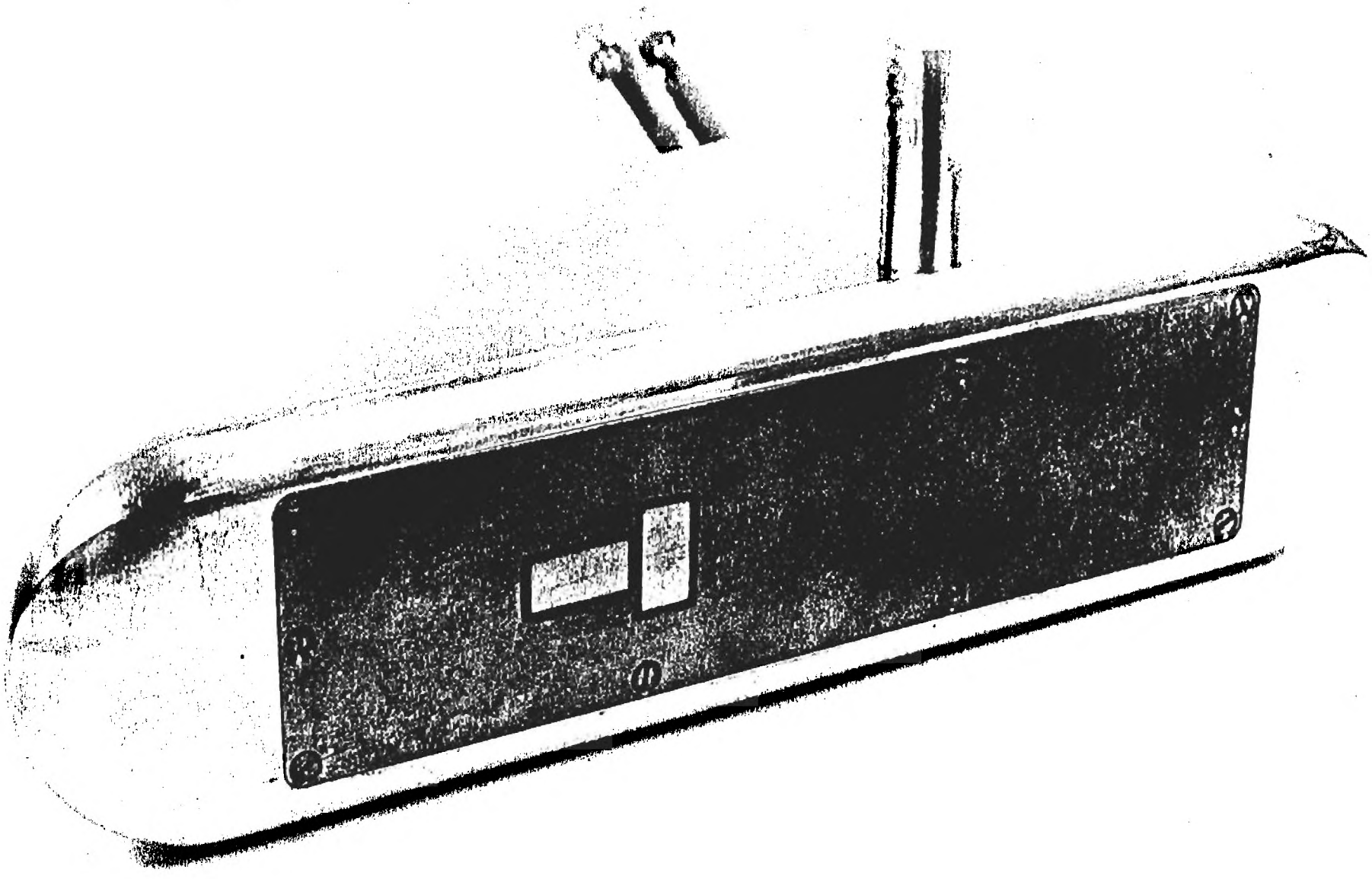

Figure 58. Photograph of Scale Model BQM-34A Pod with Scoring Antennas.

pattern measurements were taken on one T-slot antenna mounted on the pod without utilizing the main body as a part of the ground. Principal plane radiation pattern measurements for the scale model antenna (one antenna only) are shown in Figures 59 through 62. Good coverage was obtained from the antenna only on the side of the drone where the antenna was mounted. It is felt that the two antennas, each mounted on the outboard side of the wing-tip pods, will act independently of one another.

c. BOMARC Scoring Antennas

The scaled antennas were mounted onto a one-eighth scale mode BOMARC missile for the radiation pattern measurements. The antennas were mounted on the left and right sides of the fuselage and forward of the wings at the station recommended by AFATL. Radiation patterns were measured in the yaw plane with the roll angle at 0°, 45°, and 90°. Presented in Figures 63 and 64 are the horizontal polarization plots for the 0° and 90° roll angle cases. The pattern coverage is excellent except for small regions off the nose and the tail.

d. Full-Scale Measurements

Two X-Band antennas, the cylindrically shaped antenna and the conical spiral, were each mounted on a cylindrical ground plane for pattern measurements. The cylindrical antenna had good omni-directional coverage, as expected, whereas the conical spiral possessed a narrower beamwidth which made it directional. Two principal plane radiation patterns of the conical spiral are presented in Figures 65 through 68, which include both linear polarizations. This particular antenna provides the design antenna pattern coverage.

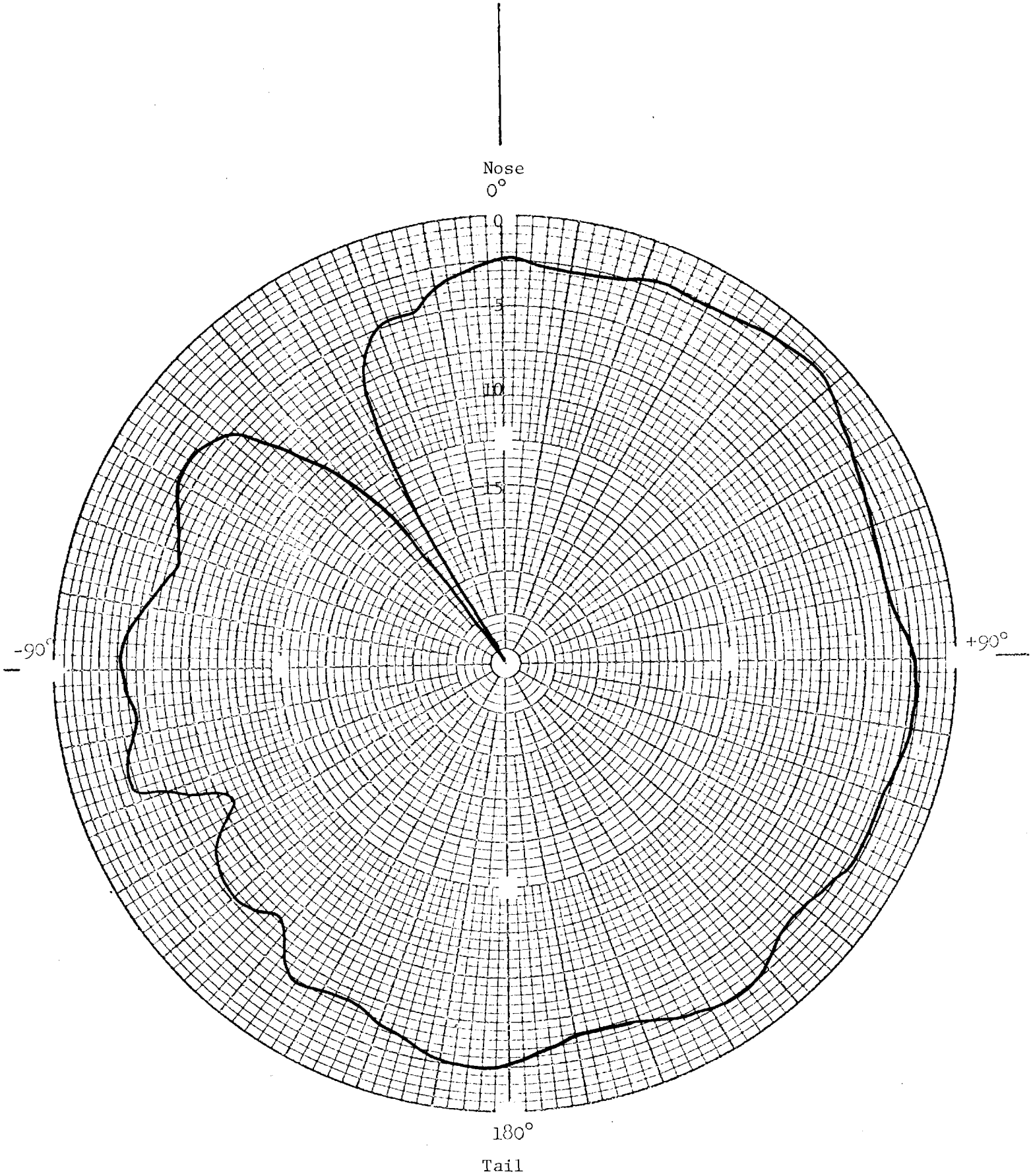

Figure 59. BQM-34A Scoring Antenna Radiation Pattern, Vertical Polarization, Variable Yaw Angle

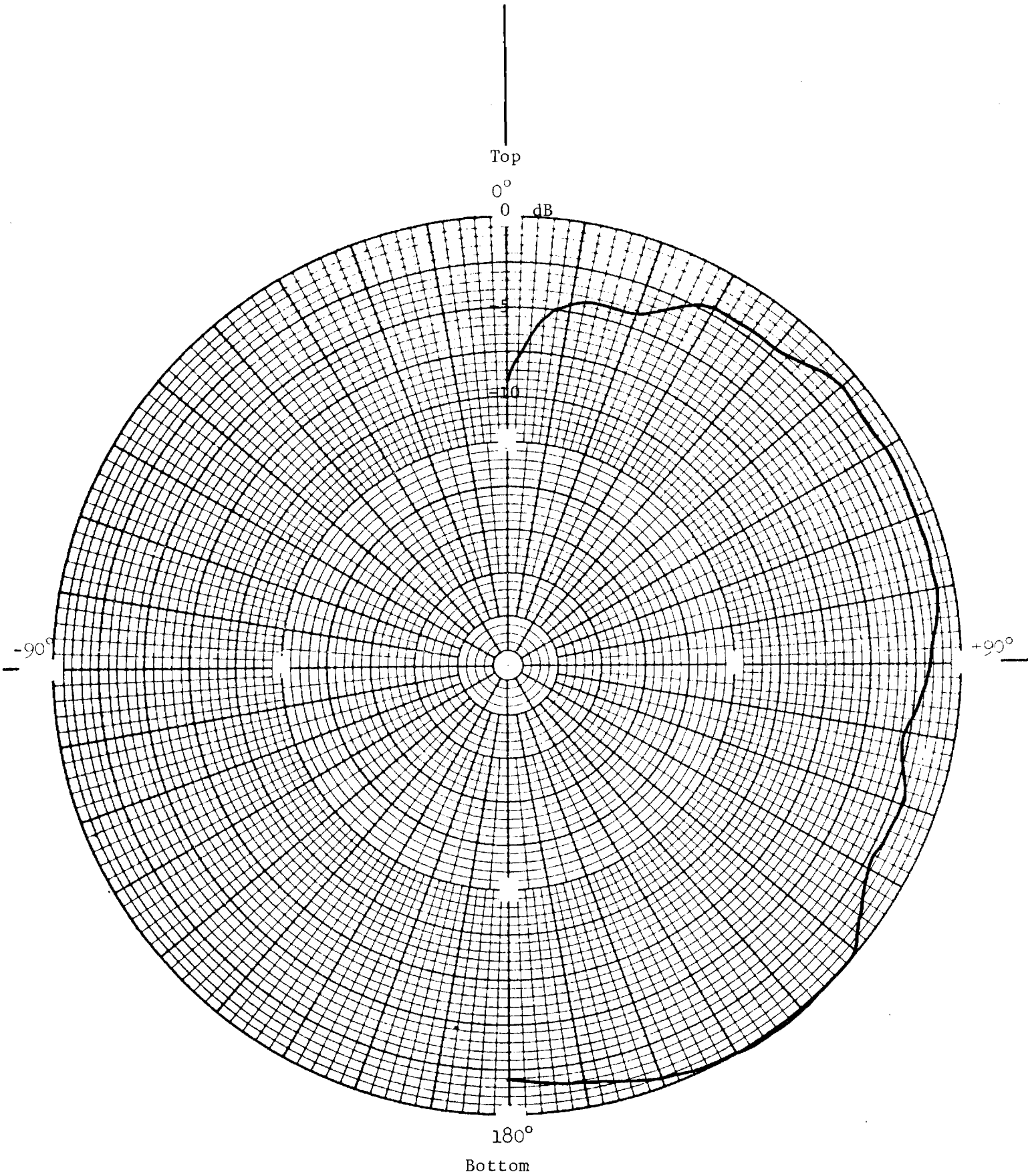

Figure 60. BQM-34A Scoring Antenna Radiation Pattern, Vertical Polarization, Variable Roll Angle

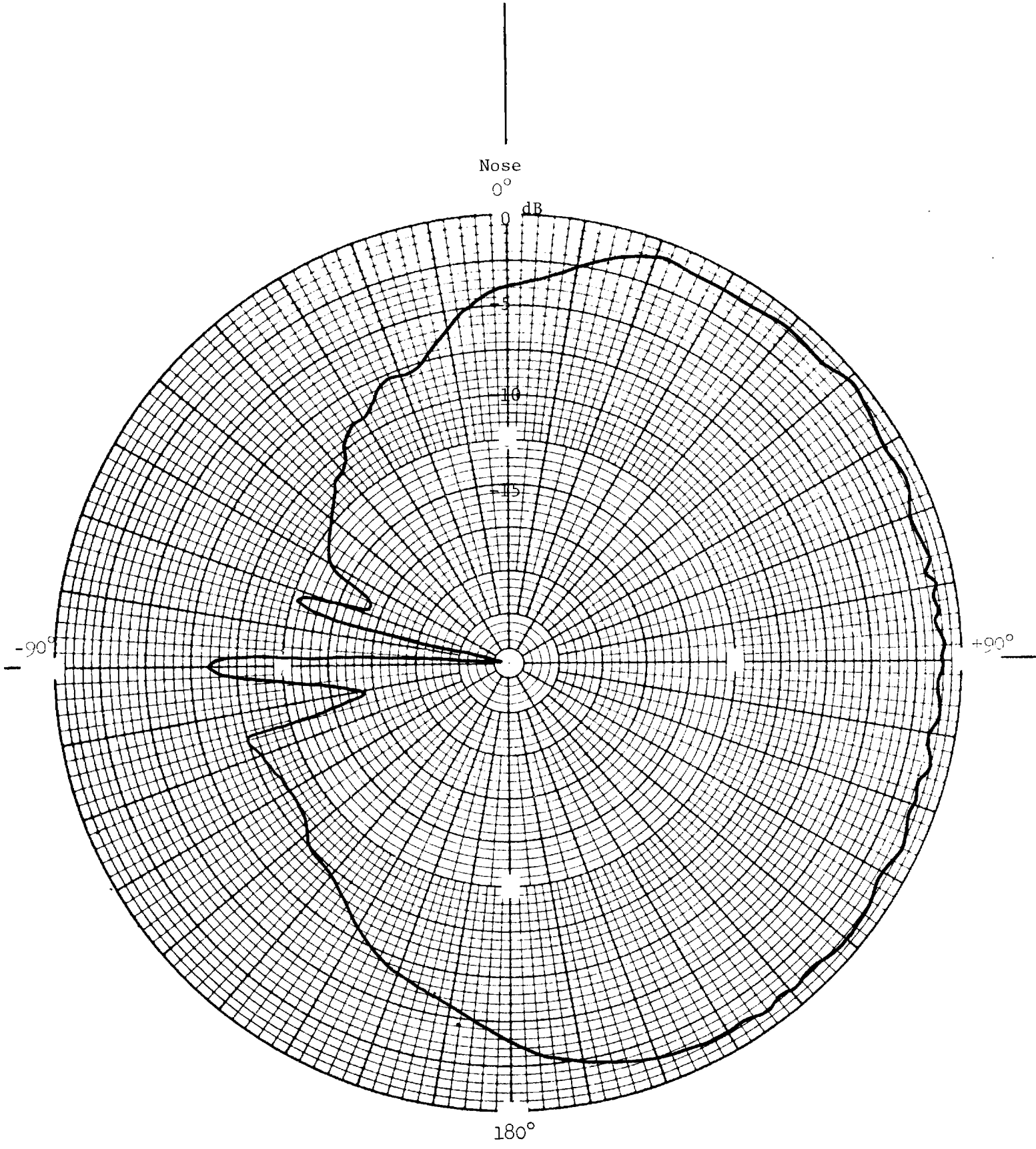

Figure 61. BQM-34A Scoring Antenna Radiation Pattern, Horizontal Polarization, Variable Yaw Angle

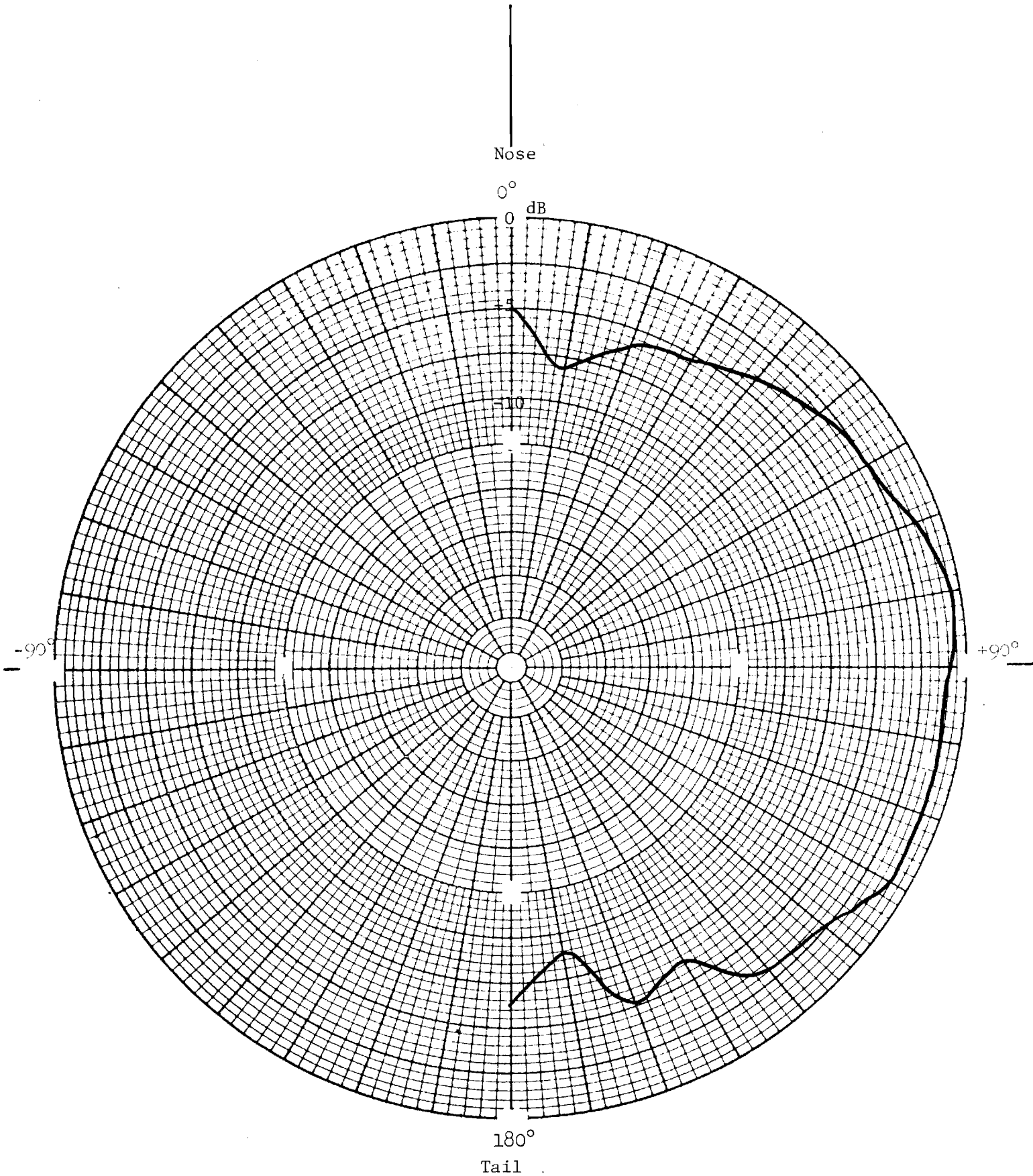

Figure 62. BQM-34A Scoring Antenna Radiation Pattern, Horizontal Polarization, Variable Roll Angle

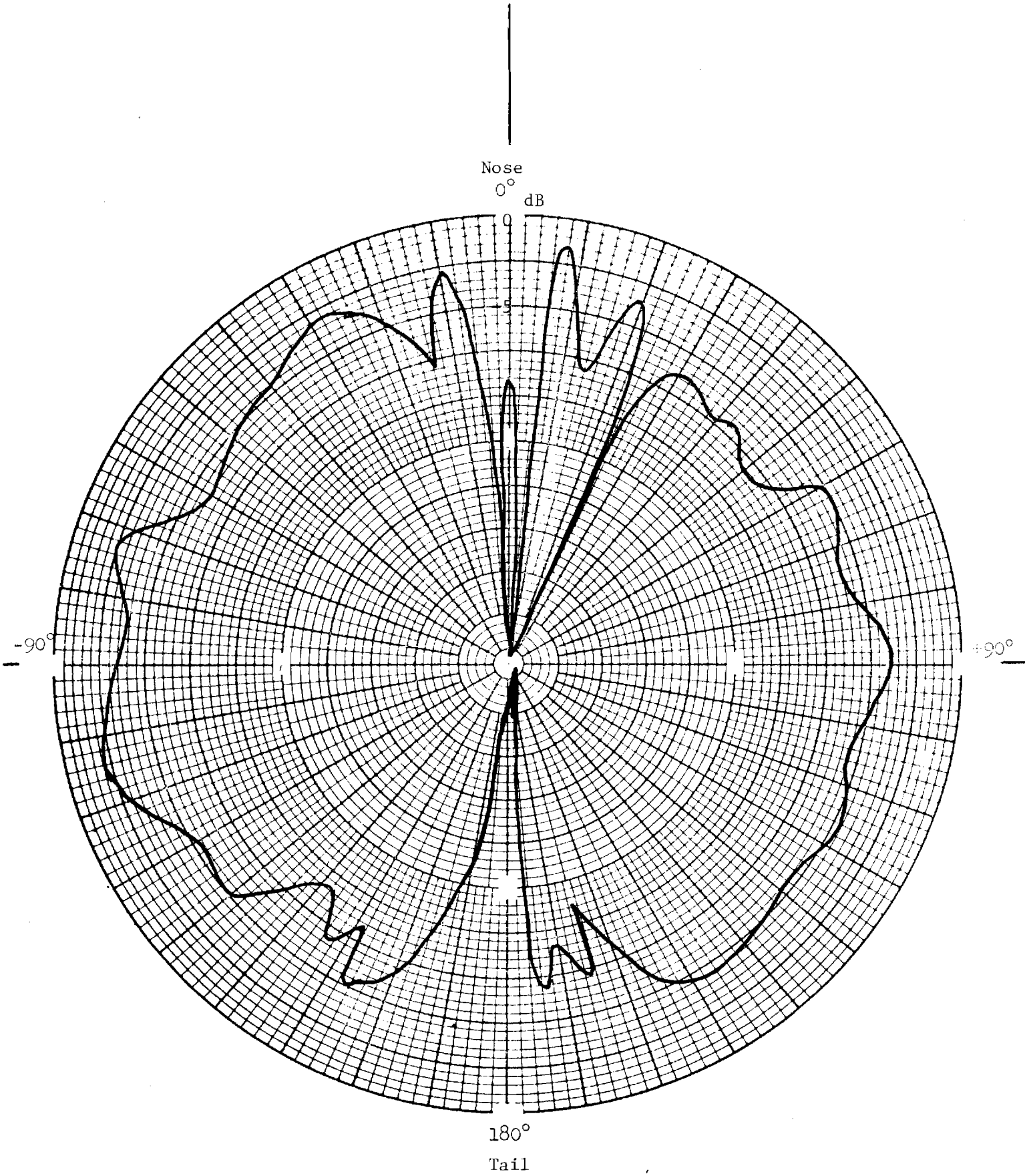

Figure 63. BOMARC Scoring Antenna Radiation Pattern, Horizontal Polarization, Variable Yaw Angle

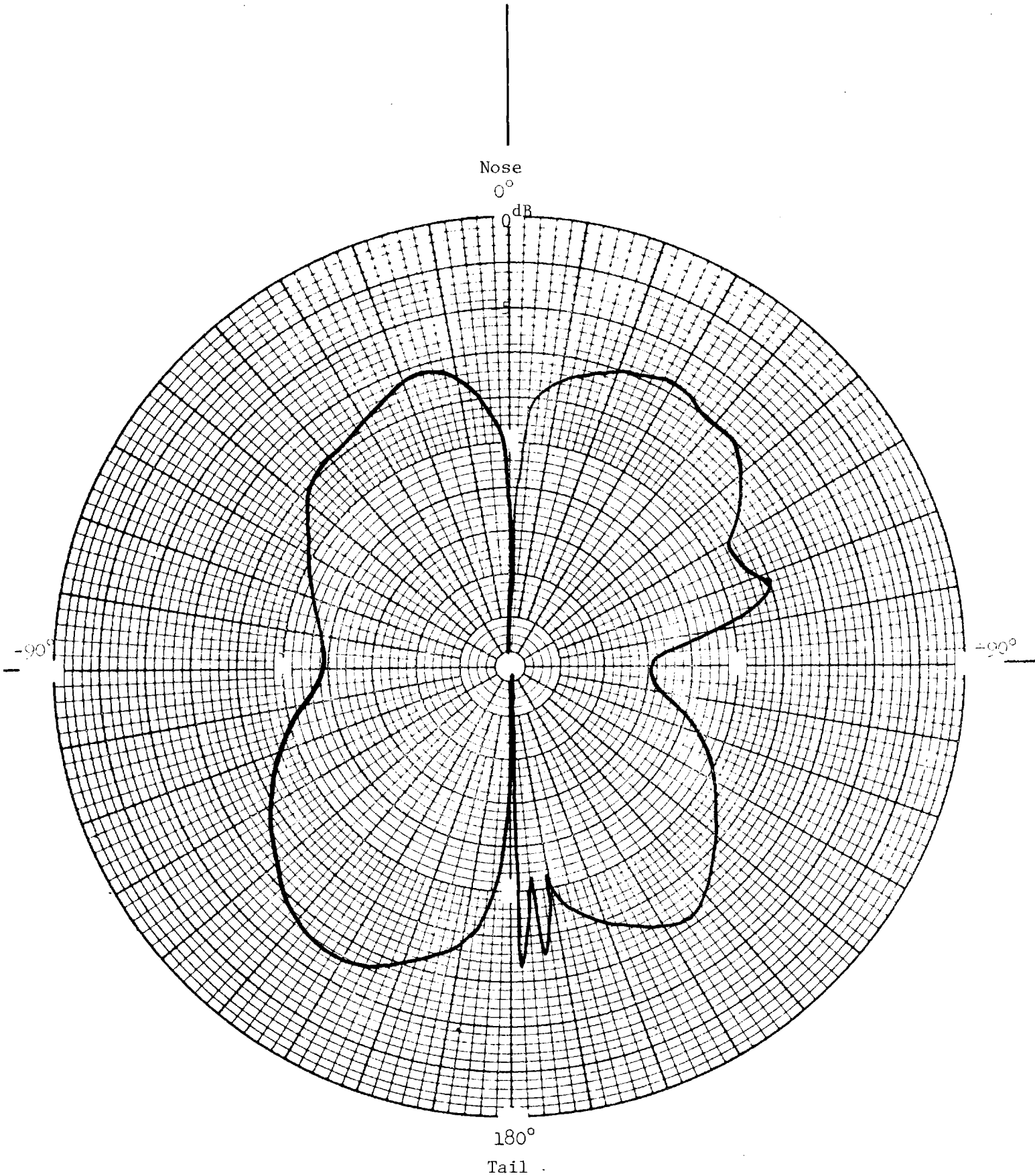

Figure 64. BOMARC Scoring Antenna Radiation Pattern, Horizontal Polarization, Roll Angle 90°, Variable Yaw Angle

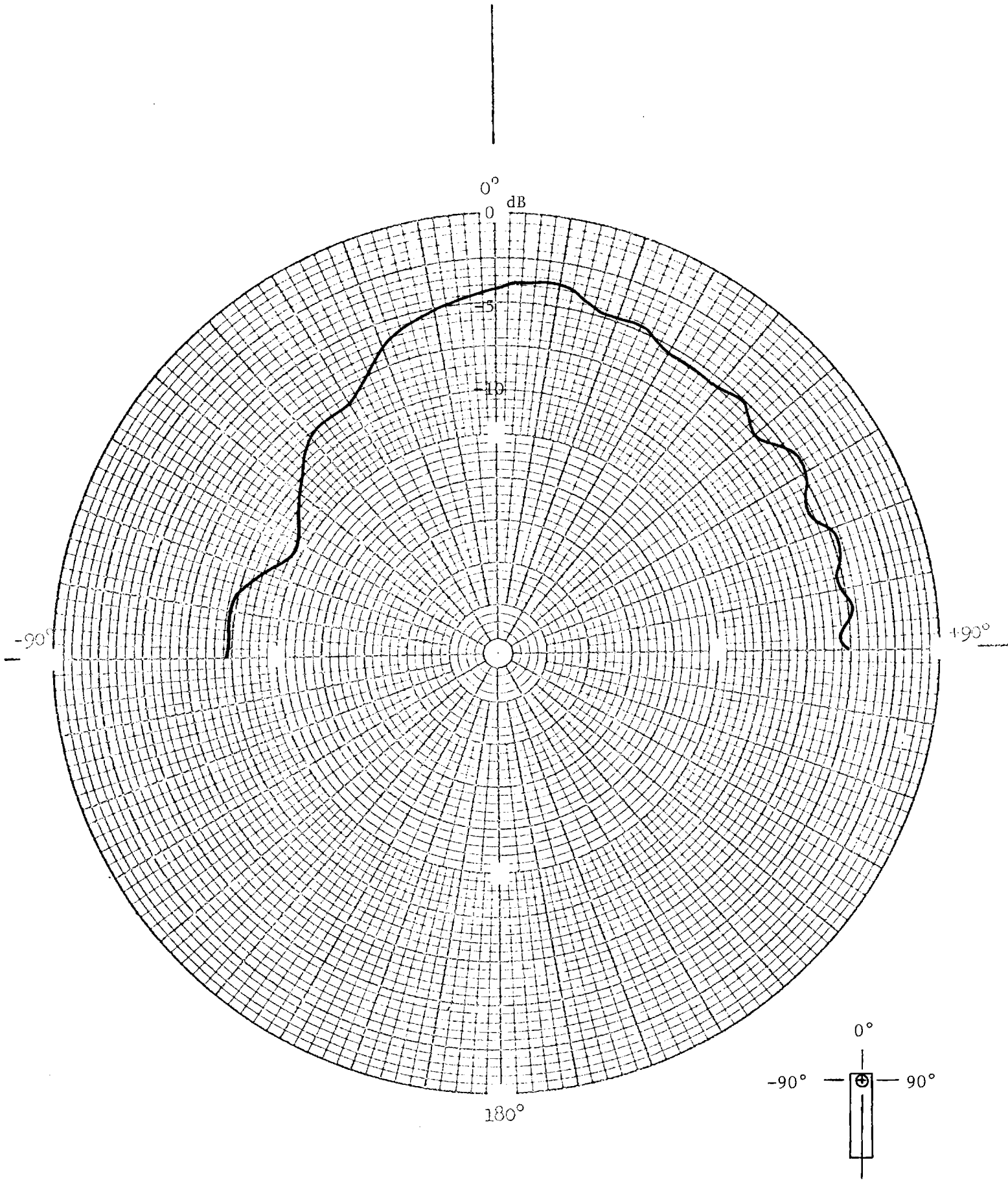

Figure 65. Conical Spiral Radiation Pattern on 14-inch Diameter Cylinder, Vertical Polarization, Variable Yaw Angle (10 GHz)

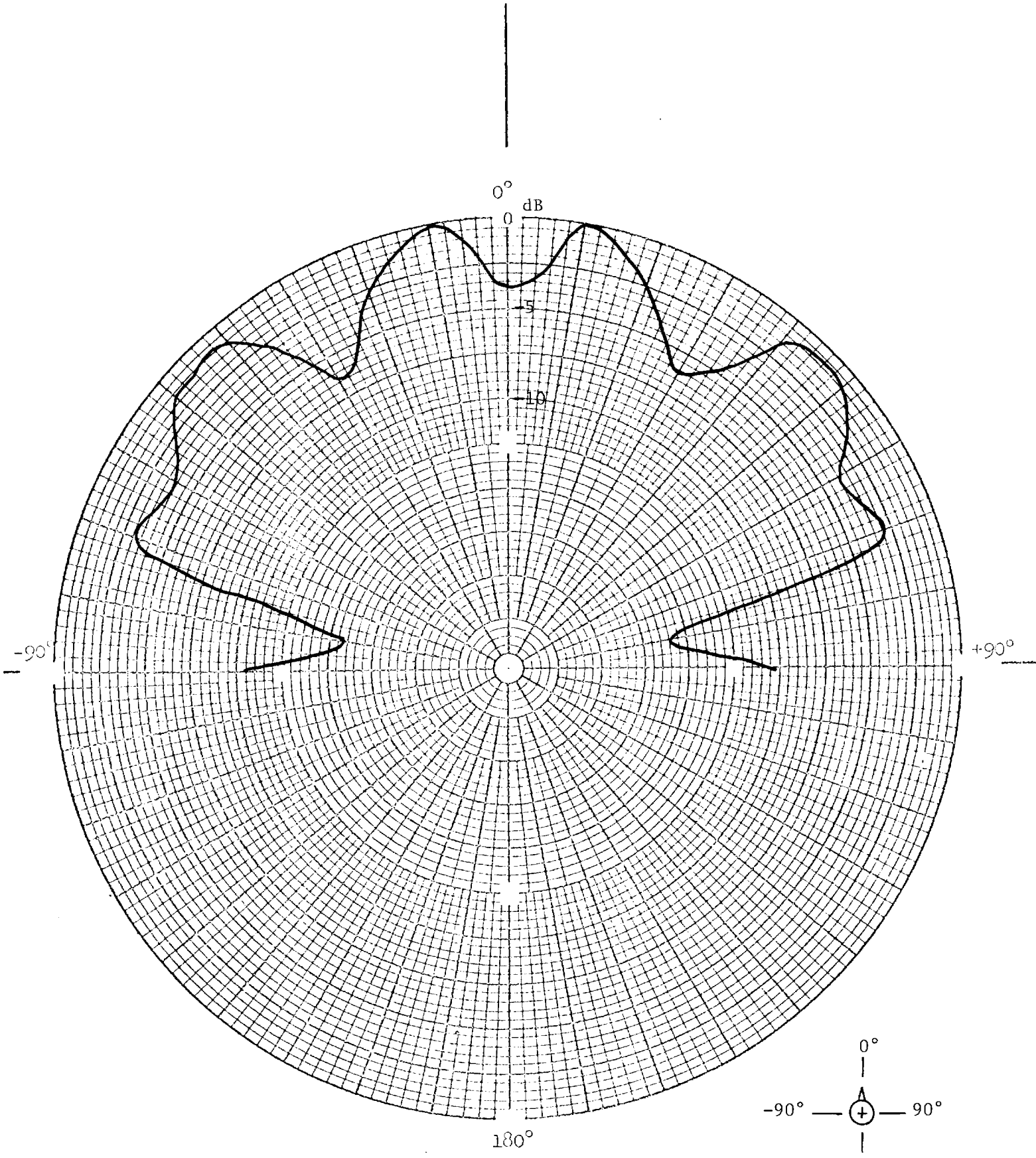

Figure 66. Conical Spiral Radiation Pattern on 14-inch Diameter Cylinder, Vertical Polarization, Variable Roll Angle (10 GHz)

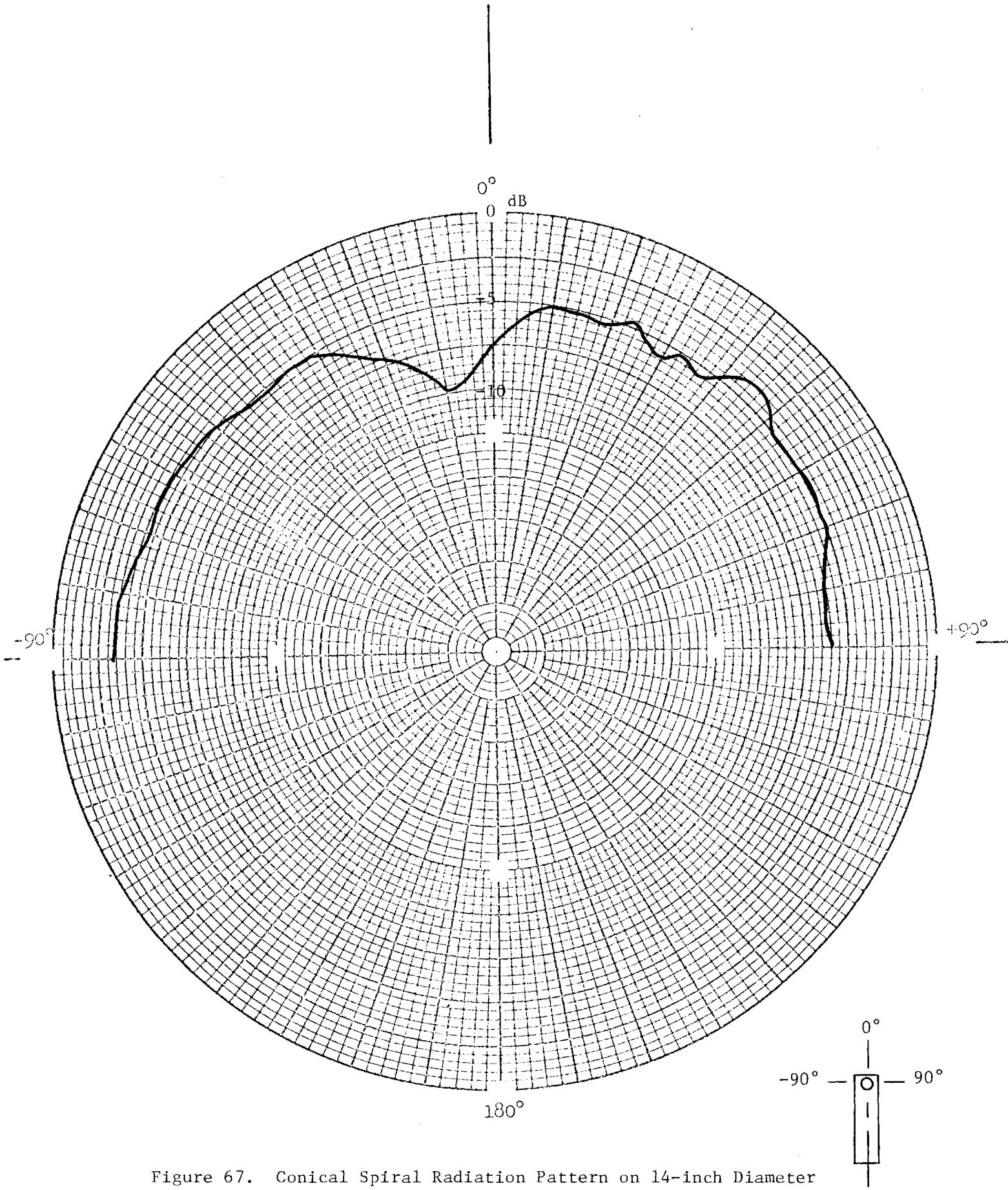

Figure 67. Conical Spiral Radiation Pattern on 14-inch Diameter Cylinder, Horizontal Polarization, Variable Yaw Angle (10 GHz)

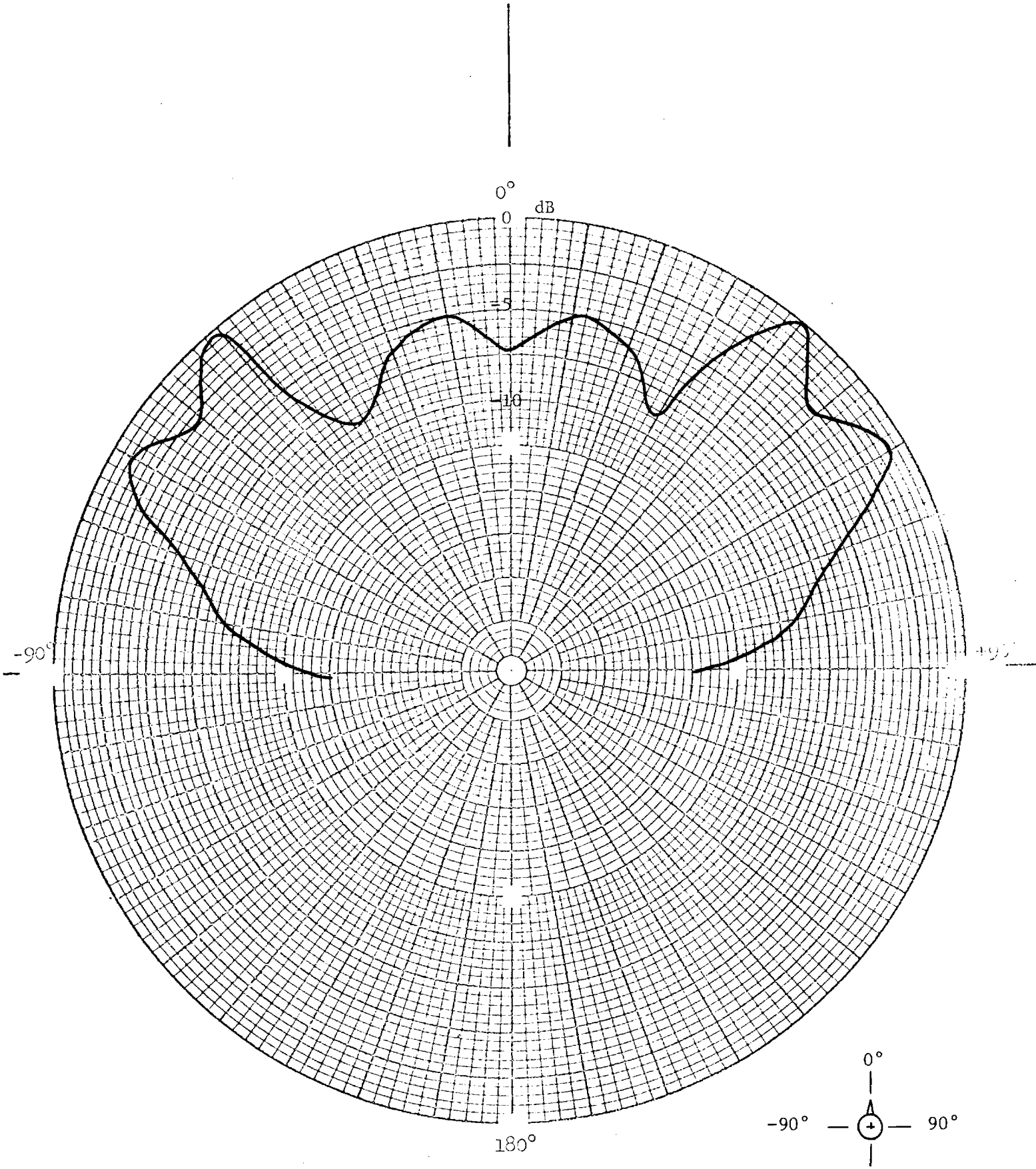

Figure 68. Conical Spiral Radiation Pattern on 14-inch Diameter Cylinder, Horizontal Polarization, Variable Roll Angle (10 GHz)

SECTION III
RESULTS

In general, it can be stated that the computer modeling technique utilized on this program is an economical approach to the calculation of antenna radiation patterns of target vehicles. The wide beamwidth characteristics of the antenna systems evaluated did have an effect on the depth and position of radiation pattern nulls in the cases where two antennas formed the system, such as the DIGIDOPS scoring antennas. But the envelope of the radiation patterns and the percent coverage of each system were predicted relatively accurately.

The location of the mounting position for the TDU-X scoring antennas was determined through the computer modeling technique as described herein. It was determined that the two antennas should be positioned on the top and bottom of the tow target and as far aft as possible. It was determined that the antennas could be displaced from one another along the fuselage axis without any serious degradation of the desired rear coverage. Once the antenna positions were determined, based on the computer prediction data and on the desire to locate the antennas in a position compatible with other TDU-X equipment, scale model radiation patterns were made that verified the coverage predicted by the computer program.

The other TDU-X tow target antennas that were evaluated did provide coverage in the areas that were predicted and expected. The computed patterns were verified by measured data on the scaled model.

The wing-tip pod-mounted scoring antennas on the BQM-34A provide pattern coverage toward each side of the vehicle with some spill-over (top and bottom), but the percent spherical coverage is much less than that of the TDU-X scoring antennas. This is caused by the near flat shape of the outboard side of the pods. Each of the two scoring antennas could be utilized individually or summed together without little change in the radiation pattern coverage.

In summary, an economical method of predicting target antenna radiation pattern coverage has been presented. For the cases where exact positions of nulls are required, the described scale model measurements also proved to be an inexpensive route to follow.

SECTION IV
RECOMMENDATIONS

It is recommended that for future target antennas the following considerations be made:

(a) Utilize the antenna pattern prediction technique for determining the location of the antennas and for an estimate of the percent coverage that will be obtained,

(b) Utilize the scale model measurements for the cases where an antenna system is formed from two or more antenna elements and where severe pattern blockages and/or reflections are predicted,

(c) Utilize the scale model measurements to provide reliable contour plots that might be required by range instrumentation personnel.

It is also recommended that consideration should be given to expanding the current antenna pattern prediction computer program to include geometrical theory of diffraction techniques. This particular computer program, although expensive to implement, would be used in situations where time was an important factor and the scale model measurement program could not be implemented.

A final recommendation concerns the design of antennas for targets. It is felt that a program should be pursued that would address the design of stripline-type, multi-antenna configurations. Microwave and antenna technology has advanced to the point where these type antenna systems are viable and economical. It is felt that by utilizing good design techniques, target antenna systems could be built to be very efficient, lightweight, and with very little structural out-cuts required. Typically, three to five antenna systems could be fabricated from a 10- to 15-inch wide strip that wraps around the fuselage of the target. In fact, a patch antenna design has recently been developed and tested in-house that looks very promising for use on target vehicles.

As a final recommendation, the DIGIDOPS scoring antennas need to be redesigned so that they are more flexible in their positioning on a target. For example, the slot antennas could be replaced by printed circuit antennas utilizing a flexible substrate. These antennas could then conform to the outer surface of most any target of interest.

At least two ideas have been discussed with the Technical Program Monitor at ADTC/DLMQ. One of these approaches would specifically address the targets that could utilize fin-mounted antennas. Because of the complexity of the scoring problem, it is felt that the antenna system should not be a contributor to any errors that might arise in the analysis of scoring data. This implies a constant VSWR over a fairly broad bandwidth and good radiation pattern coverage. These two requirements are compatible and can be realized in relatively inexpensive antenna designs.

Since each of the targets has a number of radiating systems which might cause interference between systems, it will be necessary to implement a measurement program to determine the electromagnetic interference perturbations. Although analytical techniques are available to predict these effects, past experience has shown that a measurement program is necessary because of the complexity of the problem. With the high number of transmitting and receiving systems now utilized by each target, an EMI test program based on MIL-STD-461, which tests for both emissions and susceptibilities, should be initiated.

SECTION V
REFERENCES

1. Silver, S. and W. K. Saunders, "The Radiation from a Transverse Rectangular slot in a Circular Cylinder," J. A. P., Vol. 21, August 1950, pp. 745-749.

2. Sensiper et al., "A Further Study of the Patterns of Singular Slots on Circular Conducting Cylinders," IRE Transactions on Antennas and Propagation, August 1952, pp. 240-250.

3. Bailin, L. L., "The Radiation Field Produced by a Slot in a Circular Cylinder," IRE Transactions on Antennas and Propagation, AP-3, No. 3, July 1955, pp. 128-137.